SKB

TECHNICAL REPORT 92-12

HYDRASTAR – a code for stochastic simulation of groundwater flow

Sven Norman

Starprog AB

May 1992

SVENSK KÄRNBRÄNSLEHANTERING AB
SWEDISH NUCLEAR FUEL AND WASTE MANAGEMENT CO
BOX 5864 S-102 48 STOCKHOLM
TEL 08-665 28 00 TELEX 13108 SKB S
TELEFAX 08-661 57 19

HYDRASTAR - A CODE FOR STOCHASTIC SIMULATION OF GROUNDWATER FLOW

Sven Norman

Starprog AB

May 1992

HYDRASTAR - A code for stochastic simulation of groundwater flow.

Sven Norman
Starprog AB

May 1992

ABSTRACT

The computer code HYDRASTAR was developed as a tool for groundwater flow and transport simulations in the SKB 91 safety analysis project. Its conceptual ideas can be traced back to a report by Shlomo Neuman in 1988, see the reference section.

The main idea of the code is the treatment of the rock as a stochastic continuum which separates it from the deterministic methods previously employed by SKB and also from the discrete fracture models. The current report is a comprehensive description of HYDRASTAR including such topics as regularization or upscaling of a hydraulic conductivity field, unconditional and conditional simulation of stochastic processes, numerical solvers for the hydrology and streamline equations and finally some proposals for future developments.

Der Vogel kämpft sich aus dem Ei. Das Ei ist die Welt. Wer geboren werden will, muß eine Welt zerstören. Der Vogel fliegt zu Gott. Der Gott heißt Abraxas.

Hermann Hesse, Demian.

TABLE OF CONTENTS

1 INTRODUCTION

The purpose of this report is to describe the code HYDRASTAR, developed at Starprog AB under contract from the Swedish Nuclear Fuel and Waste Management Company, SKB AB. The name HYDRASTAR is spelled out as HYDRAulic STochastic Analysis of a Repository.

HYDRASTAR is based on the following main assumptions:

- from a hydraulic point of view it is possible to treat the fractured rock as a continuum described by a hydraulic conductivity field, if the averaging scale is sufficiently large,
- the values of this continuum can be pointwise measured, with a reasonable degree of accuracy, using stationary packer tests and Moye's formula, see chapter 2.

These assumptions do not constitute something new and are in fact the assumptions classically used by SKB when modelling subsurface hydrology. None of these assumptions are undisputed, in particular one may argue that a fractured rock cannot be modelled as a continuum using averaged quantities. One of the reasons for such objections is the pattern of measured inflow into tunnels. This pattern shows indeed that the flow is concentrated at rather few points[1]. In order to clarify the picture a short discussion of the continuum approach is inserted.

The continuum description arises through the process of spatial averaging. That is quantities that only exist in the fractures of the rock such as hydrodynamic head and waterparticle velocity are averaged over spatial volumes thus defining a value of any hydrodynamic quantity at any point in space. It is clear that the averaged quantities are well defined. However, there should be no restriction on the averaging volumes such as requiring that they should be representative elementary volumes as described for instance by [Bear, 1972]. This means that any constitutional equation depends on the chosen averaging volumes. One might imagine these volumes to vary in space and being different for different quantities. Thus, the first assumption does not assume anything about the existence of the continuum fields, it is clear that these exist, but the assumption is solely that the constitutive equation known as Darcys law holds i e that there exists a

---

[1]The standard counter-argument to any discussion based on observations on tunnel walls are that these observations may to a very large extent be affected by for example degassing effects close to the tunnel wall.

hydraulic conductivity field. There are theoretical derivations of this constitutional equation that start with the constitutive equations for waterflow in the fractures and then perform the spatial averaging, see for instance [Whitaker, 1985] or [Gray and O'Neill, 1976].

The second assumption above can also be criticized, and perhaps with more reason. First it is clear that the approximations in the analysis leading to a value of a block conductivity value from a packer test are rather crude, see appendix B. Computer simulations performed in [Geier et al, 1992] suggest that the correlation between the arithmetic average of five two meter packer tests[2] and a measure of the conductivity of a surrounding cube with a side of 40m might be weak.

One can also argue, regarding the second assumption, that the low and high measurement values belong to different distributions since a low measured value can be the result of a local variation of conductivity whereas a high measured value cannot since there has to be a high conductivity path connecting the packer interval with a sink, see for example [Journel and Alabert, 1989].

The main ideas with HYDRASTAR are:

- to treat the hydraulic conductivity as a spatial stochastic function and condition it on the measurements,
- to introduce the averaging scale explicitly in the analysis using a novel technique for regularizing the conductivity measurements.

The technique necessary in order to implement the first point above is described by many authors as for instance [Delhomme, 1979] and its use in the SKB 91 project was inspired by [Neuman, 1988]. The second point was introduced partly to meet criticizm on the use of continuum methods by increasing the scale and more generally to study the influence of different scales. There were also ideas on performing simulations on different scales and then perform deregularization or deconvolution[3] towards smaller scales. In the end, however, the primary reason for introducing the second point above was the following: The size of the elements in a mesh used for solving the hydrology equations numerically must be small in comparison to the correlation scale of the hydraulic conductivity. Thus it is necessary to have large correlation scales if large regions are modelled. Since the range of the conductivity as a stochastic process increases as the averaging scale increases this

---

[2]That is the approximate equivalent of a ten meter packer test, see chapter 2.

[3]In such a process it would be advantageous to have results from several scales to start with.

large correlation scale and thus the ability to model large domains can be achieved by regularization.

The report contains fourteen chapters. The first discusses the regularization of conductivity in detail and also shows how a conductivity field is affected by regularizations. The four following chapters discuss random functions. Chapter 3 introduces some concepts and notations of stochastic functions. In chapter 4 the different types of random functions which HYDRASTAR can use are described. Chapter 5 describes how HYDRASTAR simulates the unconditional realizations of a conductivity field using the turning bands method and chapter 6 how these realizations can be conditioned on the regularized measurements.

Chapter 7 discusses the finite difference solver of the hydrology equation, chapter 8 the problem of giving the computational domain reasonable boundary conditions and chapter 9 describes the stream line equation solver.

Chapter 10 describes some special features in HYDRASTAR that are incorporated to improve transport modelling using one dimensional stream tube transport models. A further discussion of the use of these features in SKB 91 and in future developments is given in appendix A.

Chapter 11 contains some proposals for the future development of HYDRASTAR .

Two more appendices are also included, first a derivation of Moye's formula [Moye, 1967] and second a general but noncomprehensive discussion of intrinsic random functions in appendix C. A comprehensive, but mathematically very advanced text, on the subject is [Matheron, 1973].

2 SCALE AND REGULARIZATION

2.1 Regularization

The precise form of the fundamental assumption used in the stochastic analysis performed by HYDRASTAR is that :

> A stationary packer test can be evaluated by Moye´s formula to give the conductivity at an averaging scale that is related to the length of the packed off section and at a point in space identical to the midpoint of the measurement section.

Thus, employing the assumption, what is needed in order to vary the scale is a methodology to add stationary conductivity measurements together to achieve new sets of measurements on packer intervals larger than those originally used. The primary advantage with the increase of averaging scale is that the correlation scale of the studied parameter, in this case the conductivity, increases and thus makes it possible to study a larger domain. Hence if one wants to study regional flow fields, regularization is imperative. Of course it is to be noted that the cost of increasing the averaging scale is the loss of resolution.

Moreover there are other interesting questions. In general the set of measurements performed at a site consists of measurements on different scales, that is different packer interval lengths. For instance, at the Finnsjön site the measurements are predominantly performed for two and three meter sections. The question arises whether these measurements can be considered as being from the same population, or if there is a systematic difference due to the difference in scale. Secondly, we may ask how dependent our results are on the scale which we are using, that is, in the case of packer measurements, what packer interval lengths are used.

Let us first describe a mathematical model for a packer test. A similar model with subsequent numerical calculations has been developed by [Braester and Thunvik, 1982]. Figure 2.1 shows a rock block with a drilled hole in which a packer test is performed and a cylindrical coordinate system (ρ, φ, z) in which the equations will be expressed. The z-axis of the cylindrical coordinate system coincides with the borehole. The natural head field after the drilling is denoted by $h_0(\mathbf{x})$ and is assumed to satisfy the steady-state hydrology equation

$$\nabla(K(\mathbf{x})\nabla h_0(\mathbf{x})) = 0$$

along with the boundary conditions

$$h_0(\mathbf{x}) = x_3$$

for **x** at the groundwater surface. Here x_3 denotes the vertical coordinate of **x** in a Cartesian coordinate system.

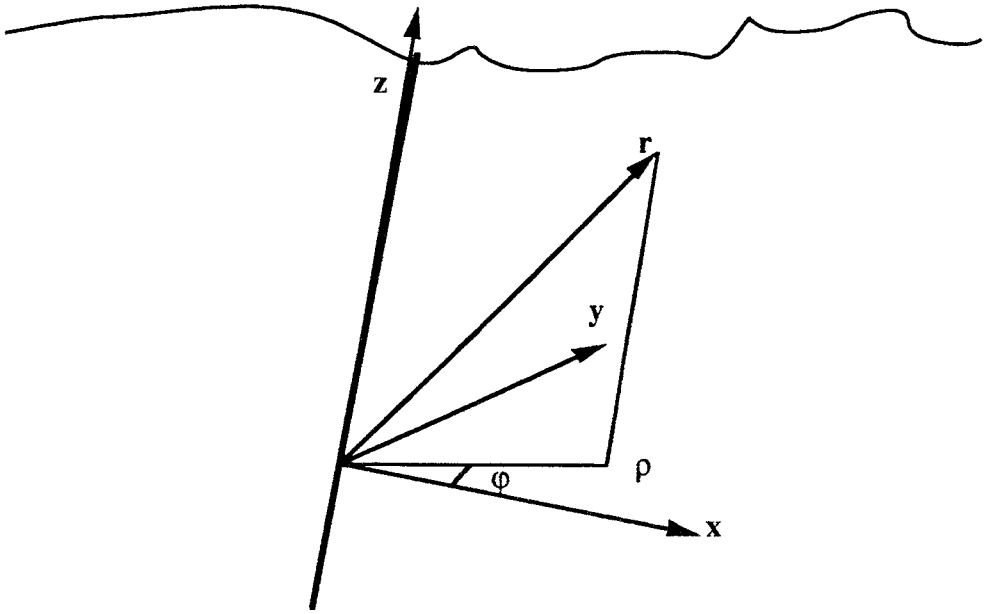

Figure 2.1 *A borehole and the corresponding cylindrical coordinate system.*

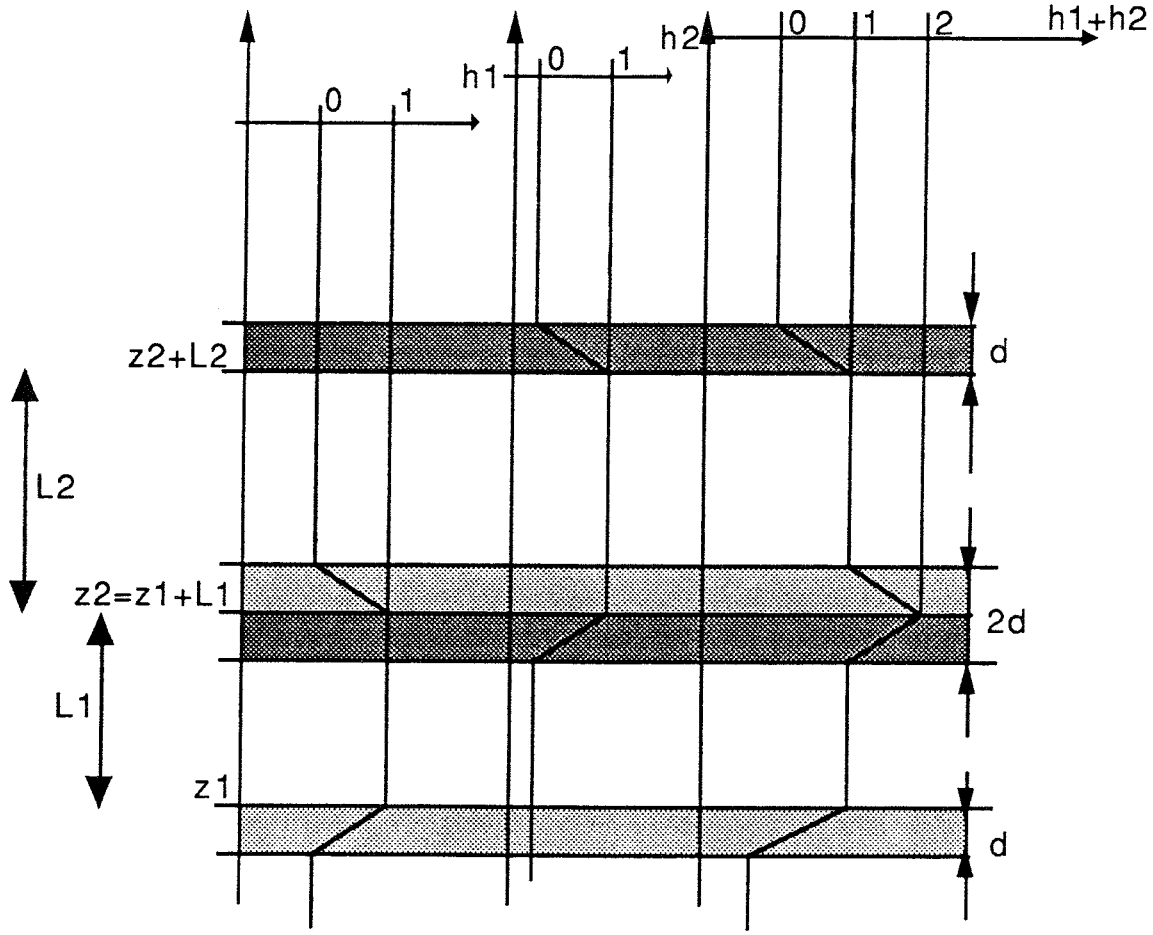

Figure 2.2 Showing the summing of two packer test responses.

Moreover it seems safe to assume[4] that along the borehole the hydraulic head equals a given constant, namely the groundwater level in the borehole.

As the next step insert the packers, without disturbing the natural field and pressurize the section between the packers to an overpressure Δp_1. This overpressure corresponds to a head difference $\Delta h_1 = \Delta p_1/\delta g$, where δ denotes the density of water and g the constant of gravity. Let us now write the head field during the steady state part of the packer test as $h_0(\mathbf{x}) + \Delta h_1 \cdot h_1(\mathbf{x})$ where Δh_1 is a dimensionless scaling factor, $h_1(\mathbf{x})$ satisfies

$$\nabla(K(\mathbf{x})\nabla h_1(\mathbf{x})) = 0$$

and

$$\begin{cases} h_1(\mathbf{x})\big|_{\rho=\rho_w} = 1 & z_1 \le z \le z_1 + L_1 \\ \left.\dfrac{\partial h_1(\mathbf{x})}{\partial \rho}\right|_{\rho=\rho_w} = -\dfrac{1}{\Delta h_1}\left.\dfrac{\partial h_0(\mathbf{x})}{\partial \rho}\right|_{\rho=\rho_w} & \begin{cases} z_1 + L_1 \le z \le z_1 + L_1 + d \\ z_1 - d \le z \le z_1 \end{cases} \\ \left.\dfrac{\partial h_1(\mathbf{x})}{\partial \rho}\right|_{\rho=\rho_w} = 0 & \begin{cases} z > z_1 + L_1 + d \\ z_1 - d > z \end{cases} \\ h_1(\mathbf{x}) = 0 & \textit{elsewhere on the boundary} \end{cases}$$

where we introduced z_1 as the position of the lowest point of interval between the packers, d as the length of the packers, L_1 as the length of the interval between the packers and ρ_w as the radius of the drill hole. The phrase "elsewhere on the boundary" is used to denote the boundary of the domain in question minus the borehole wall. For this analysis it should be interpreted as the groundwater surface. The third equality in the boundary conditions above expresses a basic approximation in this analysis, namely that the leakage back into the borehole induced by the test is negligible. The fourth equation implicitly states the assumption that the groundwater surface is assumed to be unchanged and the second equation states the flow perpendicularly to the packers is zero. Note that we supress the angle φ from the notation but that the analysis does not assume that any of the involved fields are independent of φ.

Next we will make the reasonable assumption that the natural head gradients are small in comparison to the applied head difference Δh_1 in the vicinity of the packed off section i.e.

$$-\frac{1}{\Delta h_1}\left.\frac{\partial h_0(\mathbf{x})}{\partial \rho}\right|_{\rho=\rho_w} \approx 0 \qquad z_1 - d \le z \le z_1 + L_1 + d \qquad 2.1$$

---

[4]Since the hole can be considered as very conductive a head difference along the hole cannot exist in stationary state.

so that we may write the boundary conditions of $h_1(\mathbf{x})$ as

$$\begin{cases} h_1(\mathbf{x})\big|_{\rho=\rho_w} = 1 & z_1 \le z \le z_1 + L_1 \\ \dfrac{\partial h_1(\mathbf{x})}{\partial \rho}\Big|_{\rho=\rho_w} = 0 & \begin{cases} z > z_1 + L_1 \\ z_1 > z \end{cases} \\ h_1(\mathbf{x}) = 0 & \textit{elsewhere on the boundary} \end{cases}.$$

Similar assumptions are made by [Braester and Thunvik, 1982]. However, they do not perform the above division in h_0 and h_1 but assume that the natural conditions are given by a constant potential i.e. h_0=const and treat the actual head field divided into two cases:

- No flow through the borehole wall at the packers. A constant potential along the rest of the borehole wall.
- No flow through the borehole wall i.e. the borehole is sealed.

Thus the equations resulting from our analysis above is much like the second case of [Braester and Thunvik, 1982] but the somewhat unrealistic assumtion that h_0=const is avoided. We note also that the assumptions made in 2.1 are slightly stronger than necessary for our immediate purposes. However we will make use of the remaining part of the assumption later on. Another test performed at the location z_2 is treated analogously i.e. it results in a field $h_0(\mathbf{x}) + \Delta h_2 \cdot h_2(\mathbf{x})$ where Δh_2 is a dimensionless scaling factor,

$$\nabla(K(\mathbf{x})\nabla h_2(\mathbf{x})) = 0$$

and

$$\begin{cases} h_2(\mathbf{x})\big|_{\rho=\rho_w} = 1 & z_2 \le z \le z_2 + L_2 \\ \dfrac{\partial h_2(\mathbf{x})}{\partial \rho}\Big|_{\rho=\rho_w} = 0 & \begin{cases} z_2 + L_2 < z \\ z_2 > z \end{cases} \\ h_2(\mathbf{x}) = 0 & \textit{elsewhere on the boundary} \end{cases}.$$

Now the idea is to show that the function $h_0(\mathbf{x}) + h_1(\mathbf{x}) + h_2(\mathbf{x})$ is an approximation to the field $h_{1+2}(\mathbf{x})$ arising as a result of both packer tests being performed at the same time both with an applied unit head difference. Since the aim is to predict the result of a packer test of length $L_1 + L_2$ the case of the measurement sections being adjacent, i.e.

$z_1 + L_1 = z_2$ is treated below. This case is also depicted in figure 2.2. The case of non-adjacent sections will be treated in section 2.1.1. [5]

To this end we first note that

$$0 \le h_1(\mathbf{x})\big|_{\rho=\rho_w} \le 1 \qquad \text{for} \quad \begin{cases} z_1 + L_1 < z \\ z < z_1 \end{cases}$$

and similarly for $h_2(\mathbf{x})$. This is true since $h_1(\mathbf{x})$ is equal to one on one part of the boundary and equal to zero on another so if there was a point on the remaining part of the boundary i.e along the borehole outside the packer interval not satisfying the above inequality then there would exist a extremal value of $h_1(\mathbf{x})$ somewhere along the borehole outside the injection interval[6]. This point would then act like a source or a sink, contradicting the no-flow conditions.

Thus $h_1(\mathbf{x}) + h_2(\mathbf{x})$ satisfies

$$\nabla(K(\mathbf{x})\nabla(h_1(\mathbf{x}) + h_2(\mathbf{x}))) = 0$$

and

$$\begin{cases} 1 \le (h_1(\mathbf{x}) + h_2(\mathbf{x}))\big|_{\rho=\rho_w} \le 2 & z_1 \le z \le z_1 + L_1 + L_2 \\ \dfrac{\partial(h_1(\mathbf{x}) + h_2(\mathbf{x}))}{\partial\rho}\Big|_{\rho=\rho_w} = 0 & z < z_1,\ z > z_1 + L_1 + L_2 \\ h_1(\mathbf{x}) + h_2(\mathbf{x}) = 0 & \textit{elsewhere on the boundary} \end{cases}$$

whereas for the solution $h_{1+2}(\mathbf{x})$ of the problem posed by a packer test performed over the section length $L_1 + L_2$ we would require that

---

[5] In this connection we might ponder over the overall aim of the analysis. As the reader realizes this is to use the assumption in the beginning of the current chapter, the result of the current analysis together with Moyés formula to obtain an estimate of the effective conductivity on a large averaging scale at the center of the measurement section. With this ultimate goal in mind there does not seem to be much sense in requiring that the measurement sections should be adjacent. That is only needed to simulate a packer test performed with a larger packer interval length not to obtain the effective conductivity. Thus what one should wish for is a formula that connected a set of packer measurements with the effective conductivity of a rockblock containing them.

[6] Since it is clear that any function h(x) that satisfies $\nabla(K(\mathbf{x})\nabla h(\mathbf{x}))=0$ cannot have a local maximum in the interior of the domain of interest i.e it has to attain its extremal values on the boundary.

$$\begin{cases} h_{1+2}(\mathbf{x})\big|_{\rho=\rho_w} = 1 & z_1 \le z \le z_1 + L_1 + L_2 \\ \dfrac{\partial h_{1+2}(\mathbf{x})}{\partial \rho}\Big|_{\rho=\rho_w} = 0 & z < z_1, z > z_1 + L_1 + L_2 \\ h_{1+2}(\mathbf{x}) = 0 & \textit{elsewhere on the boundary} \end{cases}$$

Thus it is clear that

$$h_{1+2}(\mathbf{x})\big|_{\rho=\rho_w} \le h_1(\mathbf{x}) + h_2(\mathbf{x})\big|_{\rho=\rho_w} \le 2h_{1+2}(\mathbf{x})\big|_{\rho=\rho_w} \qquad z_1 \le z \le z_1 + L_1 + L_2$$

and that this double inequality implies that[7]

$$\int_{z_1}^{z_1+L_1+L_2} K(\mathbf{x})\frac{\partial}{\partial \rho} h_{1+2}(\mathbf{x})\rho_w\, dz \le \int_{z_1}^{z_1+L_1+L_2} K(\mathbf{x})\frac{\partial}{\partial \rho}(h_1(\mathbf{x}) + h_2(\mathbf{x}))\,\rho_w\, dz \le 2\int_{z_1}^{z_1+L_1+L_2} K(\mathbf{x})\frac{\partial}{\partial \rho} h_{1+2}(\mathbf{x})\rho_w\, dz$$

As the notation suggests these integrals are taken over the part of the surface of the borehole between the packers. Expanding the middle term, again using the assumption that the leakage flow is negligible, and turning the inequality inside out we have

$$\tfrac{1}{2}(q_1 + q_2) \le q_{1+2} \le q_1 + q_2 \qquad 2.2$$

where

$$q_1 = \int_{z_1}^{z_1+L_1} K(\mathbf{x})\frac{\partial}{\partial \rho} h_1(\mathbf{x})\rho_w\, dz ,$$

---

[7]This is a consequence of the statement: If the function h(x) satisfies $\nabla[K(\mathbf{x})\nabla h(\mathbf{x})] = 0$ and

$$\begin{cases} h(\mathbf{x})\big|_{\rho=\rho_w} \ge 0 & z_1 \le z \le z_1 + L_1 + L_2 \\ \dfrac{\partial h(\mathbf{x})}{\partial \rho}\Big|_{\rho=\rho_w} = 0 & z < z_1, z > z_1 + L_1 + L_2 \\ h(\mathbf{x}) = 0 & \textit{elsewhere on the boundary} \end{cases}$$

then the flow from the section $[z_1, z_1+L_1+L_2]$ is nonnegative.i.e

$$\int_{z_1}^{z_1+L_1+L_2} K(\mathbf{x})\frac{\partial}{\partial \rho} h(\mathbf{x})\,\rho_w\, dz \ge 0$$

$$q_2 = \int_{z_2}^{z_2+L_2} K(\mathbf{x}) \frac{\partial}{\partial \rho} h_2(\mathbf{x}) \rho_w \, dz$$

are known quantities proportional to the measured flows per applied head difference unit and

$$q_{1+2} = \int_{z_1}^{z_1+L_1+L_2} K(\mathbf{x}) \frac{\partial}{\partial \rho} h_{1+2}(\mathbf{x}) \rho_w \, dz$$

is the flow per head difference unit that would be measured if the test was performed on the section $L_1 + L_2$. It is to be stressed here that this is the crucial point where we made strong use of the no-leakage assumption since we used that

$$\int_{z_2}^{z_2+L_2} K(\mathbf{x}) \frac{\partial}{\partial \rho} h_1(\mathbf{x}) \rho_w \, dz = \int_{z_1}^{z_1+L_1} K(\mathbf{x}) \frac{\partial}{\partial \rho} h_2(\mathbf{x}) \rho_w \, dz = 0 \quad .$$

It is moreover clear that an analysis such as this must make this kind of assumption since the leakage flows are not generally measured.

The fact that the expressions for the q:s above are proportional to the flow per head difference from a pressurized section, follows from the assumption 2.1 since the flow from a pressurized section, the section $[z_1, z_1+L_1]$ say, can be written

$$q_1 := \frac{Q_1}{2\pi \Delta h_1} = \int_{z_1}^{z_1+L_1} K(\mathbf{x}) \left(\frac{1}{\Delta h_1} \frac{\partial h_0(\mathbf{x})}{\partial \rho} + \frac{\partial h_1(\mathbf{x})}{\partial \rho} \right) \rho_w \, dz \approx$$

$$\int_{z_1}^{z_1+L_1} K(\mathbf{x}) \frac{\partial h_1(\mathbf{x})}{\partial \rho} \rho_w \, dz \quad . \qquad 2.3$$

Now Moye´s formula B.2, see appendix B or alternatively [Moye, 1967], can be written in terms of $q = Q/2\pi\Delta h$ where Q is the measured flow as

$$LK = q\left(1 - \ln\left(\frac{2\rho_w}{L}\right)\right)$$

and thus

$$(L_1 + L_2) K_{1+2} \leq (q_1 + q_2)\left(1 - \ln\left(\frac{2\rho_w}{(L_1 + L_2)}\right)\right) =$$

$$\left(1-\ln\left(\frac{2\rho_w}{(L_1+L_2)}\right)\right)\left(\frac{L_1K_1}{\left(1-\ln\left(\frac{2\rho_w}{L_1}\right)\right)}+\frac{L_2K_2}{\left(1-\ln\left(\frac{2\rho_w}{L_2}\right)\right)}\right).$$

Introducing

$$K_{reg}=\frac{\left(1-\ln\left(\frac{2\rho_w}{(L_1+L_2)}\right)\right)}{(L_1+L_2)}\left(\frac{L_1K_1}{\left(1-\ln\left(\frac{2\rho_w}{L_1}\right)\right)}+\frac{L_2K_2}{\left(1-\ln\left(\frac{2\rho_w}{L_2}\right)\right)}\right)$$

we thus have the result that

$$\tfrac{1}{2}K_{reg}\le K_{1+2}\le K_{reg} \qquad 2.4$$

and hence

$$K_{1+2}\approx\frac{3}{4}K_{reg}$$

is a reasonable estimate but HYDRASTAR uses the more conservative $K_{1+2}=K_{reg}$.[8]

These results are easily generalized to n adjacent sections with the value of K_{reg} replaced by

$$K_{reg}=\frac{\left(1-\ln\left(\frac{2\rho_w}{\sum_{i=1}^{n}L_i}\right)\right)}{\sum_{i=1}^{n}L_i}\sum_{i=1}^{n}\frac{L_iK_i}{\left(1-\ln\left(\frac{2\rho_w}{L_i}\right)\right)}.$$

but due to the presence of n added interval the estimate 2.4 instead becomes

$$\tfrac{1}{n}K_{reg}\le K_{1+2+\ldots+n}\le K_{reg}. \qquad 2.5$$

This is, however, a very pessimistic estimate. In analogy with the above discussion we can define the scaled head response from the j:th packer test participating in the regularization by $h_j(\mathbf{x})$, the corresponding packer interval length by L_j and the packer length by d. It is reasonable to assume that the $h_j(\mathbf{x})$:s are almost constant and equal to

---

[8]It may be argued that this is not conservative since choosing a certain value as a representative of a interval of possible values leads to an underestimation of the variance which in the end may lead to a more homogeneous conductivity field and thus less possibility of "fast flow paths".

zero outside the packers due to the high conductivity of the hole itself. Hence if $2d<L_j$ the analog of 2.4

$$\tfrac{1}{2}K_{reg} \le K_{1+2+\ldots+n} \le K_{reg} \qquad 2.6$$

would still hold.

We note that in the common case of constant section length $L_i = L$ for all i the regularized conductivity value equals

$$K_{reg} = \frac{\left(1 - \ln\left(\frac{2\rho_w}{nL}\right)\right)}{\left(1 - \ln\left(\frac{2\rho_w}{L}\right)\right)} \frac{1}{n} \sum_{i=1}^{n} K_i$$

i.e. a corrected arithmetic mean value of the individual conductivity measurements. This behaves very differently from the widely used geometric average. What is most striking is that the high measurement values dominate the sum and thus a plot of regularized measurements along the borehole tend to be constant in intervals, see the figures in section 2.2. This is rather natural if one consider how the conductivity of an averaging volume would vary when moved over a highly conductive fracture. We remark also that the size of the correction factor is on the order of one.

2.1.1 Imperfect match in regularization

We must consider two kinds of mismatch, positive (i.e. $z_1 + L_1 > z_2$) and negative i.e. ($z_1 + L_1 < z_2$), where the notation refers back to the two-measurement situation in the previous section. In the case of several sections added together with positive mismatch it is clear that 2.5 will always hold regardless of the magnitude of the overlap. On the other hand, following the reasoning above i.e. the assumption of constant zero head along the borehole outside the packers in each separate packer test, the estimate does not deteriorate provided that packed off sections, including the packers, do not overlap more than twice in which case 2.6 will still hold. The situation in the case of a negative mismatch is much worse since there is no way to estimate the flow that would have resulted from the gap. Declining any further theoretical analysis, which could be done in the positive-overlap case, we state that HYDRASTAR uses the following definition.

Let us denote a measurement by the triple (z_i, L_i, K_i) where, as before, z_i denotes borehole coordinate of the lowest point of the packer test, L_i denotes the length of the packer interval used and K_i denotes the obtained conductivity value according to Moye´s formula. With a set of measurements $\{(z_i, L_i, K_i), i = 1, 2, \ldots, n\}$ we associate an interval along the borehole I_{reg} and a length L_{reg} by

$$I_{reg} = \left(\min_{1 \le i \le n} (z_i), \min_{1 \le i \le n} (z_i) + S \right)$$

and

$$L_{reg} = \max_{1 \le i \le n}(z_i + L_i) - \min_{1 \le i \le n}(z_i)$$

where S is the target regularization scale. The borehole interval I_{reg} is the packer interval of the packer test we are approximating whereas the interval $(\min(z_i), \min(z_i) + L_{reg})$ is the interval of the approximation itself with its positive and negative mismatches.

Now such a set of measurements is said to constitute a regularized measurement on the scale S at the positive tolerance level ε_p and the negative tolerance level ε_n precisely if

$$e^+_{reg} = \int \left(\sum_{i=1}^{n} \chi_{(z_i, z_i + L_i)} - 1 \right)^+ < \varepsilon_p S \quad , \qquad 2.7$$

$$e^-_{reg} = \int \left(\sum_{i=1}^{n} \chi_{(z_i, z_i + L_i)} - 1 \right)^- + |S - L_{reg}| < \varepsilon_n S \qquad 2.8$$

where χ_I denotes the characteristic function for the interval I for any interval I i.e. the function that is equal to one in the interval and identically zero outside and where $(\cdot)^+$ means $\max(\cdot, 0)$ and $(\cdot)^-$ means $-\min(\cdot, 0)$. The integrals extend over the interval $(\min(z_i), \min(z_i) + L_{reg})$.

In words this would amount to saying that the set of measurements $\{(z_i, L_i, K_i), i = 1, 2, \ldots, n\}$ is a regularized measurement on scale S if the sum of all positive mismatches is less than $\varepsilon_p S$ and the sum of the negative mismatches is less than $\varepsilon_n S$. The reason for including the term $| S - L_{reg} |$ in the expression for the negative error is that it always represent a section from which the induced flow cannot be estimated in contrast to the positive type mismatch. Note that this in particular implies that

$$|S - L_{reg}| < \varepsilon_n S \quad .$$

The pair ε_n , ε_p are tolerances that a user must supply. As is clear from the above discussion it is highly recommended to take $\varepsilon_n << \varepsilon_p$. Finally then the value of the regularized measurement is taken to be

$$K_{reg} = \frac{\left(1 - \ln\left(\frac{2\rho_w}{L_{reg}}\right)\right)}{L_{reg}} \sum_{i=1}^{n} \frac{L_i K_i}{\left(1 - \ln\left(\frac{2\rho_w}{L_i}\right)\right)}$$

where ρ_w is assumed to be a constant. Also in the case the conductivity K_i is below the measurement limit the value of the limit is substituted for the true conductivity value.

2.1.2 When are two measurements identical ?

The question in the heading arises because in certain situations it may be possible to patch together measurement sections satisfying the constraints of 2.7 and 2.8 in such a way that the resulting sections cover essentially the same part of the borehole. In spite of this the values obtained can be quite different. This is to be compared with the hypothetical situation that one performs the same measurement several times but obtains different answers due to uncontrollable factors i.e. what is usually referred to as measurement errors. This line of reasoning could be used to estimate the uncertainty of the regularized measurements but we will not pursue this any further in this report.

The following definition is used in HYDRASTAR: Two regularizations $\{(z_i, L_i, K_i), i = 1, 2, \ldots, n\}$ and $\{(z_i', L_i', K_i'), i = 1, 2, \ldots, n'\}$ represent the same measurement if

$$\left|\max_{1\le i\le n}(z_i + L_i) - \max_{1\le i\le n'}(z_i' + L_i')\right| + \left|\min_{1\le i\le n}(z_i) - \min_{1\le i\le n'}(z_i')\right| < \varepsilon_n S$$

and the value of this measurement is taken to be the arithmetic mean value of the two associated regularized conductivities i.e.

$$\frac{K_{reg} + K'_{reg}}{2}.$$

The extension to several regularizations is straightforward.

2.2 The effect of regularization

In this subsection we present some graphs and histograms on original and regularized measurement sections from the Finnsjön site. The data has been retrieved from the SKB geoscientific database GEOTAB and the interpreted zone intersections shown are taken from [Ahlbom and Tiren, 1991]. The graphs clearly show the smoothing effect of the regularization procedure and the strong domination of high original measurement values on the regularized measurement values on all sections containing the original high measurement values. As for the histogram the effect of the regularization is to slightly diminish the range of the conductivity values and to even out the shape. Also there is an increase in average log conductivity with increasing scale. However, the most striking feature of these histograms are that they do not look as if taken from a normal distribution, which is a usual assumption in the literature. Thus it would be a worthwhile effort to find new Gaussian transforms. In this connection we remark that the regularization formula does not preserve log-normality, thus the possible finding of a Gaussian transform should be done separately on each scale.

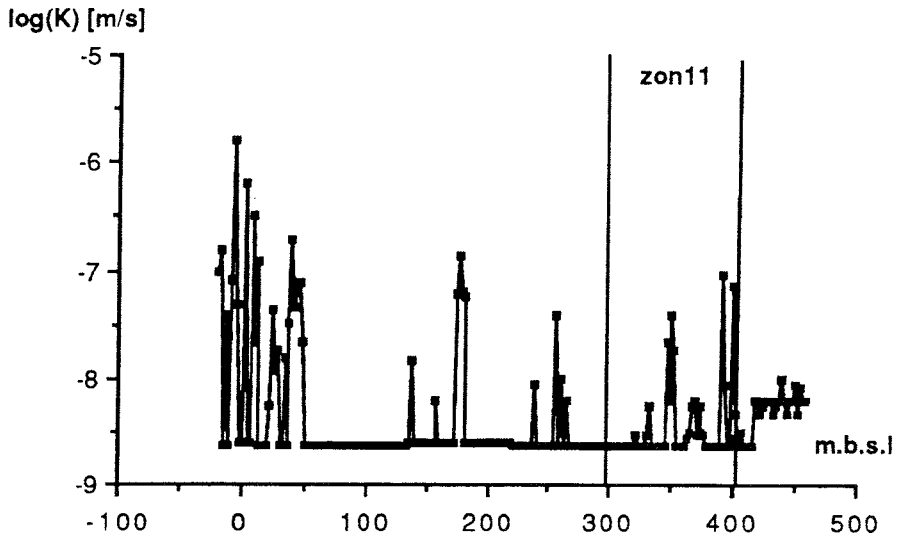

Figure 2.3 *The original measurements in borehole kfi01. The value of the measurement limit 2.4E-9 has replaced measurement values below the measurement limit.*

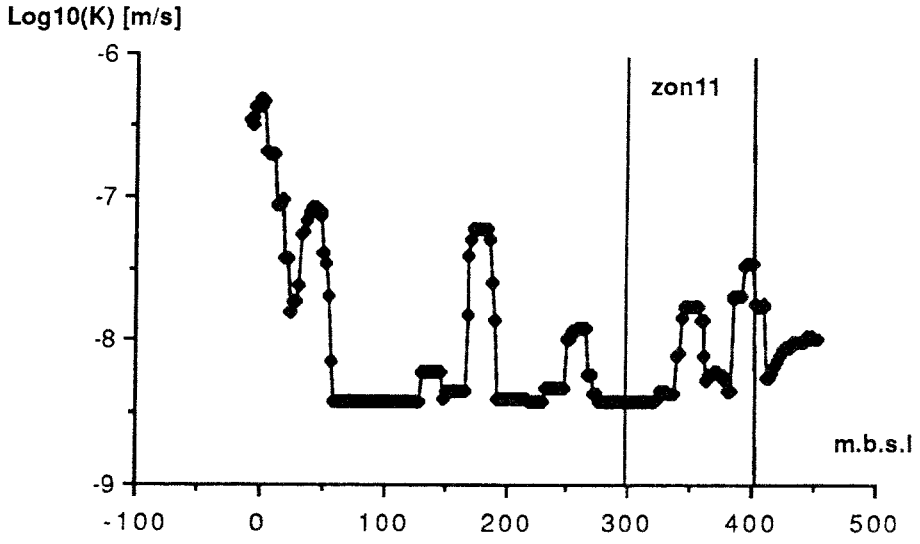

Figure 2.4 *The measurements in borehole kfi01 regularized to 18m.*

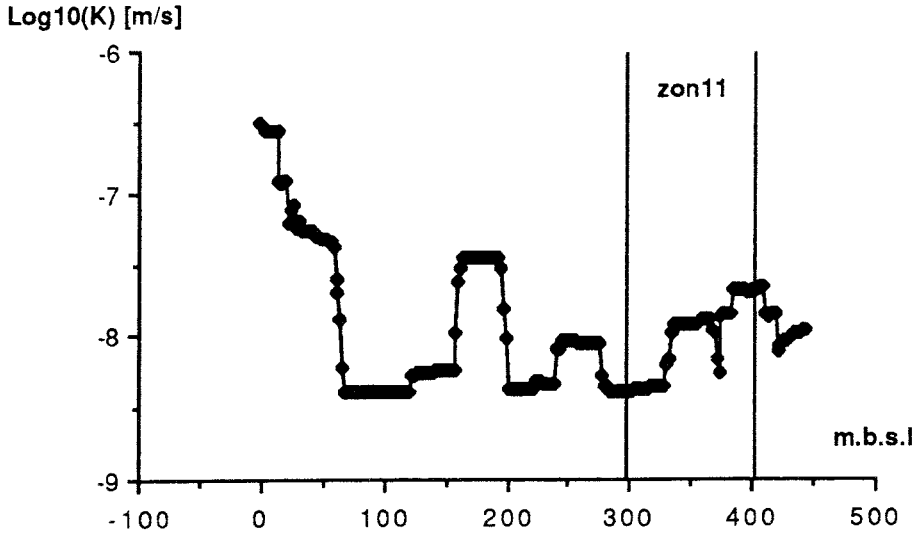

Figure 2.5 *The measurements in borehole kfi01 regularized to 36m.*

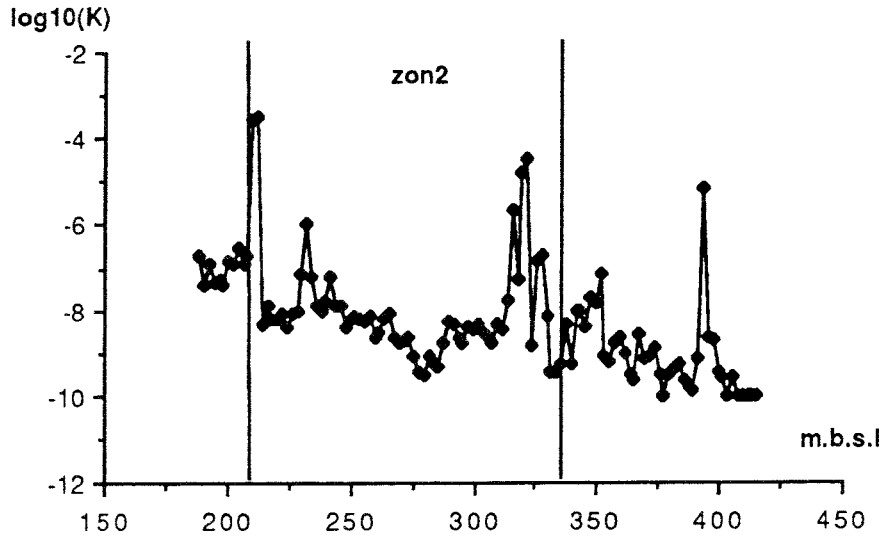

Figure 2.6 *The original measurements in borehole bfi01. The value of the measurement limit 1.0E-10 has replaced measurement values below the measurement limit.*

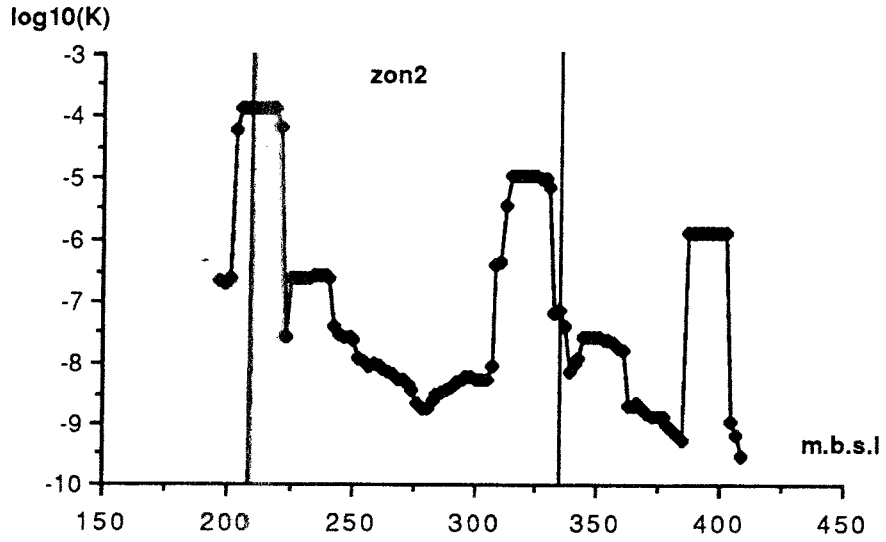

Figure 2.7 *The measurements in borehole bfi01 regularized to 18 m.*

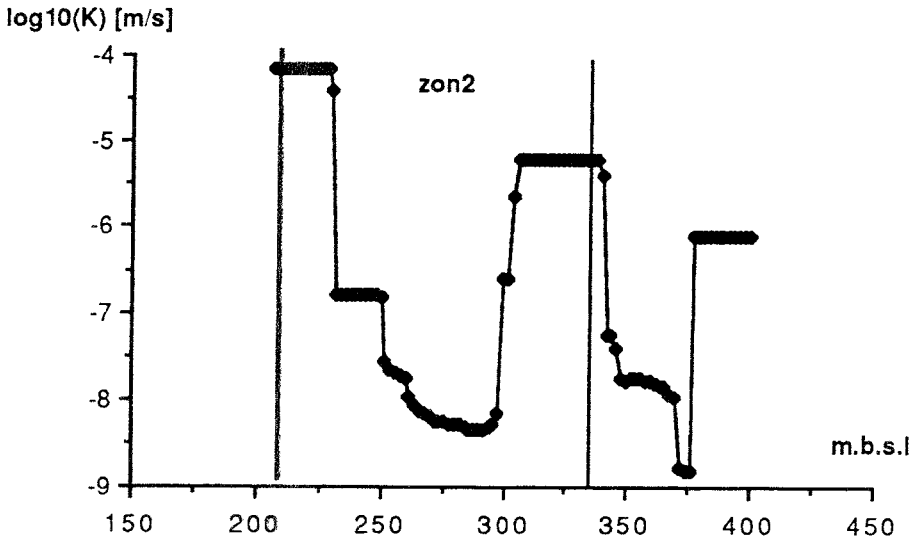

Figure 2.8 The measurements in borehole bfi01 regularized to 36m.

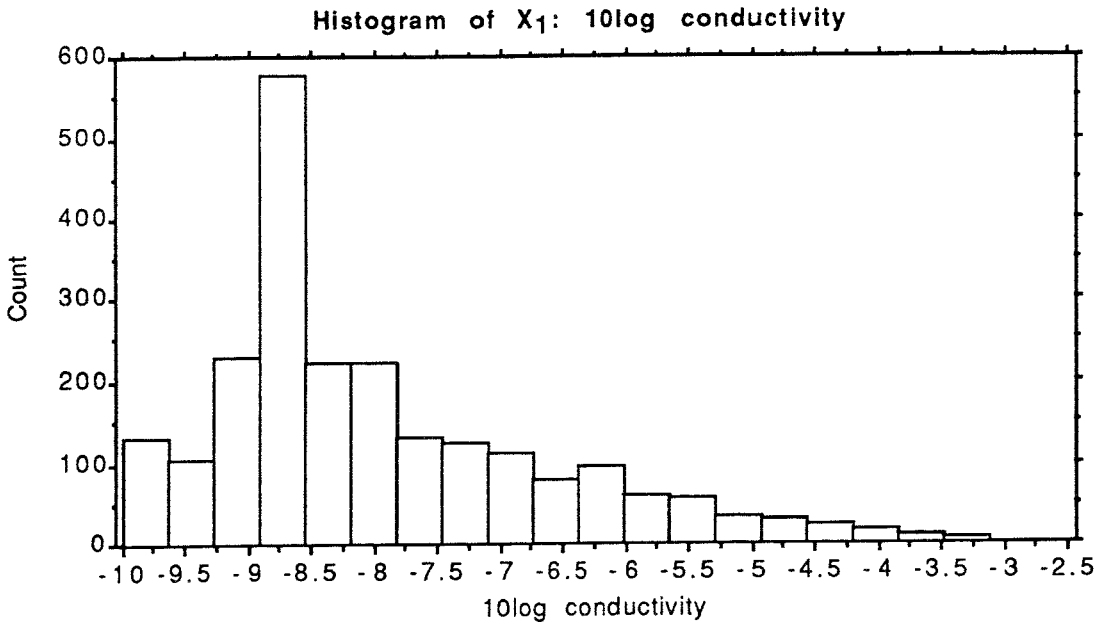

Figure 2.9. *Histogram of all (2258) original measurements of log conductivity. The value of the measurement limits have replaced measurement values below the measurement limit.*

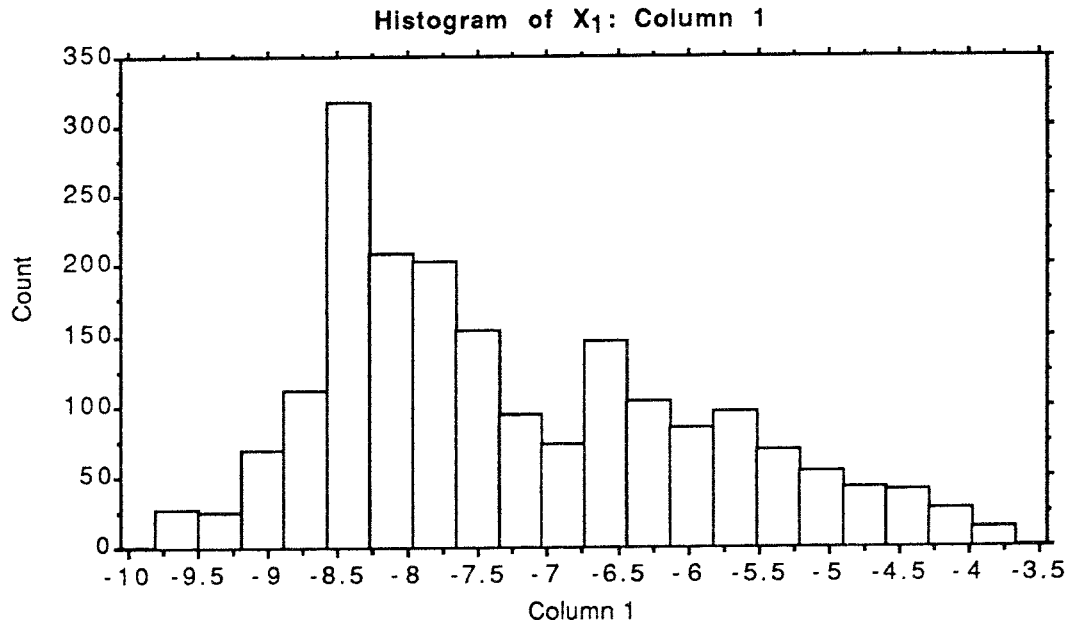

Figure 2.10. *Histogram of all (1952) 18 m measurements of log conductivity.*

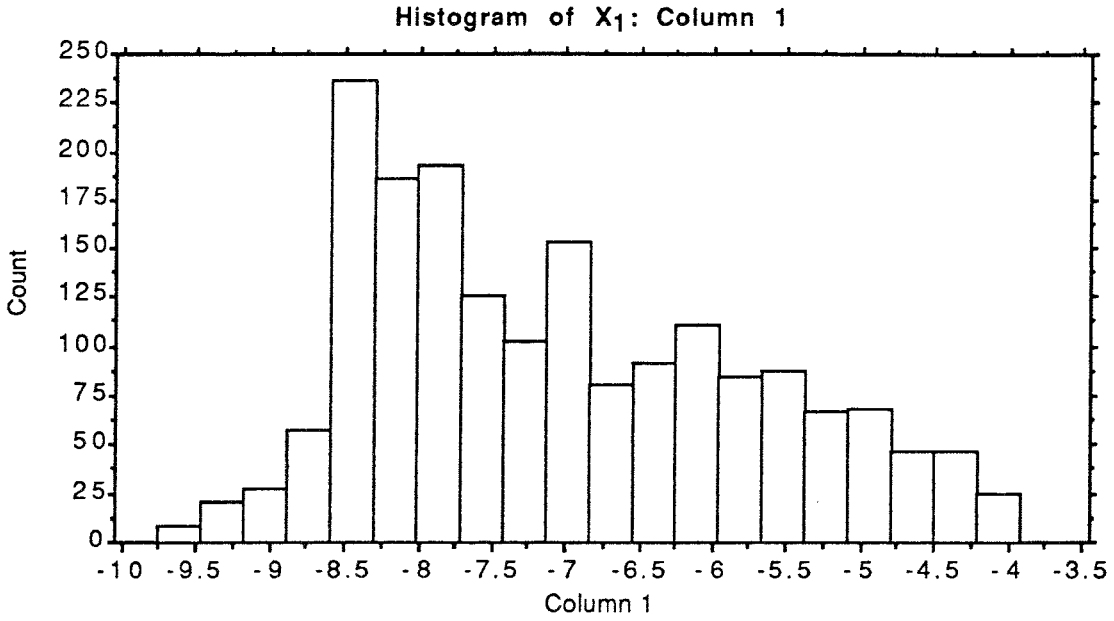

Figure 2.11. *Histogram of all (1815) 36 m measurements of log conductivity.*

3 STOCHASTIC FUNCTIONS

This chapter is inserted to give the reader some information of stochastic processes needed to read the report. It also introduces some notations.

3.1 General

In this report it will mostly suffice to think of a stochastic function Y as a function of two arguments $Y(\mathbf{x}, \omega)$, the space argument $\mathbf{x}$, and the event space argument ω. For fixed $\mathbf{x}$ the function is an ordinary stochastic variable and for fixed ω it becomes a spatial function, a realization. Let us take the opportunity to introduce some notation below that will be used throughout the rest of the report.

Define

$$m_Y(\mathbf{x}) = E[Y(\mathbf{x}, \omega)]$$

where $E[\cdot]$ denotes the expectation value operator. A primed quantity will always denote the mean removed form so for instance

$$Y'(\mathbf{x}, \omega) = Y(\mathbf{x}, \omega) - E[Y(\mathbf{x}, \omega)]$$

and $C_Y(\mathbf{x}, \xi)$ is the centered covariance function of Y, the definition of which can be written as

$$C_Y(\mathbf{x}, \xi) = E[Y'(\mathbf{x} + \xi, \omega) Y'(\mathbf{x}, \omega)]$$

where ξ denotes the vector separating two points of consideration, the so-called lag vector. A stochastic function is said to be weakly (or second order) stationary if the expectation value function $m_Y(\mathbf{x})$ and the centered covariance function $C_Y(\mathbf{x}, \xi)$ is independent of $\mathbf{x}$ i.e. if

$$\begin{cases} m_Y(\mathbf{x}) = m_Y \\ C_Y(\mathbf{x}, \xi) = C_Y(\xi) \end{cases}.$$

Finally, $\sigma(\mathbf{x})$ is the standard deviation at $\mathbf{x}$ i.e. if Y is weakly stationary

$$\sigma_Y(\mathbf{x})^2 = C_Y(\mathbf{0}).$$

In the above notational definitions $Y(\mathbf{x}, \omega)$ may be replaced by any other stochastic function without altering the meaning of the notation however the index will be dropped when it is apparent by the context which stochastic function is referred to. Furthermore, the dependence on the event space variable ω will be suppressed from now on. For a more thorough description of random functions see appendix C.

3.2 Intrinsic random functions

A stochastic function Y(**x**) is said to be intrinsic if the following requirements hold:

(i) The second order moment of an increment

$$\gamma_Y(\xi) = \tfrac{1}{2}E\left[\left(Y(\mathbf{x}+\xi) - Y(\mathbf{x})\right)^2\right] \qquad 3.1$$

exists and is independent of **x**. The function $\gamma(\mathbf{x})$ is known as the semivariogram.

(ii) The first order moment of the increment is zero i.e.

$$E[Y(\mathbf{x}+\xi) - Y(\mathbf{x})] = 0 \qquad 3.2$$

Note that the condition above is a much weaker condition than to require weak second order stationarity. In particular an intrinsic random function need not to have a finite variance i.e. need not to be of second order. In case the stochastic function has a finite variance the semivariogram is closely related to the covariance function since

$$\gamma_Y(\xi) = \tfrac{1}{2}E\left[\left(Y(\mathbf{x}+\xi) - Y(\mathbf{x})\right)^2\right] =$$

$$\tfrac{1}{2}E\left[\left(Y'(\mathbf{x}+\xi) - Y'(\mathbf{x})\right)^2\right] =$$

$$\sigma(\mathbf{x})^2 - C_Y(\xi) \qquad 3.3$$

4 MODELS OF STOCHASTIC FUNCTIONS

A stochastic function in general is a complex object.To describe it completely an enormous amount of information, the set of all finite dimensional distributions, is required. Restricting assumptions have to be made. This leads to models with few parameters that can be estimated. The typical assumption is that some kind of stationarity holds. HYDRASTAR allows a reasonable amount of different models and they will be described below. The main difference between the models that can be employed in HYDRASTAR is whether a trend is explicitly modelled, in which case we will talk of a residual type model, or if the trend is modelled implicitly by a local stationarity assumption as described in section 6.1.2. This latter case is, somewhat misleading, referred to as the intrinsic case.

4.1 Covariance models

Many properties of a stochastic function can be explained if one knows the semivariogram. However, as shown in Appendix C section C.2, not any function can be chosen as a semivariogram or for that matter a covariance function. Two models that guarantee the definiteness properties, C.6 are presented in this section and are the ones supported by HYDRASTAR. These models are both what is referred to as **transition models** [Journel and Huijbregts, 1978] which means that they possess a finite variance and thus have equivalent formulations in terms of covariance functions.

The models are basically isotropic. The first one is the so-called **spherical model** and is written in the form of a covariance function as

$$C(\xi) = \begin{cases} V\left(1 - \frac{3}{2}\frac{\|\xi\|}{a} + \frac{1}{2}\frac{\|\xi\|^3}{a^3}\right) & 0 \le \|\xi\| \le a \\ 0 & \|\xi\| > a \end{cases} \qquad 4.1$$

and the other is an **exponential model**

$$C(\xi) = V \exp(-\lambda\|\xi\|) \qquad \forall\, \xi \qquad 4.2$$

where, in both these expressions, V signifies the variance, ξ is the vector separating two measurement points, i.e. the lag vector and a and λ are parameters determining the range of the stochastic function with the corresponding covariance function.[9] The **range**, or correlation length, of a stochastic function Y(**x**) is the maximum distance separating two

---

[9]These models could of course have been stated in the semivariogram form.

points $\mathbf{x}_1$ and $\mathbf{x}_2$ over which the the stochastic variables $Y(\mathbf{x}_1)$ and $Y(\mathbf{x}_2)$ are correlated. We note that as a rule of thumb the practical range of a stochastic function with an exponential covariance function is $3/\lambda$ whereas for a stochastic function with a spherical covariance function the range is equal to a.

A simple way to model stochastically anisotropic fields is to use so-called geometrical anisotropy i.e. to write

$$C(\xi) = C_{iso}(\mathbf{G}\xi)$$

where C_{iso} is an isotropic model and $\mathbf{G}$ is the matrix of geometrical anisotropy. This will transform the level surfaces of the covariance functions from concentric spheres to confocal ellipsoids. The mapping

$$\eta = \mathbf{G}\xi$$

will be said to transform the (lag) space into the isotropic (lag) space.

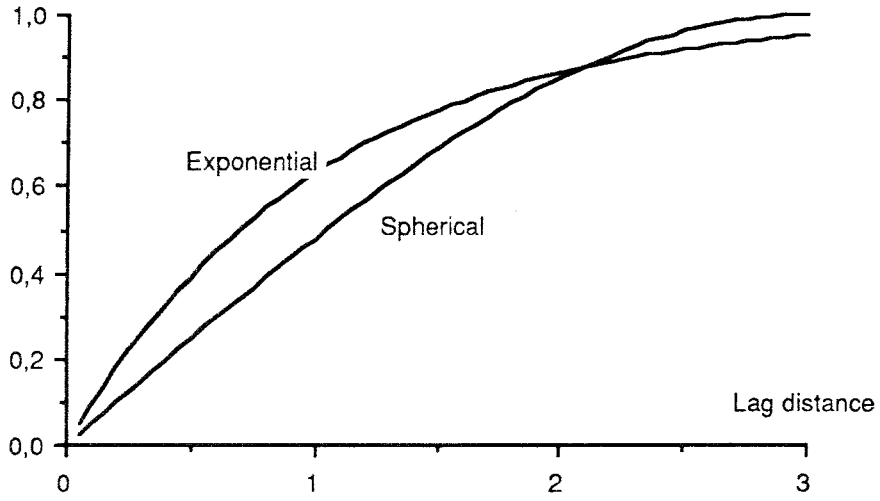

Figure 4.1 *Showing the exponential and spherical variogram models. They both have finite variance equal to 1.0 and practical range equal to 3.0.*

Further models of covariance functions can be obtained by adding covariance functions of the above classes to obtain what is known as nested models [Journel and Huijbregts, 1978]. This is a possible future development of HYDRASTAR.

4.2 Kriging neighbourhoods

Kriging neighbourhoods are discussed in chapter 6.1. The basic form of these that can be used in HYDRASTAR are inclined slices, for instance the kriging neighbourhood for the point $\mathbf{x}_1$ is given by

$$D(\mathbf{x}_1) = \left\{ \mathbf{x} \in \mathbf{R}^3 : -o \leq (\mathbf{x} - \mathbf{x}_p(\mathbf{x}_1)) \bullet \hat{\mathbf{n}} \leq w + o \right\}$$

where the width w and the overlap o are positive real numbers, $\hat{\mathbf{n}}$ is the normal of the slices and $\mathbf{x}_p(\mathbf{x}_1)$ is a point defining a kriging set[10] . The kriging set containing the point $\mathbf{x}_1$, $E(\mathbf{x}_1)$ is defined as

$$E(\mathbf{x}_1) = \left\{ \mathbf{x} \in \mathbf{R}^3 : 0 \leq (\mathbf{x} - \mathbf{x}_p(\mathbf{x}_1)) \bullet \hat{\mathbf{n}} < w \right\}$$

and thus consists of slices of width w inclined in the same direction as the kriging neighbourhoods.

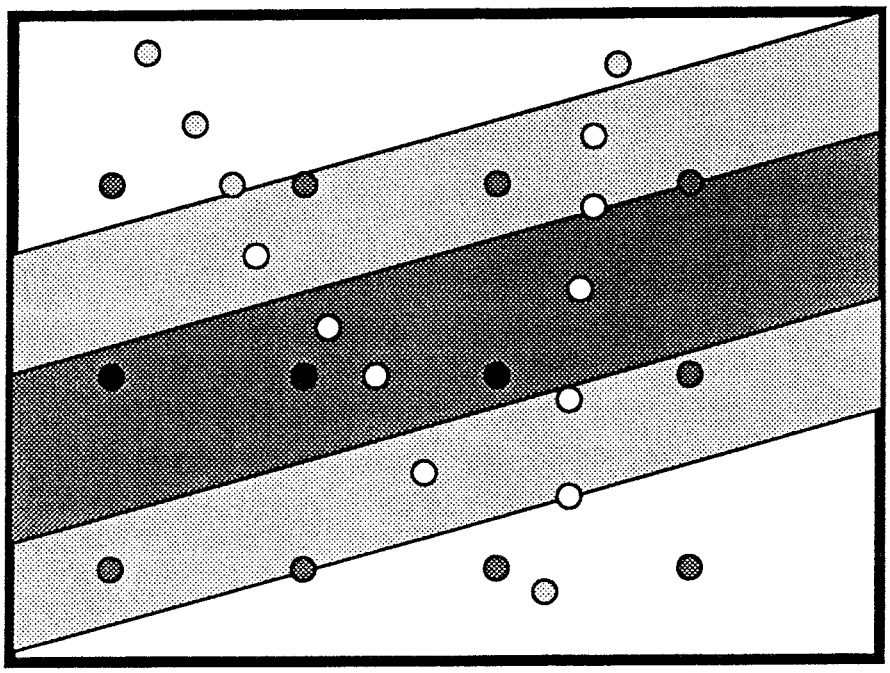

Figure 4.2 *Showing a kriging set and a corresponding kriging neighbourhood.*

- ● *Nodes inside the kriging set i.e.* $\in E(\mathbf{x}_1)$.
- ◍ *Nodes outside the kriging set.*
- ◎ *Measurements outside the kriging neighbourhood i.e.* $\notin D(\mathbf{x}_1)$.
- ○ *Measurements inside the kriging neighbourhood.*

This implies that the kriging neighbourhood is unchanged for all points in a kriging set

$$D\left(\mathbf{x}_p(\mathbf{x}_1) + s\hat{\mathbf{n}} + \mathbf{b}\right) = D(\mathbf{x}_1)$$

---

[10]This is a nonstandard notation invented by the author.

if $s \leq w$ is a real number and $\mathbf{b}$ is any vector orthogonal to the kriging neighbourhood normal $\hat{\mathbf{n}}$. The function $\mathbf{x}_p(\mathbf{x}_1)$ is chosen so that the set of all kriging sets covers the domain of interest and is mutually disjoint, i.e. there is no point that lies in two kriging sets.

Since, as explained in chapter 6.1, the primary requirement on a kriging neighbourhood is the constancy of the expected value function this choice of kriging neighbourhoods is motivated by the well known decrease of hydraulic conductivity with increasing depth. This decrease will thus be achieved without the use of an explicit trend function. Also inclination of the slices can be motivated by an assumption that the level surfaces of the hydraulic conductivity is oriented parallel with the subhorizontal zone 2.

As for the parameter w it should not be too small in comparison to the correlation scale of the stochastic function considered. On the other hand it should not be too large in view of the constancy requirement.

To this basic structure of kriging neighbourhoods a possibility is added in HYDRASTAR to perform a subdivision of the considered rock block prior to the slicing described above. The reason for this is that it is likely that the modeller wants to use models that allow different expectation values for the conductivity in more generally shaped regions and then overlay the trendlike behaviour obtained by the slicing in some direction. The main example of regions with different expectation values being inferred fracture zones.

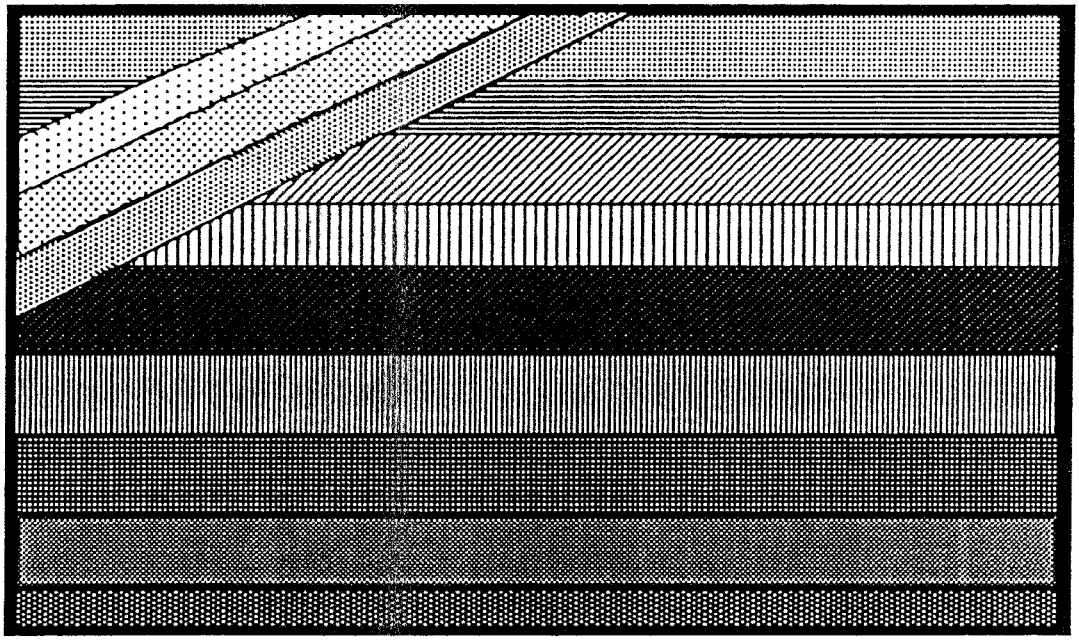

Figure 4.3 *Showing a possible slicing of a computational domain for the Finnsjön rock block where we have used one primary kriging set for zone 2 and another for the rest of the domain. The primary kriging*

set for zone 2 has then been divided into three secondary kriging neighbourhoods.

To be specific the modeller may define a primary kriging set as the union of several basic sets constructed as the intersection of halfspaces. This may be useful for instance when one considers many fracture zones and only have measurements in some of them. It is then possible to assume that the fracture zones have identical properties and to lump them together in one primary kriging neighbourhood and then perform the secondary slicing on this disconnected set. Also need may arise to use more general nonconvex primary kriging sets. For more details on how to specify this input to HYDRASTAR, see [HYDRASTAR].

If one does not believe that a zero:th order intrinsic model, even using kriging neighbourhoods, is sufficient for describing the phenomenon at hand one may want to include the expectation value functions explicitly in the analysis. In HYDRASTAR one may use any trend function. The user must however, if he cannot use one of or a linear combination of the already supplied trend functions, write his own FORTRAN subroutine and link it with HYDRASTAR. See [HYDRASTAR] for details.

5 UNCONDITIONAL SIMULATIONS

In the following chapter we shall describe in detail how HYDRASTAR generates unconditional Gaussian regionalization with a given covariance or semivariogram function. The method used is the turning bands algorithm as described by [Journel and Huijbregts, 1978], [Tompson, Ababou and Gelhar, 1989] and [Matheron, 1973]. The main goal of this section is to give a reasonably comprehensive derivation and discussion of the formulas 5.21 and 5.22 used in HYDRASTAR for generating random fields and also a discussion on the reasons for the way the user may specify the lines distributions used in the generation, see section 5.3.

5.1 The turning bands method

Regard the problem of simulating a three dimensional random function Y. We assume it to be weak second order stationary as defined in chapter 3. Let us further assume that the random function Y is Gaussian and that its second order moments m_Y and $C_Y(\xi)$ are known. This, in fact, specifies the distribution of the regionalization completely.

Now the basic idea with the turning bands algorithm is to write

$$Y(\mathbf{x}) = \int_{S_{1/2}} Y_1((\mathbf{x},\mathbf{l}),\mathbf{l})\sqrt{f(\mathbf{l})}\,dS(\mathbf{l})$$

where $\mathbf{l}$ is a unit vector on the half unit sphere $S_{1/2}$, $dS(\mathbf{l})$ is a infinitesimal surface element, $f(\mathbf{l})$ is a probability density function on $S_{1/2}$, $(\cdot\,,\,\cdot)$ signifies the ordinary scalar product and $Y_1(\cdot\,,\,\mathbf{l})$ is a family of stochastic processes indexed by $\mathbf{l}$ and with the following properties:

- $Y_1(\cdot\,,\,\mathbf{l}_1)$ and $Y_1(\cdot\,,\,\mathbf{l}_2)$ are uncorrelated if $\mathbf{l}_1 \neq \mathbf{l}_2$

and

- $Y_1(\cdot\,,\,\mathbf{l}_1)$ is stationary with zero expectation and a covariance function $C_1(\cdot\,,\,\mathbf{l}_1)$.

Above we also introduced a general notation exemplified with $Y_1(\cdot\,,\,\mathbf{l}_1)$. This simply means that this object is a function or process of one variable obtained by fixing the variable given as the second argument to the value $\mathbf{l}_1$.

As an approximation for the case of a uniform distribution on the half unit sphere, i.e. $f = 1/2\pi$ identically, we write

$$Y(\mathbf{x}) = \frac{1}{\sqrt{N}} \sum_{i=1}^{N} Y_1((\mathbf{x}, \mathbf{l}_i), \mathbf{l}_i) \qquad 5.1$$

where $\{\mathbf{l}_i\}_{i=1}^{N}$ is a set of unit vectors on $S_{1/2}$. The first thing to note is that the marginal distributions of this process obtained by fixing one point in space will tend to a normal distributions as the number of lines tends to infinity as follows from the central limit theorem [Fisz, 1963, p 196.]. The second thing to notice is that trivially the stationarity of Y follows from the stationarity of $Y_1(\cdot, \mathbf{l})$. In particular

$$E[Y_1(\cdot, \mathbf{l})] = 0, \forall \mathbf{l} \Rightarrow E[Y] = 0.$$

However, the main thing about the method is to find the covariances $C_1(\xi, \mathbf{l})$, where ξ is the lag coordinate on the line, which produces the given covariance $C(\xi)$. To that end we express the covariance of Y in the covariances of $Y_1(\cdot, \mathbf{l})$ using the properties of the family $Y_1(\cdot, \mathbf{l})$ as[11]

$$C_Y(\xi) = \int_{S_{1/2}} C_1((\xi, \mathbf{l}), \mathbf{l}) f(\mathbf{l}) dS(\mathbf{l}) \qquad 5.2$$

and in the approximate case

$$C_Y(\xi) = \frac{1}{N} \sum_{i=1}^{N} C_i((\xi, \mathbf{l}_i), \mathbf{l}_i).$$

Using the spectral theorem [Yaglom, 1962] we write, utilizing 5.2

$$\frac{1}{4\pi^2} \int_{\mathbf{R}^3} S_Y(\lambda) e^{i(\lambda, \xi)} d\lambda = \int_{S_{1/2}} \int_{-\infty}^{\infty} S_1(\lambda_1, \mathbf{l}) e^{i(\xi, \lambda_1 \mathbf{l})} f(\mathbf{l}) d\lambda_1 dS(\mathbf{l}) \qquad 5.3$$

where $S_Y(\cdot)$ and $S_1(\cdot, \mathbf{l})$ are the spectra of the processes $Y(\cdot)$ and $Y_1(\cdot, \mathbf{l})$ respectively.

The idea is now to rewrite the right hand side into the same form as the left hand side. As a first step in doing this divide the right hand side into two parts

$$\int_{S_{1/2}} \int_{0}^{\infty} S_1(\lambda_1, \mathbf{l}) e^{i(\xi, \lambda_1 \mathbf{l})} f(\mathbf{l}) d\lambda_1 dS(\mathbf{l}) + \int_{S_{1/2}} \int_{-\infty}^{0} S_1(\lambda_1, \mathbf{l}) e^{i(\xi, \lambda_1 \mathbf{l})} f(\mathbf{l}) d\lambda_1 dS(\mathbf{l})$$

---

[11] To produce a stringent derivation of 5.2 necessitates the introduction of a whole machinery and is therefore excluded.

and then perform a change of variables as

$$\begin{cases} \lambda_1 \mathbf{l} = \lambda \\ \lambda_1 = |\lambda| \\ \mathbf{l} = \lambda/|\lambda| \\ |\lambda|^2 d\lambda_1 dS(\mathbf{l}) = d\lambda \end{cases}$$

for the first integral and

$$\begin{cases} \lambda_1 \mathbf{l} = \lambda \\ \lambda_1 = -|\lambda| \\ \mathbf{l} = -\lambda/|\lambda| \\ |\lambda|^2 d\lambda_1 dS(\mathbf{l}) = d\lambda \end{cases}$$

for the second. Introducing the notation $\Re^3_{1/2}$ for the part of $\Re^3$ intersected by rays through $S_{1/2}$ and $\Re^3_{-1/2}$ for $-\Re^3_{1/2} = \{-\mathbf{x}:\mathbf{x} \in \Re^3_{1/2}\}$ we then rewrite the previous expression as

$$\int_{\Re^3_{1/2}} S_1(|\lambda|, \lambda/|\lambda|) e^{i(\xi,\lambda)} f(\lambda/|\lambda|) \frac{d\lambda}{|\lambda|^2} + \int_{\Re^3_{-1/2}} S_1(-|\lambda|, -\lambda/|\lambda|) e^{i(\xi,\lambda)} f(-\lambda/|\lambda|) \frac{d\lambda}{|\lambda|^2}.$$

Finally, the line passing through -**l** is the same as the one passing through **l** so f(-**l**) = f(**l**) and $S_1(\lambda_1, -\mathbf{l}) = S_1(-\lambda_1, \mathbf{l})$ for $\mathbf{l} \in S_{1/2}$ .Thus the covariance function of the turning bands representation of Y can be written as

$$\int_{\Re} S_1(|\lambda|, \lambda/|\lambda|) e^{i(\xi,\lambda)} f(\lambda/|\lambda|) \frac{d\lambda}{|\lambda|^2}$$

and so by the uniqueness of Fourier transforms and 5.3 we have

$$S_Y(\lambda) = 4\pi^2 S_1(|\lambda|, \lambda/|\lambda|) \frac{f(\lambda/|\lambda|)}{|\lambda|^2}. \qquad 5.4$$

Now in the particular case that the probability density function, f, is uniform, i.e. equal to $1/2\pi$, and the family of line processes $Y_1(\cdot, \mathbf{l})$ satisfies the additional condition that $C_1(\xi, \mathbf{l})$ is independent of **l** we have

$$S_Y(\lambda) = S_1(|\lambda|) \frac{2\pi}{|\lambda|^2}.$$

This result together with 5.4 is also obtained by [Tompson, Ababou and Gelhar, 1989] although they use another definition of the spectral density with regard to the factor 2π. These expressions are then used to determine the spectral density along each line from the given spectral density S_Y.

In the case of isotropic processes and uniform probability density function f one may directly relate the covariances of Y and $Y_1(\cdot, \mathbf{l})$ by the following computation given in [Journel and Huijbregts, 1978]. Starting from 5.2 and suppressing the direct dependence of C_1 on $\mathbf{l}$, i.e. the second argument, we have

$$C_Y(\xi) = C_Y(|\xi|) = \frac{1}{2\pi} \int_{S_{1/2}} C_1((\xi,\mathbf{l}))dS(\mathbf{l}) = \frac{1}{4\pi} \int_S C_1((\xi,\mathbf{l}))dS(\mathbf{l})$$

where we used the symmetry of C_1 and the notation S for the unit sphere.

Switching to polar coordinates with the direction of the polar axis parallel to ξ and θ as the angle between the radius vector and the polar axis we rewrite the right hand side as

$$\frac{1}{4\pi} \int_0^{2\pi} d\varphi \int_0^{\pi} C_1(|\xi|\cos\ \theta)\sin\ \theta d\theta = \frac{1}{2} \int_0^{\pi} C_1(|\xi|\cos\ \theta)\sin\ \theta d\theta .$$

Employing the change of variables

$$\begin{cases} |\xi|\cos\ \theta = s \\ -|\xi|\sin\ \theta d\theta = ds \end{cases}$$

and the symmetry of C_1 once again we have

$$C_Y(|\xi|) = \int_0^{|\xi|} C_1(s)\frac{ds}{|\xi|}$$

or

$$C_1(|\xi|) = \frac{d}{d|\xi|}(|\xi|C_Y(|\xi|)). \qquad 5.5$$

In practice one generates a finite number of lines, N, each line is divided in bands of width T. If the value of the i:th line process $Y_1(\cdot, \mathbf{l}_i)$ in the k:th band is taken to be constant and equal $y_{i,k}$ 5.1 is replaced by

$$Y(\mathbf{x}) = \frac{1}{\sqrt{N}} \sum_{i=1}^{N} y_{i,k} \qquad 5.6$$

where k is chosen so that

$$(k-1)T \le (\mathbf{x},\mathbf{l}_i) < kT .$$

In order to make this a useful algorithm one has to find out how to generate the line processes $Y_1(\cdot\, \mathbf{l})$ and the lines themselves so that the result is "sufficiently good". We will treat this in the following two sections.

5.2 Line processes

This section will solely describe methods for simulating one dimensional stochastic processes with a given covariance function $C_1(\xi)$. This will be based on convolution techniques and follows essentially [Journel and Huijbregts, 1978]. We stress from the beginning that no importance whatsoever will be given to the form of the distribution of the generated process but only to its first two moments.

We start with the observation that a covariance function $C_1(\xi)$ always allows a convolution representation as

$$C_1(\xi) = f * \grave{f}(\xi) = \int_{-\infty}^{\infty} f(\xi - u) f(-u)\, du =$$

$$\int_{-\infty}^{\infty} f(\xi + u) f(u) du\,, \qquad 5.7$$

where f is a realvalued function and `f is a nonstandard notation defined by

$$\grave{f}(x) = f(-x).$$

This result follows easily from Bochners theorem [Yaglom, 1962] if we assume that C_1 corresponds to a spectral density function [12]. This is since in that case it is possible to write

$$C_1(\xi) = \frac{1}{2\pi} \int_{-\infty}^{\infty} e^{i\xi\lambda} dF(\lambda) = \frac{1}{2\pi} \int_{-\infty}^{\infty} e^{i\xi\lambda} S(\lambda) d\lambda$$

with S as the spectral density function and F as the spectral distribution function. From Bochners theorem we know that $F(\omega)$ is a nondecreasing function and thus $dF(\omega) \geq 0$ and $S(\lambda) \geq 0$.

Introducing the tilde sign ~ for Fourier transform and superindex * for complex conjugate we see that 5.7 gives

$$\tilde{C}_1(\lambda) = \tilde{f}(\lambda)\tilde{f}(\lambda)^* = \left|\tilde{f}(\lambda)\right|^2$$

---

[12] That is we are assuming for simplicity that the covariance function has an absolutely continuous Fourier transform.

and thus the choice of the function f only needs to satisfy

$$S(\lambda) = \left|\tilde{f}(\lambda)\right|^2 \qquad 5.8$$

which has an infinite number of real valued solutions since $S(\lambda) \geq 0$.

Now letting f be a continuous function satisfying 5.8 and taking the definition of a function against a stochastic measure for granted we write

$$Y_1(u) = \int_{-\infty}^{\infty} f(u + r)dT(r)$$

as a candidate for a stochastic process having the required covariance function $C_1(\xi)$. Here dT(r) is a stochastic measure on the real line such that for two intervals I_1 and I_2 with lengths $|I_1|$ and $|I_2|$ we have

$$\begin{cases} E[T(I_1)] = E\left[\int_{I_1} dT(r)\right] = 0 \\ E[T(I_1)T(I_2)] = E\left[\int\int_{I_1 I_2} dT(r)dT(r')\right] = |I_1 \cap I_2|\sigma_T^2 \end{cases} . \qquad 5.9$$

It is now possible to show, at least formally [13] that the process so defined has the desired covariance function. In fact

$$C_1(s) = E[Y_1(u + s)Y_1(u)] = E\left[\int_{-\infty}^{\infty}\int_{-\infty}^{\infty} f(u + s + r)f(u + r')dT(r)dT(r')\right] =$$

$$\int_{-\infty}^{\infty} f(s + r)f(r)dr\sigma_T^2$$

which is what we wanted apart from the constant factor σ_T^2.

In practise we will make a discrete approximation of these formulas on a grid with spacing b by

$$Y_1(ib) = \int_{-\infty}^{\infty} f(r)dT(r - ib) = \sum_{k=-\infty}^{\infty} \int_{\left(k-\frac{1}{2}\right)b}^{\left(k+\frac{1}{2}\right)b} f(r)dT(r - ib) \approx$$

$$\sum_{k=-\infty}^{\infty} f(kb) \int_{\left(k-\frac{1}{2}\right)b}^{\left(k+\frac{1}{2}\right)b} dT(r - ib) = \sum_{k=-\infty}^{\infty} f(kb) \int_{\left(k-i-\frac{1}{2}\right)b}^{\left(k-i+\frac{1}{2}\right)b} dT(r) = \sum_{k=-\infty}^{\infty} f(kb)t_{k-i} . \qquad 5.10$$

---

[13] It does not pose any serious problems to prove this if we define all involved integrals as Riemann integrals. We only approximate with Riemann sums.

Here t_k by the implicit definition in the equation above are independent stochastic variables with moments following directly from 5.9 i.e.

$$\begin{cases} E[t_k] = 0 \\ E\left[t_k^{\,2}\right] = b\sigma_T^{\,2} = \sigma_t^{\,2} . \end{cases}$$

This approximation is simple and in principle the one used by [Journel and Huijbregts, 1978]. The disadvantage is of course that in order for it to be a good approximation the grid spacing b has to be small. One could contemplate better integration schemes as for instance the trapetzoidal rule. For use in the turning bands method i.e. in formula 5.6 we want to have the values of the stochastic process generated in the points with spacing equal to the bandwidth T whereas the method described above generates values at points with spacing b, the magnitude of which is determined by the need of a sufficiently good approximation. Thus we will require that

$$T = N_q b \qquad 5.11$$

where N_q is some integer.

Another method for generating realizations of one dimensional processes is the FFT method which is advocated in [Tompson, Ababou and Gelhar, 1989].

5.2.1 Random number generator

The random number generator currently used in HYDRASTAR to generate random reals uniformly distributed on the interval [0, 1] is based on a combined linear congruential generator taken from [Brately, Fox and Schrage, 1987], claimed to originate from L'Ecuyer:

$$x_{i+1} = 40014 * x_i \bmod 2147483563$$

$$y_{i+1} = 40692 * y_i \bmod 2147483399$$

$$z_{i+1} = (x_{i+1} + y_{i+1}) \bmod 2147483563$$

yielding a random real

$$r_{i+1} = z_{i+1}/2147483563 . \qquad 5.12$$

This has proven to be fast and is claimed to have been extensively checked. In particular it has good spectral properties, a very large period and does not suffer from the well known weakness of linear congruential generators of having successive overlapping sequences of numbers falling on parallel hyperplanes. It should be portable across all machines having a word length of at least 32 bits.

In order to validate this generator further we have also used the following generator employed by the PROPER Monitor, see [McGrath and Irving, 1975],

$$x_{i+1} = 5^{15} * x_i \bmod 2^{47}. \qquad 5.13$$

that has been thoroughly tested [Pörn, 1986], [Coveyou and MacPherson, 1967]. Comparisons have been performed between semivariogram functions estimated from series of one dimensional realizations using either one of these random number generators and the results are almost identical.

Due to the difficulties in handling the large integers involved in the generator 5.13 it is slower than the generator 5.12 and this is the reason for choosing the latter.

5.2.2 Application to spherical and exponential models

Two isotropic covariance models C(r) are often used [Journel and Huijbregts, 1978], the spherical model

$$C(r) = \begin{cases} V\left(1 - \frac{3}{2}\frac{r}{a} + \frac{1}{2}\frac{r^3}{a^3}\right) & 0 \le r \le a \\ 0 & r > a \end{cases}$$

and the exponential

$$C(r) = V \exp(-\lambda r) \qquad r \ge 0$$

where V signifies the variance, r the norm of the lag vector, a and λ are range parameters.

According to 5.5 we derive the corresponding covariances required for the line processes as

$$C_1(s) = \begin{cases} V\left(1 - 3\frac{s}{a} + 2\frac{s^3}{a^3}\right) & 0 \le s \le a \\ 0 & s > a \end{cases}$$

and

$$C_1(s) = V(1 - \lambda s)\exp(-\lambda s) \qquad s \ge 0$$

respectively.

For these two models we propose to use convolution separations of the type 5.7 with the convolution function f given by [Journel and Huijbregts, 1978, p 507 - 508]

$$f(u) = \begin{cases} \left(\frac{12V}{a^3}\right)^{1/2} u & |u| \le \frac{a}{2} \\ 0 & |u| > \frac{a}{2} \end{cases} \qquad 5.14$$

and

$$f(u) = \begin{cases} 2(V\lambda)^{1/2}(1-\lambda u)e^{-\lambda u} & u > 0 \\ 0 & u < 0 \end{cases} \qquad 5.15$$

respectively. It is easily verified by direct, although somewhat tedious, computation that these functions satisfy the equation 5.7. However it is not clear whether these particular choices are the best.

Now we want to specialize the approximate formula 5.10 to these two cases. In the spherical case we write

$$Y(ib) = \int_{-a/2}^{a/2} f(r)dT(r-ib) = \sum_{k=-R}^{R} \int_{\left(k-\frac{1}{2}\right)b}^{\left(k+\frac{1}{2}\right)b} f(r)dT(r-ib)$$

$$\approx \sum_{k=-R}^{R} f(kb)\, t_{k-i} \qquad 5.16$$

with

$$t_k = \int_{\left(k-\frac{1}{2}\right)b}^{\left(k+\frac{1}{2}\right)b} dT(r)$$

and thus we require that

$$a = (2R+1)b. \qquad 5.17$$

For the choice of the important parameter R [Journel and Huijbregts, 1978] recommends the value R = 20.

In the exponential case we first approximate

$$Y(ib) = \int_{0}^{\infty} f(r)dT(r-ib) = \int_{0}^{4/\lambda} f(r)dT(r-ib)$$

the error associated with this approximation can be estimated by

$$\frac{E\left[\left(\int_{4/\lambda}^{\infty} f(r)dT(r-ib)\right)^2\right]}{E\left[\left(\int_{0}^{4/\lambda} f(r)dT(r-ib)\right)^2\right]} = \frac{\int_{4/\lambda}^{\infty} f(r)^2 dr}{\int_{0}^{4/\lambda} f(r)^2 dr} = \frac{25e^{-8}}{1-25e^{-8}} \approx 3.3E-4.$$

Approximating further setting $a = 1/\lambda$

$$Y(ib) = \int_0^{4a} f(r)dT(r - ib) = \sum_{k=0}^{8R} \int_{kb}^{(k+1)b} f(r)dT(r - ib) \approx$$

$$\sum_{k=0}^{8R} f\left(\left(k + \frac{1}{2}\right)b\right) t_{k-i} \qquad 5.18$$

and we require that

$$(8R + 1)b = 4a. \qquad 5.19$$

where the value of the parameter R again is recommended to be chosen equal to 20 by [Journel and Huijbregts, 1978].

These formulas differ in details only from those of [Journel and Huijbregts, 1978]. However the formula 5.16 together with 5.17 generates five to ten times more accurate values than the corresponding formulas in [Journel and Huijbregts, 1978] due to better integral approximation. Unfortunately no such cheap improvements resulted by using the formula 5.18 together with 5.19 instead of the counterparts in [Journel and Huijbregts, 1978]. As pointed out in the end of paragraph 5.2 one should try to improve the scheme for numerical integration in the exponential case.

5.2.3 Corrections of the approximative formulas

In order to check and correct the approximations above resulting in the formulas 5.16 and 5.18 we calculate the covariances from the approximative expressions directly. Starting with the spherical case we note the formula

$$E[Y(ib)Y(ib + sb)] = \sum_{k'=-R}^{R} \sum_{k=-R}^{R} f(kb)f(k'b)E\left[t_{k-i}\, t_{k'-i-s}\right].$$

Since

$$E\left[t_{k-i}\, t_{k'-i-s}\right] = \begin{cases} \sigma_t^2 & \text{if } k + s = k' \\ 0 & \text{if } k + s \neq k' \end{cases}$$

we have in the case s > 0 (note that s is an integer)

$$E[Y(ib)Y(ib + sb)] = \sigma_t^2 \sum_{k=-R}^{R} f(kb)f((k + s)b) =$$

$$\sigma_t^2 b^2 \frac{12V}{a^3} \sum_{k=-R}^{R-s} k(k+s) =$$

14

$$\sigma_t^2 b^2 \frac{12V}{a^3}\left(\frac{s^3}{6} - \left(R^2 + R + \frac{1}{6}\right)s + \frac{1}{3}(2R^3 + 3R^2 + R)\right) \qquad 5.20$$

and in particular by putting s = 0 we obtain the variance as

$$E[Y(ib)^2] = \sigma_t^2 b^2 \frac{4V}{a^3}(2R^3 + 3R^2 + R).$$

This should be compared with the required value V.

The approximative formula 5.16 is then corrected with a multiplicative constant

$$\left[\sigma_t^2 b^2 \frac{4}{a^3}(2R^3 + 3R^2 + R)\right]^{-1/2}$$

in order to give the correct value of the variance. Thus

$$Y(ib) = \sqrt{\frac{3V}{\sigma_t^2(2R^3 + 3R^2 + R)}} \sum_{k=-R}^{R} kt_{k-i} \qquad 5.21$$

which is the formula used in HYDRASTAR for simulating processes with spherical covariances. The value of R currently used is 20, the stochastic variables t_k are uniformly distributed in the interval [-0. 5, 0. 5] and thus $\sigma_t = 1/12$.

Turning to the exponential model we perform a similar computation

$$E[Y(ib)Y(ib + sb)] = \sigma_t^2 \sum_{k=0}^{8R-s} f\left(\left(k + \tfrac{1}{2}\right)b\right) f\left(\left(k + \tfrac{1}{2} + s\right)b\right) =$$

$$4V\lambda\sigma_t^2 e^{\lambda b(s+1)} \sum_{k=0}^{8R-s} \left(1 - \lambda b\left(k + \tfrac{1}{2}\right)\right)\left(1 - \lambda b\left(k + s + \tfrac{1}{2}\right)\right) e^{-2\lambda bk}.$$

This series is possible to calculate by for instance neglecting the influence of the tail of this power series and using the formula for a geometrical series. Since this involves tedious computations we put s = 0 and write instead

$$E[Y(ib)^2] = 4V\lambda\sigma_t^2 e^{-\lambda b} \sum_{k=0}^{8R} \left(1 - \lambda b\left(k + \tfrac{1}{2}\right)\right)^2 e^{-2\lambda bk} = 4V\lambda\sigma_t^2 e^{-\lambda b}\,\Sigma$$

with

---

[14]This equality requires some calculations.

$$\Sigma = \sum_{k=0}^{8R} \left(1 - \lambda b\left(k + \tfrac{1}{2}\right)\right)^2 e^{-2\lambda b k}.$$

Recognizing that this should be equal to V we get the correction factor

$$\left(4\lambda\sigma_t^{\,2} e^{-\lambda b}\,\Sigma\right)^{-1/2}$$

and thus the formula used in HYDRASTAR for simulating one dimensional processes with a covariance function of exponential type is

$$Y(ib) = \sqrt{\frac{V}{\sigma_t^{\,2}\Sigma}} \sum_{k=0}^{8R} \left(1 - \lambda\left(k + \frac{1}{2}\right)b\right) e^{-\lambda k b} t_{k-i}\,. \qquad 5.22$$

where the value of R and the stochastic variables t_k are the same as the ones used in the generation of the spherical model.

5.3 Line generation

Given the possibility to generate the one dimensional processes Y one would then proceed to generate three dimensional realizations from the approximative formula

$$Y(\mathbf{x}) = \frac{1}{\sqrt{N}} \sum_{i=1}^{N} Y_i((\mathbf{x},\mathbf{l}_i),\mathbf{l}_i).$$

Recalling formula 5.2 it would be natural to choose the lines $\mathbf{l}_i$ in an evenly spread fashion over the unit sphere as if evaluating an integral numerically. However it is not easy to identify directions that are evenly distributed on the unit sphere for an arbitrary number of lines. Therefore this method is usually restricted to taking N = 15 lines joining the mid-points of the opposite edges of a regular icosahedron. We will in the following refer to such a set of lines as an icosahedron set. For a discussion on how to do this in practice see [Journel and Huijbregts, 1978, p. 503]. On the other hand writing formula formula 5.2 as

$$C_Y(\xi) = \int_{S_{1/2}} C_1((\xi,\mathbf{l}),\mathbf{l}) f(\mathbf{l}) dS(\mathbf{l}) = E\left[C_1((\xi,\mathbf{l}),\mathbf{l})\right]$$

it suggests drawing the lines randomly from a uniform distribution on the half unit sphere.

A study of the merits of different schemes for line generation has been made by [Tompson, Ababou and Gelhar, 1989] from which the following discussion is inferred.

The use of N = 15 evenly spaced lines reproduces the mean and variance statistics rather well but the realizations show a number of sets of parallel, linelike patterns. The appearance of these is explained by the following reasoning.

In Fig. 5.1 the process of simulating a random function with the turning bands method is depicted in two dimensions and using three lines. It is then clear that when averaging the contributions from the three lines the spatial variability along lines of type A becomes roughly σ if the variability of each line process is σ. However the spatial variability on lines of type B only becomes roughly $2\sigma/3$ since the contribution from the line perpendicular to it, i.e. line 2, is constant in each separate realization. Also the spatial average along the line of type A becomes approximately zero whereas the spatial average along lines of type B is determined by the contribution from line 2.

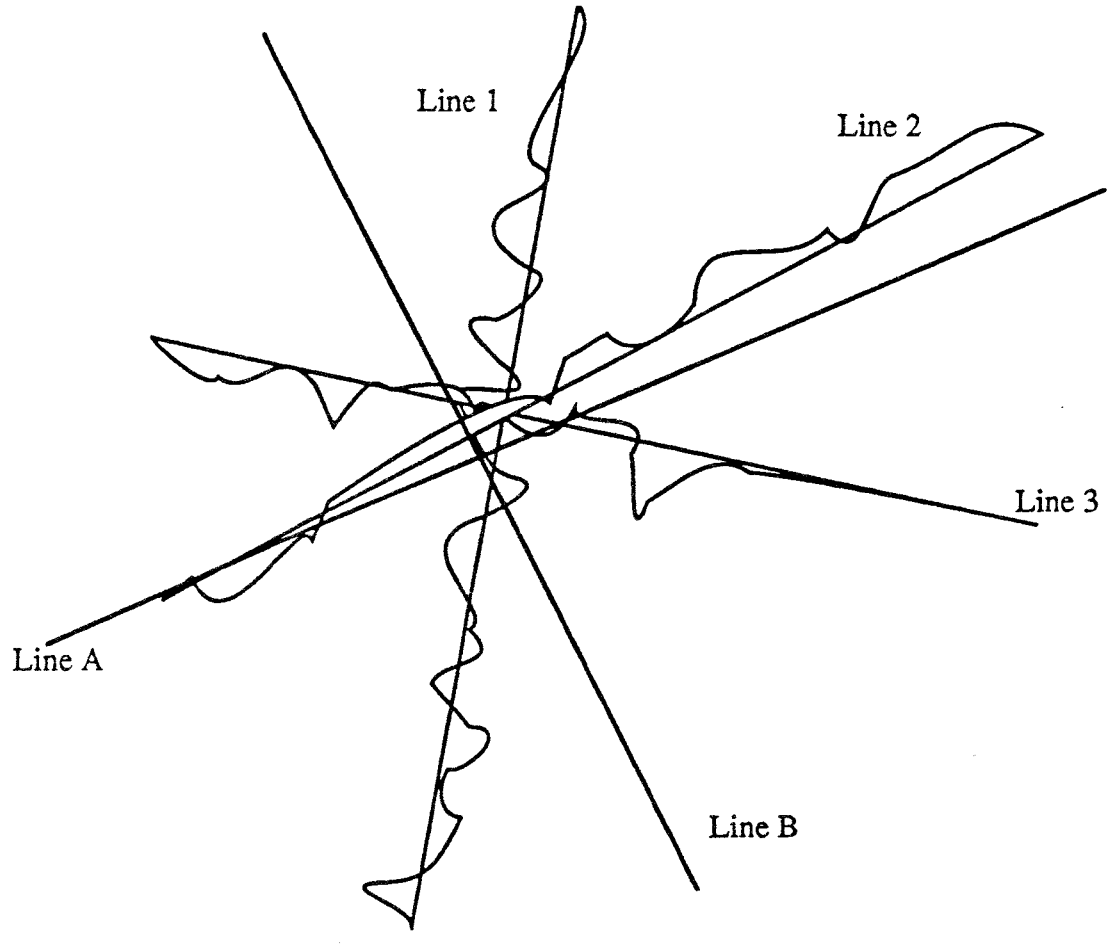

Figure 5.1 *Explaining the origin of linelike patterns.*

It is important to realize that the magnitude of this effect depends on the number of lines and not on their orientation. We will make use of this fact later on.

The alternative approach of using a larger number of randomly chosen lines, N = 100 seems to be the recommended value, removes this effect but will of course increase the computational burden. Also the variability for the covariance estimates, both between different directions of the lag vectors used in the covariance estimation, and between successive runs are increased in comparison with the case of evenly spaced lines.

Thus it seems to be a good idea to use several icosahedron sets all subjected to a random rotation characterized by a rotation vector chosen from a uniform distribution i.e

$$\omega_j = 2\pi U_j \qquad j = 1, 2, 3$$

where U_j is uniformly distributed over [0, 1] and ω_j, j = 1, 2, 3 are the components of the random rotation vector each giving the rotation angle around the j:th coordinate axis. For these reasons the HYDRASTAR can simulate random fields using a combination of random lines and random icosahedron sets. The user requests the number of each that is going to be used. Comparative results of use of different sets of lines can be found in [Norman, 1991]. See also [HYDRASTAR].

6 CONDITIONAL SIMULATIONS

Given is the possibility to simulate realizations from a stationary random field as described in section 5. In order to improve the similarities between these realizations and the structure of the conductivity field given by geological investigations and the packer tests, HYDRASTAR conditions the realizations on the regularized measurement. To clarify, this means that all realizations of the stochastic process simulated with HYDRASTAR attains the measured values at the measurement locations. This chapter contains a description on how this is achieved starting from the beginning with a discussion of kriging. The reader familiar with the theory of kriging can jump directly to section 6.2 perhaps with a glance at section 6.1.4 which includes some information on how HYDRASTAR solves the kriging systems.

6.1 Kriging

Assume that we have a random function Y(**x**) which is known at a number of points, the data support, $\mathbf{x}_i$, i = 1, 2, . . . , N. What is the best linear unbiased estimator Y(**x**)*

$$Y(\mathbf{x})^* = \sum_{i=1}^{N} \lambda_i(\mathbf{x}) Y(\mathbf{x}_i) \qquad 6.1$$

of Y(**x**), given this information, in the sense that the centered variance of the interpolation error i.e.

$$V[(Y(\mathbf{x})^* - Y(\mathbf{x}))] = E\left[(Y(\mathbf{x})^* - Y(\mathbf{x}))^2\right] - E[(Y(\mathbf{x})^* - Y(\mathbf{x}))]^2$$

should be minimal ? Here V[·] is the centered variance operator. The multiplicators $\lambda_i(\mathbf{x})$ appearing in 6.1 will be referred to as the kriging weights at **x**. These are functions of the point of estimation, **x**. The reader is urged to make clear the difference between the estimator Y(**x**)*, which is a stochastic variable, and the estimate y*(**x**) which is a realization of Y(**x**)*. The best estimator of type 6.1 is the so-called kriging estimator and the process of employing it for estimating for instance level curves of a stochastic function is known as kriging.

There are a number of different approaches to this simple problem and we shall consider them one by one.

6.1.1 Residual kriging

Here we assume that the trend, E[Y(**x**)], is known i.e. in some way estimated. We may then work with the residual process Y´(**x**) = Y(**x**) - E[Y(**x**)] only. Since the expectation

of both the residual and any linear estimator of it then becomes zero the centered variance of interpolation error above is written as

$$V\left[(Y'(\mathbf{x})^* - Y'(\mathbf{x}))\right] = E\left[(Y'(\mathbf{x})^* - Y'(\mathbf{x}))^2\right] = \sum_{i,j=1}^{N} \lambda_i(\mathbf{x})\lambda_j(\mathbf{x})C(\mathbf{x}_i - \mathbf{x}_j) - 2\sum_{i=1}^{N}\lambda_i(\mathbf{x})C(\mathbf{x}_i - \mathbf{x}) + C(\mathbf{0})$$

where $C(\cdot)$ is the covariance function for Y and thus $C(\mathbf{0})$ is the variance of Y.

By differentiating with respect to $\lambda_i(\mathbf{x})$ we see that the centered variance is minimized[15] when

$$\sum_{i=1}^{N}\lambda_j(\mathbf{x})C(\mathbf{x}_i - \mathbf{x}_j) = C(\mathbf{x}_i - \mathbf{x}) \qquad i = 1, \ldots N \tag{6.2}$$

which are the so-called kriging equations. Inserting this equality into the above expression for the interpolation error, we obtain the kriging variance as

$$E\left[(Y'(\mathbf{x})^* - Y'(\mathbf{x}))^2\right] = C(\mathbf{0}) - \sum_{i=1}^{n}\lambda_i(\mathbf{x})C(\mathbf{x}_i - \mathbf{x}) .$$

6.1.2 Kriging in the locally stationary case

If one does not know the trend, E[Y(**x**)], or wants to avoid estimating it, one can instead make the assumption that the trend is locally stationary . This means that for the task of determining the best linear estimator of Y at **x**, $Y^*(\mathbf{x})$, one makes the assumption that in a neighbourhood of **x**, the trend E[Y(**x**)] is unknown but approximately equal to a constant. To this neighborhood there corresponds a set D(**x**) of measurement locations defined by the requirement that the points in D(**x**), i.e. $\{\mathbf{x}_i\}_{i\in D(\mathbf{x})}$, belongs to the neighbourhood. The question of finding the best linear unbiased estimator is then restricted to using only points in D(**x**) i.e. $Y(\mathbf{x})^*$ is given by

$$Y(\mathbf{x})^* = \sum_{i\in D(\mathbf{x})} \lambda_i(\mathbf{x})Y(\mathbf{x}_i) . \tag{6.3}$$

The set D(**x**) is usually called a kriging neighbourhood and can also be used, in general, to restrict the size of the kriging equation system by taking only the closest points into account.

---

[15]That this stationary point is in fact a minimum follows, since a covariance function is always positive definite.

With these assumptions we easily see that in order to ensure that the linear estimator should be unbiased, that is have the correct expectation value, we have only to require that

$$\sum_{j \in D(\mathbf{x})} \lambda_j(\mathbf{x}) = 1 \qquad 6.4$$

Next, with this in mind, we can write the centered variance of the interpolation error as

$$V\left[(Y(\mathbf{x})^* - Y(\mathbf{x}))\right] = E\left[(Y(\mathbf{x})^* - Y(\mathbf{x}))^2\right] =$$

$$E\left[\left(\sum_{i \in D(\mathbf{x})} \lambda_i(\mathbf{x}) Y(\mathbf{x}_i) - Y(\mathbf{x})\right)^2\right] =$$

$$E\left[\left(\sum_{i \in D(\mathbf{x})} \lambda_i(\mathbf{x})(Y(\mathbf{x}_i) - m(\mathbf{x}_i)) - (Y(\mathbf{x}) - m(\mathbf{x}))\right)^2\right] =$$

$$\sum_{i,j \in D(\mathbf{x})} \lambda_i(\mathbf{x}) \lambda_j(\mathbf{x}) C(\mathbf{x}_i - \mathbf{x}_j) - 2 \sum_{i \in D(x)} \lambda_i(\mathbf{x}) C(\mathbf{x}_i - \mathbf{x}) + C(\mathbf{0}) \qquad 6.5$$

in principle as before, here as always $m(\mathbf{x}) = E[Y(\mathbf{x})]$. Note the use of the assumption of local stationarity in the first and third equality above i.e. we used

$$m(\mathbf{x}) - \sum_{j \in D(\mathbf{x})} \lambda_i(\mathbf{x}) m(\mathbf{x}_i) = 0 \qquad 6.6$$

which is equivalent with the assumption 6.4 if Y is locally stationary.

The minimization of this interpolation error 6.5 under the constraint of unbiasedness 6.4 is obtained by differentiating the Lagrangian function

$$\sum_{i,j \in D(\mathbf{x})} \lambda_i(\mathbf{x}) \lambda_j(\mathbf{x}) C(\mathbf{x}_i - \mathbf{x}_j) - 2 \sum_{i \in D(\mathbf{x})} \lambda_i(\mathbf{x}) C(\mathbf{x}_i - \mathbf{x}) + C(\mathbf{0}) +$$

$$2\mu(\mathbf{x}) \left[\sum_{j \in D(\mathbf{x})} \lambda_j(\mathbf{x}) - 1\right]$$

which leads to the linear system for determining a stationary point[16]

$$\begin{cases} \sum_{j \in D(\mathbf{x})} \lambda_j(\mathbf{x}) C(\mathbf{x}_i - \mathbf{x}_j) + \mu(\mathbf{x}) = C(\mathbf{x}_i - \mathbf{x}) & i \in D(\mathbf{x}) \\ \sum_{i \in D(\mathbf{x})} \lambda_j(\mathbf{x}) = 1 \end{cases} \qquad 6.7$$

---

[16]Which is also a minimum since if C is positive semi definite it is positive semi definite on any subspace as well.

where $\mu(\mathbf{x})$ is a Lagrange multiplier for the kriging system at $\mathbf{x}$. The interpolation error associated with the above approach is given by inserting the kriging system into the expression for centered variance of the interpolation error 6.5 as

$$E\left[\left(Y(\mathbf{x})^{*} - Y(\mathbf{x})\right)^{2}\right] = C(\mathbf{0}) - \mu(\mathbf{x}) - \sum_{i \in D(\mathbf{x})} \lambda_i(\mathbf{x}) C(\mathbf{x}_i - \mathbf{x}) \quad . \quad 6.8$$

The above approach can be generalized to more general forms of local trend. That is, instead of assuming that the trend is locally constant we may assume another, more complicated form. The most common form of the local trend is a second order polynomial, where we assume that locally the expectation of Y(**x**) is given by

$$E[Y(\mathbf{x})] = m_0 + \mathbf{m}_1 \bullet \mathbf{x} + \mathbf{m}_2 \bullet \mathbf{x}^T \mathbf{x}$$

where m_0 is a constant scalar, $\mathbf{m}_1$ is a constant vector, $\mathbf{m}_2$ a constant symmetric matrix and $\bullet$ signifies the inner (tensor) product [17]. The nonbias equation 6.6 is thus replaced by

$$m_0\left(1 - \sum_{i \in D(\mathbf{x})} \lambda_i(\mathbf{x})\right) + \mathbf{m}_1 \bullet \left(\mathbf{x} - \sum_{i \in D(\mathbf{x})} \lambda_i(\mathbf{x}) \mathbf{x}_i\right) + \mathbf{m}_2 \bullet \left(\mathbf{x}\mathbf{x}^T - \sum_{i \in D(\mathbf{x})} \lambda_i(\mathbf{x}) \mathbf{x}_i \mathbf{x}_i^T\right) = 0$$

or since we want this to hold independent of the choice of m_0, $\mathbf{m}_1$ and $\mathbf{m}_2$ with the ten conditions

$$\begin{cases} 1 - \sum_{j \in D(\mathbf{x})} \lambda_i(\mathbf{x}) = 0 \\ \mathbf{x} - \sum_{j \in D(\mathbf{x})} \lambda_i(\mathbf{x}) \mathbf{x}_i = 0 \\ \mathbf{x}\mathbf{x}^T - \sum_{j \in D(\mathbf{x})} \lambda_i(\mathbf{x}) \mathbf{x}_i \mathbf{x}_i^T = 0 \end{cases}$$

and thus the number of Lagrange multipliers is likewise increased to ten. This is known as universal kriging. The disadvantage of this approach, independent of the number of constants to describe the trend (also in the main case of one constant above), is that one

---

[17]The inner matrix (tensor) product is defined as: Let $\mathbf{S}_1$ and $\mathbf{S}_2$ be two arbitrary NxM matrices then their inner product **S** is given by

$$\mathbf{S} = \sum_{i=1}^{N} \sum_{j=1}^{M} S_{1_{i,j}} S_{2_{i,j}}$$

must estimate the form of the covariance function of the residuals. First of all this is a difficult task and secondly, if one completes the task, one obtains the trend as a part of the result. See for instance [de Marsily, 1986, pp 310-312].

6.1.3 Kriging in the intrinsic case

When using intrinsic random functions in relation to kriging, one usually assumes that 3.2 i.e

$$E[Y(\mathbf{x}+\xi) - Y(\mathbf{x})] = 0$$

holds only locally. This equation is equivalent to the corresponding assumption made on the expectations in the section above.

To derive the kriging system in this case one first notes that the condition for unbiasedness again becomes

$$\sum_{j \in D(\mathbf{x})} \lambda_j(\mathbf{x}) = 1 \qquad 6.9$$

And because of this, one may express the (centered) variance of the kriging error as

$$V[(Y(\mathbf{x})^* - Y(\mathbf{x}))] = E\left[(Y(\mathbf{x})^* - Y(\mathbf{x}))^2\right] =$$

$$E\left[\left(\sum_{i \in D(\mathbf{x})} \lambda_i(\mathbf{x}) Y(\mathbf{x}_i) - Y(\mathbf{x})\right)^2\right] =$$

$$E\left[\left(\sum_{i \in D(\mathbf{x})} \lambda_i(\mathbf{x})[Y(\mathbf{x}_i) - Y(\mathbf{x})]\right)^2\right] =$$

$$\sum_{i,j \in D(\mathbf{x})} \lambda_i(\mathbf{x})\lambda_j(\mathbf{x}) E\left[(Y(\mathbf{x}_i) - Y(\mathbf{x}))(Y(\mathbf{x}_j) - Y(\mathbf{x}))\right]$$

Now what is needed is the following observation

$$2(Y(\mathbf{x}_i) - Y(\mathbf{x}))(Y(\mathbf{x}_j) - Y(\mathbf{x})) =$$

$$(Y(\mathbf{x}_i) - Y(\mathbf{x}))^2 + (Y(\mathbf{x}_j) - Y(\mathbf{x}))^2 - (Y(\mathbf{x}_i) - Y(\mathbf{x}_j))^2$$

Making use of this identity we can express the variance of the interpolation error in terms of the semivariogram γ as

$$2\sum_{i \in D(\mathbf{x})} \lambda_i(\mathbf{x})\gamma(\mathbf{x}_i - \mathbf{x}) - \sum_{i,j \in D(\mathbf{x})} \lambda_i(\mathbf{x})\lambda_j(\mathbf{x})\gamma(\mathbf{x}_i - \mathbf{x}_j)$$

and differentiation of the corresponding Lagrangian function, incorporating the side condition 6.9, with respect to the kriging weights gives the kriging system

$$\begin{cases} \sum_{j \in D(\mathbf{x})} \lambda_j(\mathbf{x})\gamma(\mathbf{x}_i - \mathbf{x}_j) - \mu(\mathbf{x}) = \gamma(\mathbf{x}_i - \mathbf{x}) & i \in D(\mathbf{x}) \\ \sum_{i \in D(\mathbf{x})}^{n} \lambda_j(\mathbf{x}) = 1 \end{cases} \quad . \qquad 6.10$$

where $\mu(\mathbf{x})$ again is a Lagrange multiplier for the kriging system at $\mathbf{x}$.

The interest in this derivation is mainly in the differences as compared to the derivation for the locally constant case. The kriging variance is obtained as previously by inserting the kriging system into the expression for the variance of the interpolation error to give

$$\sum_{i \in D(\mathbf{x})} \lambda_i(\mathbf{x})\gamma(\mathbf{x}_i - \mathbf{x}) - \mu(\mathbf{x}) \quad .$$

For an alternative and more elegant derivation of the results of this section see appendix C.

6.1.4 Solution of the kriging equations

First of all let us stress the fact that any covariance matrix $\mathbf{C} = \{C(\mathbf{x}_i - \mathbf{x}_j)\}_{i,j}$ is positive semidefinite, a fact that we have already used extensively. This is easily seen since

$$\lambda^T \mathbf{C}\lambda = \sum_{1 \le i,j \le n} \lambda_i C_Y(\mathbf{x}_i - \mathbf{x}_j)\lambda_j = V\left[\sum_{1 \le i \le n} \lambda_i Y(\mathbf{x}_i)\right] \ge 0$$

This is an important quality to keep when solving the kriging system. Now the kriging matrix i.e. the matrix in the solution in the kriging system 6.7 or its corresponding generalization to universal kriging is

$$\mathbf{D} = \begin{bmatrix} \mathbf{C} & \mathbf{X} \\ \mathbf{X}^T & 0 \end{bmatrix} \qquad 6.11$$

or in the case 6.10 [18]

$$\mathbf{D} = \begin{bmatrix} \Gamma & \mathbf{X} \\ \mathbf{X}^T & 0 \end{bmatrix} \qquad 6.12$$

are both indefinite and thus it is good strategy to write the solution of the kriging system

---

[18] Or its generalization to intrinsic random functions of order higher than zero,see Appendix C.

$$\mathbf{D}\begin{bmatrix} \lambda(\mathbf{x}) \\ \mu(\mathbf{x}) \end{bmatrix} = \begin{bmatrix} \mathbf{c}(\mathbf{x}) \\ 1 \end{bmatrix} \qquad 6.13$$

or

$$\mathbf{D}\begin{bmatrix} \lambda(\mathbf{x}) \\ \mu(\mathbf{x}) \end{bmatrix} = \begin{bmatrix} \gamma(\mathbf{x}) \\ 1 \end{bmatrix} \qquad 6.14$$

in terms of the inverse of the covariance matrix, $\mathbf{C}^{-1}$. In the first case 6.11 we note that

$$\mathbf{D} = \begin{bmatrix} \mathbf{C} & \mathbf{X} \\ \mathbf{X}^T & \mathbf{0} \end{bmatrix} = \begin{bmatrix} \mathbf{C} & \mathbf{0} \\ \mathbf{X}^T & -\mathbf{X}^T\mathbf{C}^{-1}\mathbf{X} \end{bmatrix} \begin{bmatrix} \mathbf{I} & \mathbf{C}^{-1}\mathbf{X} \\ \mathbf{0} & \mathbf{I} \end{bmatrix}$$

and thus the solution to the kriging system 6.13 can be written

$$\mu = \frac{1 - \mathbf{X}^T\mathbf{C}^{-1}\mathbf{c}(\mathbf{x})}{s}$$

$$\lambda(\mathbf{x}) = \mathbf{C}^{-1}\mathbf{c}(\mathbf{x}) - \mu\mathbf{w}$$

where we introduced

$$\mathbf{w} = \mathbf{C}^{-1}\mathbf{X}$$

$$s = -\mathbf{X}^T\mathbf{C}^{-1}\mathbf{X}.$$

We call the vector **w** the "Lagrange correction vector" since it arises from the Lagrange multiplier formulation of the minimum variance formulation above.

In the case 6.12, where the matrix Γ results from a semivariogram without a sill, a pseudo covariance [Journel and Huijbregts, 1978, p 306] $C_p(\mathbf{x})$ is defined by

$$\gamma(\xi) = C_0 - C_p(\xi)$$

and thus

$$\mathbf{C}_p = C_0\mathbf{1}\mathbf{1}^T - \Gamma \qquad 6.15$$

where C_0 is a constant greater than the maximum element of Γ, 1 is a vector with all components equal 1 and superindex T denotes matrix transpose. Note however that it is not certain that the resulting matrix is positive definite.

6.2 Construction of conditional simulations

The idea used to construct conditional simulations is to simulate the kriging error. Let $Z(\mathbf{x})$ be a process independent of, but with the same covariance function as $Y(\mathbf{x})$ and regard the process

$$Y_s(\mathbf{x}) = Y(\mathbf{x})^* + Z(\mathbf{x}) - Z(\mathbf{x})^*.$$

We want to show that this process has the same moments as Y(**x**). The following discussion follows the lines in [Journel and Huijbregts,1978, p 494-498].

6.2.1 The residual case

Dropping the primes and just remembering that we work with residual quantities with zero expectation we note that

$$E[Y_s(\mathbf{x})] = E[Y(\mathbf{x})] = 0.$$

Secondly since Z(**x**) and Y(**x**) are independent and E[Z(**x**) - Z*(**x**)] = E[Y(**x**)] = 0 we have

$$E[Y_s(\mathbf{x})Y_s(\xi)] = E[Y(\mathbf{x})^*Y(\xi)^*] + E[(Z(\mathbf{x}) - Z(\mathbf{x})^*)(Z(\xi) - Z(\xi)^*)]$$

whereas

$$E[Y(\mathbf{x})Y(\xi)] = E[Y(\mathbf{x})^*Y(\xi)^*] + E[(Y(\mathbf{x}) - Y(\mathbf{x})^*)(Y(\xi) - Y(\xi)^*)] +$$
$$E[Y(\mathbf{x})^*(Y(\xi) - Y(\xi)^*)] + [E(Y(\mathbf{x}) - Y(\mathbf{x})^*)Y(\xi)^*].$$

So we see that what is needed for equality of the second order moment is that Y(**x**)* and Z(**x**) - Z(**x**)* are orthogonal. In the residual case this is easy

$$E[Y(\mathbf{x})^*(Y(\xi) - Y(\xi)^*)] =$$
$$\sum_{i=1}^{n}\lambda_i(\mathbf{x})C(\mathbf{x}_i - \xi) - \sum_{i,j=1}^{n}\lambda_i(\mathbf{x})\lambda_j(\xi)C(\mathbf{x}_i - \mathbf{x}_j) =$$
$$\sum_{i=1}^{n}\lambda_i(\mathbf{x})\left[C(\mathbf{x}_i - \xi) - \sum_{j=1}^{n}\lambda_j(\xi)C(\mathbf{x}_i - \mathbf{x}_j)\right] = 0$$

since the λ(ξ):s satisfies the kriging equations.[19]

6.2.2 Locally constant case

It is clear from the nonbias condition 6.4 that

$$E[Y_s(\mathbf{x})] = E[Y(\mathbf{x})] = m(\mathbf{x}).$$

---

[19]We note that this is a direct consequence of Hilbert space theory if one considers the Hilbert space $L^2(\Omega, \aleph, P)$ with Ω, ℵ, P signifying the event space, the σ-algebra and the probability measure respectively and the scalar product being defined as (Y(**x**), Y(ξ)) = E[Y(**x**), Y(ξ)], see [Journel ,1977].

For the second order moment we can write again since Z(**x**)and Y(**x**) are independent

$$E\left[(Y_s(\mathbf{x}) - m(\mathbf{x}))(Y_s(\xi) - m(\xi))\right] =$$

$$E\left[(Y(\mathbf{x})^* - m(\mathbf{x}))(Y(\xi)^* - m(\xi))\right] +$$

$$E\left[(Z(\mathbf{x}) - Z(\mathbf{x})^*)(Z(\xi) - Z(\xi)^*)\right]$$

whereas

$$E\left[(Y(\mathbf{x}) - m(\mathbf{x}))(Y(\xi) - m(\xi))\right] =$$

$$E\left[(Y(\mathbf{x})^* - m(\mathbf{x}))(Y(\xi)^* - m(\xi))\right] + E\left[(Y(\mathbf{x}) - Y(\mathbf{x})^*)(Y(\xi) - Y(\xi)^*)\right] +$$

$$E\left[(Y(\mathbf{x})^* - m(\mathbf{x}))(Y(\xi) - Y(\xi)^*)\right] + E\left[(Y(\xi)^* - m(\xi))(Y(\mathbf{x}) - Y(\mathbf{x})^*)\right]$$

which does not become identical to the expression for the simulated field since

$$E\left[(Y(\mathbf{x})^* - m(\mathbf{x}))(Y(\xi) - Y(\xi)^*)\right] = E\left[Y'(\mathbf{x})^*(Y'(\xi) - Y'(\xi)^*)\right] =$$

$$\sum_{i \in D(\mathbf{x})} \lambda_i(\mathbf{x}) C(\mathbf{x}_i - \xi) - \sum_{i \in D(\mathbf{x}),\, j \in D(\xi)} \lambda_i(\mathbf{x}) \lambda_j(\xi) C(\mathbf{x}_i - \mathbf{x}_j) =$$

$$\sum_{i \in D(\mathbf{x})} \lambda_i(\mathbf{x}) \left[C(\mathbf{x}_i - \xi) - \sum_{j \in D(\xi)} \lambda_j(\xi) C(\mathbf{x}_i - \mathbf{x}_j) \right] = \mu(\xi) \sum_{i \in D(\mathbf{x})} \lambda_i(\mathbf{x}) \qquad 6.16$$

Note that we have tacitly used 6.6 twice in the first equality above. Similarly by just interchanging **x** with ξ in 6.16

$$E\left[(Y(\xi)^* - m(\xi))(Y(\mathbf{x}) - Y(\mathbf{x})^*)\right] =$$

$$\sum_{i \in D(\xi)} \lambda_i(\xi) \left[C(\mathbf{x}_i - \mathbf{x}) - \sum_{j \in D(\mathbf{x})} \lambda_j(\mathbf{x}) C(\mathbf{x}_i - \mathbf{x}_j) \right] = \mu(\mathbf{x}) \sum_{i \in D(\xi)} \lambda_i(\xi)$$

hence the difference between the covariance function of simulated field $Y_S(\mathbf{x})$ and the covariance function of the actual field Y(**x**) is

$$\mu(\mathbf{x}) \sum_{i \in D(\xi)} \lambda_i(\xi) + \mu(\xi) \sum_{i \in D(\xi)} \lambda_i(\mathbf{x}) = \mu(\mathbf{x}) + \mu(\xi) \,.$$

However, let us view the variogram of the simulated fields

$$E\left[(Y_s(\mathbf{x}) - Y_s(\xi))^2\right] =$$

$$E\left[(Y(\mathbf{x})^* - Y(\xi)^*)^2\right] + E\left[((Z(\mathbf{x}) - Z(\mathbf{x})^*) - (Z(\xi) - Z(\xi)^*))^2\right]$$

whereas

$$E\left[(Y(\mathbf{x}) - Y(\xi))^2\right] =$$

$$E\left[\left(Y(\mathbf{x})^{*}-Y(\xi)^{*}\right)^{2}\right]+E\left[\left(\left(Y(\mathbf{x})-Y(\mathbf{x})^{*}\right)-\left(Y(\xi)-Y(\xi)^{*}\right)\right)^{2}\right]+$$

$$2E\left[\left(Y(\mathbf{x})^{*}-Y(\xi)^{*}\right)\left(\left(Y(\mathbf{x})-Y(\mathbf{x})^{*}\right)-\left(Y(\xi)-Y(\xi)^{*}\right)\right)\right]$$

which is equal to the variogram of the simulated field since we have by 6.16

$$E\left[\left(Y(\mathbf{x})^{*}-Y(\xi)^{*}\right)\left(\left(Y(\mathbf{x})-Y(\mathbf{x})^{*}\right)-\left(Y(\xi)-Y(\xi)^{*}\right)\right)\right]=$$

$$\mu(\mathbf{x})\sum_{i\in D(\mathbf{x})}\lambda_i(\mathbf{x})-\mu(\xi)\sum_{i\in D(\mathbf{x})}\lambda_i(\mathbf{x})-\mu(\mathbf{x})\sum_{i\in D(\xi)}\lambda_i(\xi)+\mu(\xi)\sum_{i\in D(\xi)}\lambda_i(\xi)=0$$

Hence the variograms for Y and Y_S are equal but the covariances are not. Here one may think that there is a contradiction since variograms and covariances are coupled through the identity 3.3. However the explanation is simple, by 6.8 we know that

$$E\left[\left(Y(\mathbf{x})^{*}-Y(\mathbf{x})\right)^{2}\right]=C(\mathbf{0})-\mu(\mathbf{x})-\sum_{i\in D(\mathbf{x})}\lambda_i(\mathbf{x})C(\mathbf{x}_i-\mathbf{x})$$

and in general for locally constant stochastic functions

$$E\left[\left(Y(\mathbf{x})^{*}-m(\mathbf{x})\right)^{2}\right]=\sum_{i,j\in D(\mathbf{x})}\lambda_i(\mathbf{x})\lambda_j(\mathbf{x})C(\mathbf{x}_i-\mathbf{x}_j)=\sum_{i\in D(\mathbf{x})}\lambda_i(\mathbf{x})C(\mathbf{x}_i-\mathbf{x})-\mu(\mathbf{x})$$

so that

$$E\left[\left(Y(\mathbf{x})^{*}-m(\mathbf{x})\right)^{2}\right]+E\left[\left(Y(\mathbf{x})^{*}-Y(\mathbf{x})\right)^{2}\right]=C(\mathbf{0})-2\mu(\mathbf{x}).$$

Thus the simulated field does not have the same variance as the original field and moreover the simulated fields are not stationary but they are intrinsic and have the same semivariogram as the original.

7 THE HYDROLOGY EQUATION AND ITS NUMERICAL SOLUTION

The hydrology equation solved by HYDRASTAR is

$$\nabla\left(K_s(\mathbf{x})\nabla\langle h\rangle^s(\mathbf{x})\right) = 0 \qquad 7.1$$

where K_S is the isotropic hydraulic conductivity at the averaging scale s and $\langle h\rangle^s$ is the averaged hydraulic head i.e.

$$\langle h\rangle^s(\mathbf{x}) = \frac{1}{\left|V_s(\mathbf{x}) \cap \Omega_f\right|} \int_{V_s(\mathbf{x})\cap\Omega_f} h(\xi)\,d\xi$$

where Ω_f is the void space i.e. the fractures, $V_S(\mathbf{x})$ is the averaging volume and $|\cdot|$ is a general notation for volume, or size, of a set. For more details on this see for example chapter 3 and 4 in [de Marsily, 1986].

The corresponding integral equation is

$$\int_S K_s(\xi)\nabla\langle h\rangle^s(\xi)\,d\mathbf{S}(\xi) = 0 \qquad 7.2$$

where S is the surface of an arbitrary volume V and dS its directed surface differential.

The integral equation above is solved numerically by a finite difference approximation derived from the specialization of 7.2 to parallelepipeds. These parallelepipeds are referred to as the mass balance elements and their boundary surface consists of six rectangular faces. This is represented by a staggered prismatic mesh, that is the head nodes are situated at the midpoint of the parallelepipeds and are given by

$$(i_1 - 1)\mathbf{s}_1 + (i_2 - 1)\mathbf{s}_2 + (i_3 - 1)\mathbf{s}_3 \qquad 1 \le i_k \le N_k,\ k = 1,2,3 \qquad 7.3$$

where $\mathbf{s}_j$, j = 1, 2, 3 are the basis vectors of the prismatic mesh and N_k are the number of head nodes in the direction k, k = 1, 2, 3. The conductivities are given on the translated nodes situated on the faces of the parallelepipeds i.e. at

$$\begin{cases} \left(i_1 - \frac{1}{2}\right)\mathbf{s}_1 + (i_2 - 1)\mathbf{s}_2 + (i_3 - 1)\mathbf{s}_3 & 1 \le i_1 \le N_1 - 1,\ 1 \le i_k \le N_k,\ k = 2,3 \\ (i_1 - 1)\mathbf{s}_1 + \left(i_2 - \frac{1}{2}\right)\mathbf{s}_2 + (i_3 - 1)\mathbf{s}_3 & 1 \le i_2 \le N_2 - 1,\ 1 \le i_k \le N_k,\ k = 1,3 \\ (i_1 - 1)\mathbf{s}_1 + (i_2 - 1)\mathbf{s}_2 + \left(i_3 - \frac{1}{2}\right)\mathbf{s}_3 & 1 \le i_3 \le N_3 - 1,\ 1 \le i_k \le N_k,\ k = 1,2 \end{cases}$$

7.4

The values of the conductivities at these nodes are denoted

$$\begin{cases} K_1(i_1, i_2, i_3) & 1 \le i_1 \le N_1 - 1,\ 1 \le i_k \le N_k,\ k = 2,3 \\ K_2(i_1, i_2, i_3) & 1 \le i_2 \le N_2 - 1,\ 1 \le i_k \le N_k,\ k = 1,3 \\ K_3(i_1, i_2, i_3) & 1 \le i_3 \le N_3 - 1,\ 1 \le i_k \le N_k,\ k = 1,2 \end{cases}$$

respectively. See Fig. 7.1 where the computational molecule is depicted.

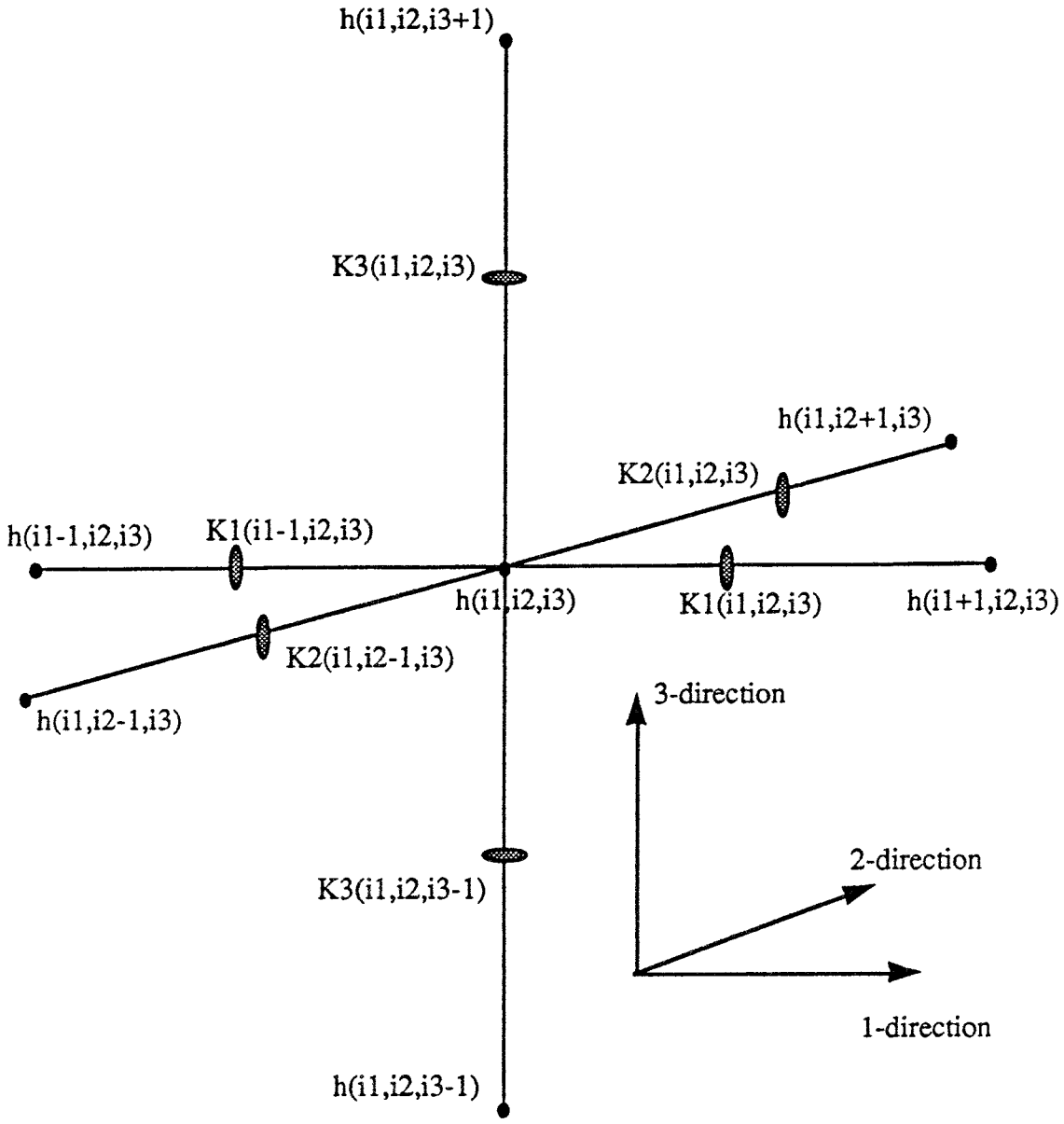

Figure 7.1 *The computational molecule for the hydrology equation 7.1 employed in HYDRASTAR.*

The advantage with a staggered mesh is threefold, all resulting from the absence of the need for interpolation of conductivity values. First a, admittedly minor, speed increase results in the solver as a result of the fact that no interpolation takes place. Secondly, there is no uncontrolled smoothing of the simulated conductivity field which would result

from interpolation. Finally, one avoids a somewhat arbitrary choice of interpolation formula. The obvious disadvantage is the increased need for storage since the number of conductivity nodes are, in principle, three times the number of head nodes. Another less obvious disadvantage is a more complicated situation when designing the streamline algorithm, see chapter 8.

From these meshes the finite difference equation at the node (i_1, i_2, i_3), $2 \le i_j \le N_j - 1$ resulting from 7.1 is written

$$\begin{aligned} &T_1(i_1 - 1, i_2, i_3)h(i_1 - 1, i_2, i_3) + T_1(i_1, i_2, i_3)\, h(i_1 + 1, i_2, i_3) + \\ &T_2(i_1, i_2 - 1, i_3)h(i_1, i_2 - 1, i_3) + T_2(i_1, i_2, i_3)\, h(i_1, i_2 + 1, i_3) + \\ &T_3(i_1, i_2, i_3 - 1)h(i_1, i_2, i_3 - 1) + T_3(i_1, i_2, i_3)\, h(i_1, i_2, i_3 + 1) - \\ &D(i_1, i_2, i_3)\, h(i_1, i_2, i_3) = 0 \end{aligned} \qquad 7.5$$

where

$$\begin{cases} T_1(i_1, i_2, i_3) = \dfrac{S_2 S_3}{S_1} K_1(i_1, i_2, i_3) \\ T_2(i_1, i_2, i_3) = \dfrac{S_1 S_3}{S_2} K_2(i_1, i_2, i_3) \\ T_3(i_1, i_2, i_3) = \dfrac{S_1 S_2}{S_3} K_3(i_1, i_2, i_3) \end{cases}, \qquad 7.6$$

$s_j = |s_j|$ for $j = 1,2,3$ and

$$\begin{aligned} &D(i_1, i_2, i_3) = T_1(i_1 - 1, i_2, i_3) + T_1(i_1, i_2, i_3) + \\ &T_2(i_1, i_2 - 1, i_3) + T_2(i_1, i_2, i_3) + T_3(i_1, i_2, i_3 - 1) + T_3(i_1, i_2, i_3) \end{aligned} \qquad 7.7$$

These equations are then solved employing a conjugate gradient algorithm, see for instance [Golub and van Loan, p 353 - 380]. Comparisons with other FD codes as well as with FEM codes and analytical solutions are to be found in [Norman, 1991].

Finally, after the solution for the hydraulic head has been obtained the Darcy velocities may be approximately calculated as

$$
\begin{cases}
U_1(i_1, i_2, i_3) = -K(i_1, i_2, i_3)\dfrac{h(i_1+1, i_2, i_3) - h(i_1, i_2, i_3)}{s_1} \\
\qquad\qquad \text{for} \quad 1 \le i_1 \le N_1 - 1,\ 1 \le i_k \le N_k,\ k = 2,3 \\
U_2(i_1, i_2, i_3) = -K(i_1, i_2, i_3)\dfrac{h(i_1, i_2+1, i_3) - h(i_1, i_2, i_3)}{s_2} \\
\qquad\qquad \text{for} \quad 1 \le i_2 \le N_2 - 1,\ 1 \le i_k \le N_k,\ k = 1,3 \\
U_3(i_1, i_2, i_3) = -K(i_1, i_2, i_3)\dfrac{h(i_1, i_2, i_3+1) - h(i_1, i_2, i_3)}{s_3} \\
\qquad\qquad \text{for} \quad 1 \le i_3 \le N_3 - 1,\ 1 \le i_k \le N_k,\ k = 1,2
\end{cases}
\qquad 7.8
$$

i.e calculated by the same difference formula that is used to derive the massbalance equations.

8 BOUNDARY CONDITIONS

Given is the method to simulate the hydraulic conductivity field and the method to solve a certain hydrology equation as described in sections 5, 6 and 7 respectively. With known boundary conditions, the solution would be straight-forward. However, this is not the case. Ordinarily one then tries to make some plausible guesses which are mainly based on two grounds:

- a groundwater divide is identified which leads to the assumption of no flow boundary conditions. A groundwater divide is a valley (discharge area) or a ridge (recharge area).
- a fracture zone with "high conductivity" is inferred. This leads to the assumption of constant head along the fracture zone and not no flow boundaries unless the fracture zone is also considered as a groundwater divide.

These ways of inferring boundary conditions may of course lead to serious misjudgment of the flow situation at depth as discussed in [Nyberg and Voss, 1991]. The problem can be summarized by stating that the boundary conditions can be reasonably well described by the above considerations close to the ground surface. However, at large depths the boundary conditions are subjected to a very large uncertainty. Stated in another fashion it is to say that the recharge and discharge areas of the repository may be located very much outside the domain used for hydrological modelling. This may be due to either large scale topographical qualities or large scale hydrological structures.

The choice of boundary conditions also has a direct influence on the kind of information to be obtained from calculating the stream lines. From a safety analysis point of view, one of the prime outputs must be the travel time of water particles from the repository to the biosphere, that is the surface. If we use head boundary conditions the normal case is that the stream lines end at the lateral boundaries and thus the information obtained is that "the travel time to the biosphere is larger that T". To choose head boundary conditions is natural when using a stochastic approach since the hydraulic head is a stochastic function involved in the analysis and can thus be subjected to uncertainty analysis. On the other hand choosing no flow boundary conditions leads automatically to a situation where all particles reach the surface. This is a fact that may steer the modelers choice of boundary conditions toward no flow type even if it is not justified on other grounds.

The nonflexible mesh in HYDRASTAR prevents any direct application of the tricks mentioned above and the restrictions of time prevented the development of the method that takes the uncertainty of the boundary condition into account systematically. This is why the current solution in HYDRASTAR is to take the boundary conditions from a

deterministic hydrology simulation in a block including the computational parallelepiped and using plausible boundary conditions in that outer block. There are a number of disadvantages

- the uncertainty of the boundary conditions cannot be taken into account systematically but only through explicit variations in the modelling of the outer block.
- the procedure is not mathematically sound since even if the head values are transferred there may well exist discontinuities in the velocity field.

There also exist some supplementary methods in HYDRASTAR to generate the boundary conditions namely to calculate them from a given function or to specify noflow conditions at any side of the computational parallelepiped.

9 STREAM LINE EQUATION SOLVER

The support for transport modelling given from HYDRASTAR is the possibility to calculate stream lines and groundwater travel times to the boundaries. This chapter contains a description of the stream line equation solver as implemented in HYDRASTAR.

Introducing $\mathbf{r}(t)$ for the location of a water particle[20] at time t initially at $\mathbf{r}(0)$ and $\mathbf{u}(\mathbf{x})$ for the pore velocity at the point $\mathbf{x}$ the stream line equation is

$$\frac{d\mathbf{r}}{dt} = \mathbf{u}(\mathbf{r}(t)) \qquad 9.1$$

Finding the stream lines and thereby the associated ground water travel times thus consists of two main parts:

1) Calculate the pore velocity field $\mathbf{u}(\mathbf{x})$ given the head field computed according to section 7. In practice, that amounts to first calculate the Darcy velocity $\mathbf{U}$ by a finite difference approximation in points defined by the mesh according to 7.8, divide by the flow porosity ε_f to obtain the pore velocity and then choose an interpolation for each of the three pore velocity components.

2) Use a suitable method for numerical integration of the streamline equation 9.1.

9.1 Interpolation

This paragraph solely treats the interpolation of the 1- component of the pore velocity field. The 2- and 3- components are treated analogously.

Take any point $\mathbf{r}$, with components r_1, r_2 and r_3 , in space such that

$$\begin{cases} \frac{1}{2}s_1 \le r_1 < \left(N_1 - \frac{3}{2}\right)s_1 \\ s_2 \le r_2 < (N_2 - 2)s_2 \\ s_3 \le r_3 < (N_3 - 2)s_3 \end{cases} \qquad 9.2$$

where N_k, k = 1,2,3, as before are the number of head nodes in the k:th coordinate direction and s_k, k = 1,2,3 is the distance between two consecutive head nodes in the k:th coordinate direction.

Obviously the point $\mathbf{r}$ belongs to a set of the type

---

[20]For an elaboration on this concept see, for instance, [Bear, p 16-18].

$$\begin{cases} (i_1 - \frac{1}{2})s_1 \le r_1 < (i_1 + \frac{1}{2})s_1 \\ (i_2 - 1)s_2 \le r_2 < i_2 s_2 \\ (i_3 - 1)s_3 \le r_3 < i_3 s_3 \end{cases} \qquad 9.3$$

for some values of the integers i_1, i_2, i_3 such that

$$\begin{cases} 1 \le i_1 \le N_1 - 2 \\ 2 \le i_2 \le N_2 - 2 \\ 2 \le i_3 \le N_3 - 2 \end{cases}.$$

In fact it is easy to see that

$$i_1 = \begin{cases} \text{int}\left(\frac{r_1}{s_1} + \frac{1}{2}\right) & \text{if } \frac{r_1}{s_1} + \frac{1}{2} \ge 0 \\ \text{int}\left(\frac{r_1}{s_1} - \frac{1}{2}\right) & \text{if } \frac{r_1}{s_1} + \frac{1}{2} < 0 \end{cases}$$

$$i_2 = \begin{cases} \text{int}\left(\frac{r_2}{s_2} + 1\right) & \text{if } \frac{r_2}{s_2} + 1 \ge 0 \\ \text{int}\left(\frac{r_2}{s_2}\right) & \text{if } \frac{r_2}{s_2} + 1 < 0 \end{cases}$$

$$i_3 = \begin{cases} \text{int}\left(\frac{r_3}{s_3} + 1\right) & \text{if } \frac{r_3}{s_3} + 1 \ge 0 \\ \text{int}\left(\frac{r_3}{s_3}\right) & \text{if } \frac{r_3}{s_3} + 1 < 0 \end{cases} \qquad 9.4$$

give these values. Here the lower alternatives in each formula are given for completeness.

A set such as 9.3 is named a computational cell for the 1 - velocity see figure 9.1. Denoting, in the obvious fashion, the 1-velocities in the eight corners of this cell by $v_{i,j,k}$ where i,j,k takes the values 0 or 1 we write the interpolation polynomial employed, v, as

$$v(x_1, x_2, x_3) = \frac{1}{s_1 s_2 s_3}($$

$$v_{0,0,0}(s_1 - x_1)(s_2 - x_2)(s_3 - x_3) +$$

$$v_{1,0,0}x_1(s_2 - x_2)(s_3 - x_3) +$$

$$v_{0,1,0}(s_1 - x_1)x_2(s_3 - x_3) +$$

$$v_{0,0,1}(s_1 - x_1)(s_2 - x_2)x_3 +$$

$$v_{1,1,0}x_1x_2(s_3 - x_3) +$$

$$v_{1,0,1}x_1(s_2 - x_2)x_3 +$$

$$v_{0,1,1}(s_1 - x_1)x_2x_3 +$$

$$v_{1,1,1}x_1x_2x_3) \qquad 9.5$$

Here we also introduced the local coordinates x_1, x_2 and x_3. These are defined by shifting the origin to the 1-velocity node with the smallest indices of all the 1-velocity nodes constituting the computational cell i.e the node with indices given by 9.4. Using this formula we may express the local coordinates as

$$\begin{cases} x_1 = \begin{cases} r_1 - \left[\text{int}\left(\frac{r_1}{s_1} + \frac{1}{2}\right) - \frac{1}{2}\right]s_1 & \text{if } \frac{r_1}{s_1} + \frac{1}{2} \geq 0 \\ r_1 - \left[\text{int}\left(\frac{r_1}{s_1} - \frac{1}{2}\right) - \frac{1}{2}\right]s_1 & \text{if } \frac{r_1}{s_1} + \frac{1}{2} < 0 \end{cases} \\ x_2 = \begin{cases} r_2 - \left[\text{int}\left(\frac{r_2}{s_2}\right)\right]s_2 & \text{if } \frac{r_2}{s_2} + 1 \geq 0 \\ r_2 - \left[\text{int}\left(\frac{r_2}{s_2}\right) - 1\right]s_2 & \text{if } \frac{r_2}{s_2} + 1 < 0 \end{cases} \\ x_3 = \begin{cases} r_3 - \left[\text{int}\left(\frac{r_3}{s_3}\right)\right]s_3 & \text{if } \frac{r_3}{s_3} + 1 \geq 0 \\ r_3 - \left[\text{int}\left(\frac{r_3}{s_3}\right) - 1\right]s_3 & \text{if } \frac{r_3}{s_3} + 1 < 0 \end{cases} \end{cases}$$

Clearly this polynomial is an interpolating polynomial and moreover using this formulae in each computational cell we obtain a continuous 1-velocity field in the domain given by 9.2. Outside this domain no particle tracking takes place. The reason for not using the whole domain i.e.

$$\begin{cases} \frac{1}{2}s_1 \leq r_1 \leq \left(N_1 - \frac{3}{2}\right)s_1 \\ 0 \leq r_2 \leq (N_2 - 1)\, s_2 \\ 0 \leq r_3 \leq (N_3 - 1)\, s_3 \end{cases}$$

is that on the boundary the velocities are not subjected to the requirement of mass balance as expressed by 7.2 and 7.5 but results directly from the given head boundary conditions and the simulated conductivities on the boundary.

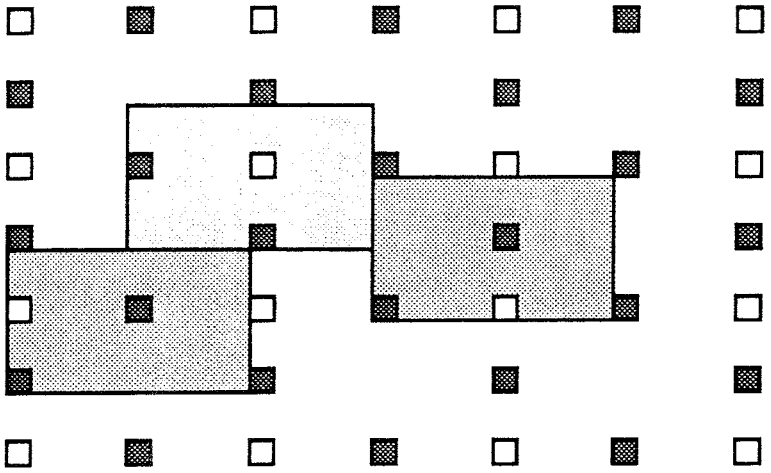

Figure 9.1 *Showing the staggered mesh. The symbols □, ■ and ■ signifies a head, 1-velocity and 2-velocity node respectively, all placed in the lower left corner of the symbol. The rectangles with marking ▭, ▭ and ▭ mark a mass balance element and computational cells for the 1- and 2- velocities respectively.*

We point out that the choice of this particular interpolating polynomial has the following qualities:

- The velocity field is continuous.
- In general the interpolated velocity field **u** does not satisfy $\nabla \mathbf{u} = 0$.

Finally, in this section, we insert a short discussion of other interpolation schemes not implemented in HYDRASTAR but possible alternatives in the future:

- Linear interpolation in every mass balance element using the two boundary velocities for each velocity direction. The advantages of this method are at least threefold. First, since the stream line equation in each mass balance cell becomes

$$s_i \frac{dx_i}{dt} = u_i(0)(s_i - x_i) + u_i(s_i)x_i \quad i = 1,2,3$$

it can be solved analytically for each cell from which a higher computational efficiency derives. This would be particularly important in case one were to analyze the transport with random walk methods. Secondly, as opposed to the trilinear method used, the velocity fields obtained with this method is not continuous which might be more accurate in presence of rapid conductivity changes i.e this interpolation scheme favours channeling. Finally, the interpolated velocity field satisfy $\nabla \mathbf{u} = 0$ since

$$\nabla \mathbf{u}(\mathbf{x}) = \sum_{i=1}^{3} \frac{u_i(s_i) - u_i(0)}{s_i} = 0$$

and where the final equality is seen by factoring out $(\varepsilon_f s_1 s_2 s_3)^{-1}$ using ε_f for the flow porosity.

- Using kriging as interpolator. The obvious disadvantage of this alternative is that one needs to have the covariance function of the velocity. This can in practice only be obtained from a previous simulation series. The matrix to be inverted could be made identical at almost all points, presuming that the velocity is second order stationary, due to the fixed mesh so the method should be computationally feasible.

- Simulating the velocities conditioned on the mesh values. This is similar to the previous method but leads to complications since the points at which simulated values are needed are determined by the solution algorithm for the stream line equation. So if we imagine the simulation being performed using the turning bands method the one dimensional simulations need to be saved during the streamline calculations so that a simulated value of the velocity at a given point can be obtained. This discussion is continued in paragraph 9.3.1.

- Further interpolators such as the so called grad scheme, [Goode, 1990].

9.2 Integration

Given the interpolation ν above of the pore velocity field $\mathbf{u}$ we are in a position to solve the streamline equation in a domain

$$\begin{cases} s_1 \le r_1 \le (N_1 - 2)\, s_1 \\ s_2 \le r_2 \le (N_2 - 2)\, s_2 \\ s_3 \le r_3 \le (N_3 - 2)\, s_3 \end{cases}$$

that is, the intersection of the domains of definition for the interpolators of the pore velocities in the 1- 2- and 3- direction, as defined in the previous paragraph.

Previous experience leads us toward numerical integration methods of high order, hence we choose the 4:th order Runge-Kutta [Dahlquist and Björck, p 346]

$$\mathbf{r}^{n+1} = \mathbf{r}^n + \tfrac{1}{6}(\mathbf{k}^1 + 2\mathbf{k}^2 + 2\mathbf{k}^3 + \mathbf{k}^4)$$

where

$$\begin{cases} \mathbf{k}^1 = \delta t\, v(\mathbf{r}^n) \\ \mathbf{k}^2 = \delta t\, v\left(\mathbf{r}^n + \frac{\mathbf{k}^1}{2}\right) \\ \mathbf{k}^3 = \delta t\, v\left(\mathbf{r}^n + \frac{\mathbf{k}^2}{2}\right) \\ \mathbf{k}^4 = \delta t\, v(\mathbf{r}^n + \mathbf{k}^3) \end{cases}$$

and $\mathbf{r}^n$ is the radius vector of the tracer after the completion of the n:th time step and δt is the length of the time step.

The time steps in the integration are controlled in two ways. If the weighted square of the step length is "too large" i.e. if

$$\sum_{i=1}^{3}\left(\frac{r_i^{n+1} - r_i^n}{s_i}\right)^2 > \varepsilon^2 \qquad 9.6$$

the time step is shortened by a experimental factor 0.3. If, on the other hand more than five steps are taken inside a cell without the tracer exiting the time step is doubled. There is no theoretical ground for the choice of the numerical values of these factors, nor for the value of the tolerance ε. There is also a parameter that maximizes the number of steps inside a single cell and another that maximizes the number of changes of computational cell. Those maximizing parameters are primarily intended to prevent infinite loops from occurring in the case of the solution to the hydrology equation 7.1 having too poor mass balance but may also be a proper criterion for termination in case of extended domain, see paragraph 9.3 below.

For simplicity the successive evaluations of $\mathbf{k}_j$, j = 1,2,3,4 in each Runge-Kutta step uses the interpolation formula derived from the computational cell that contains r^n. This may lead to inaccuracies if the streamline is allowed to proceed too far out from the initial computational cell in one step. Therefore, as an option the code moves the tracer backwards along the straight line connecting r^n and r^{n+1} until the boundary of the computational cell is reached. To avoid the case that the tracer starts the next step precisely on the boundary between the two computational cells a small length is subtracted from the backward movement. The elapsed time for the current timestep is scaled by the factor obtained by dividing the length of the backward movement with the length of the original line segment.

When tracing in the extended domain, see subsection 9.3 below, this kind of backward interpolation is always used. The reason is that the large contrasts between the elements of the interior and exterior domains togther with the stepsize control criterion 9.2 could lead to very large steps into the interior domain from the exterior.

It would be interesting to improve upon the methods used. In particular since the velocity field is highly variable, a method designed for stiff problems might be better. This is particularly true since the stepsize control described above has no theoretical foundation. For instance the MOLCOL (Modified One-Leg COLlocation) algorithm, see [Eriksson] that is employed in the NEAR21 nearfield model, see [Norman and Kjellbert, 1991] could be tried.

9.3 Extended Domain

9.3.1 Reason for performing particle tracking in an extended mesh.

A standard problem in subsurface hydrology is the need for a finite computational domain and specified boundary conditions. This need arises as a result of the strategy of analysis namely:

1. collecting information in a site. The information is of type inferred fracture zones with interpreted hydraulic conductivity values, packer test, interference test, measurements or estimation of water table elevation etc.

2. derivation of an appropriate mathematical model. In our case, denoting the computational domain Ω and its boundary $\partial\Omega$ this might be written symbolically as

$$K|_{\Omega}, h|_{\partial\Omega} \rightarrow \mathbf{U}|_{\Omega} \qquad 9.7$$

for the Darcy velocity U and

$$K|_{\Omega}, h|_{\partial\Omega} \rightarrow t_{\Omega} \qquad 9.8$$

for the travel time to the boundary of Ω, t_{Ω}.

It is characteristic for the situation that the data is accumulated around the imagined repository and that it is successively depleted further away from the site. Looking at 9.7 the question on how to choose the domain may be posed. The smaller it is chosen the better is the quality of the information. It would thus be natural to choose as small a domain as possible with the allowance for the tricks dicussed in chapter 8 for finding reasonable head boundary conditions. The problem is that for small domains none of the streamlines will reach the surface unless noflow boundary conditions are used[21]. The alternative, which was used in the SKB 91-study, is to extend the validity of the statistical information of the conductivity field to a much larger domain than the sample

---

[21] A related method is to reflect the tracers at the boundary.

domain allowing for interpreted fracture zones and then perform the particle tracking. This method has the disadvantage that the large computational domain nessecitates large regularization scales or large meshes or both. Thus the resolution becomes bad.

Now the idea with extended domain tracking is simply to replace the extrapolation of the conductivity field with the extrapolation of the velocity field. That is to recognize that the role of the computational domain in this problem is to translate the knowledge (uncertainty) about conductivity into knowledge (uncertainty) about Eulerian or Lagrangian Darcy velocity and that strictly speaking when this task is completed there is no further need for the computational domain.

Hence one should try to find an optimal domain with respect to the factors mentioned above. Then, secondly, design a model for the velocity field from repeated simulations in the smaller block and finally extrapolate this model and use it for global simulations. Note that it is essential for such an approach to be able to guarantee that the simulated fields satisfy the constraints of mass balance, i.e that have no sources or sinks.

The advantages are that one can use smaller scales in the calculations and that one eliminates the problem of tracers not reaching the surface level since we can continue to simulate indefinitely. Moreover the simulations can, in principle, be conditioned on measured values of the velocity. The most notable disadvantage is that one looses the coupling to reality obtained from inserting interpreted fracture zones away from the actual data support.

A variation of the idea would be to extrapolate the head field or extrapolate a traveltime function $\tau(\mathbf{x},z)$ defined by the time needed for a particle at $\mathbf{x}$ to reach the level z. The advantages as compared with simulating the velocity field is that we avoid the problems with simulating a velocity field without sources and sink, the function at hand is a scalar and tracers leaving the computational domain prematurely may be treated as censored statistics. The disadvantage is that the stochastic function is defined on a four dimensional space instead of a three dimensional.

In the current version of HYDRASTAR this is not completely implemented. But the basis is the idea described above.

9.3.2 Algorithm for external particle tracking

As explained in previous paragraph the basic idea for external particle tracking is the same as in regression or statistical inference and simulation. Since time has not allowed us to develop a particle tracking algorithm in a stochastic velocity field we have settled for something more modest, still keeping the main line of thought however.

As said, we cannot simulate the velocity field outside the computational domain hence we try at least to predict it. For reason of the discussion, in which we only treat the 1 -component of the pore velocity u_1 the other components treated analogously, take a point $\mathbf{x}$ outside the domain. Then the best linear unbiased predictor of u_1, neglecting any influence from the crosssvariogram between u_1 and u_2 , u_1 and u_3, is written in analogy with paragraph 6.1 as

$$u_1(\mathbf{x})^* = \sum_{j \in D_1(\mathbf{x})} \lambda_j(\mathbf{x}) u_1(\mathbf{x}_j) \qquad 9.9$$

where $D_1(\mathbf{x})$ is a selected kriging neighbourhood of $\mathbf{x}$ consisting of (the indices of) the used mesh points and where $\lambda_i(\mathbf{x})$ satisfies the kriging equations i.e.

$$\begin{cases} \sum_{j \in D_1(\mathbf{x})} \lambda_j(\mathbf{x}) C_{u_1}(\mathbf{x}_i - \mathbf{x}_j) + \mu(\mathbf{x}) = C_{u_1}(\mathbf{x}_i - \mathbf{x}) \quad i \in D(\mathbf{x}) \\ \sum_{j \in D_1(\mathbf{x})} \lambda_j(\mathbf{x}) = 1 \end{cases} \qquad 9.10$$

The idea is now to extend the mesh and use the predictions of type 9.9 for the pore velocities in the extended mesh. The impact on the travel times of such an approach is difficult to judge since the consequence is to smooth the velocity field. This intuitively results in a underestimation of the tortuosity of the flow paths and also a removal of the fastest flow paths.

Since it is desired to avoid the estimation of the covariance functions of the (pore) velocities the algorithm was further simplified by the following reasoning.

If the row sums of the covariance matrix are approximately constant and $\mathbf{x}$ is chosen so that its distance from the nearest meshpoint is larger than the correlation scale of u_1 then the solution to the system 9.10 is approximately given by

$$\lambda_j(\mathbf{x}) = \frac{1}{|D_1(\mathbf{x})|} \quad j = 1, 2, \ldots, |D_1(\mathbf{x})| \qquad 9.11$$

where $|D_1(\mathbf{x})|$, as usual, denotes the number of points in $D_1(\mathbf{x})$. Thus in the absence of any covariance function for the velocity field we appoint 9.9 together with 9.11 to our estimator of the velocity at $\mathbf{x}$. However, even with this approximation there is still need for an estimate of the correlation scale of u_1.

In this connection we remark that 9.11 holds in two particular cases. When $|D_1(\mathbf{x})|$ equals four, the involved covariance function is isotropic and certain, easily calculated, conditions hold between $\mathbf{x}$ and the mesh geometry, $D_1(\mathbf{x})$ refers to the indices of four

points at the surface of the computational cube. In that case the row sum is constant and equal to

$$C_{u_1}(0) + C_{u_1}(s_1) + C_{u_1}(s_2) + C_{u_1}\left(\sqrt{s_1^2 + s_2^2}\right)$$

where as before s_1 and s_2 are the lengths of the mesh basis vectors $\mathbf{s}_1$ and $\mathbf{s}_2$.

A similar dicussion applies to the case when $|D_1(\mathbf{x})|$ equals nine.

Let us now extend our mesh for u_1 in the following way

$$s_1(i_1)\mathbf{e}_1 + s_2(i_1)\mathbf{e}_2 + s_3(i_3)\mathbf{e}_3 \quad -1 \le i_1 \le N_1 + 1, 0 \le i_k \le N_k + 1, k = 2,3,$$

see Fig. 9.2, where $\mathbf{e}_k$, k = 1,2,3 are the standard basis vectors and the stepvectors $s_1(i_1)$, $s_2(i_2)$ and $s_3(i_3)$ are given by

$$s_1(i_1) = \begin{cases} \frac{1}{2}s_1 - t_{1,1} - u_\infty & i_1 = -1 \\ \frac{1}{2}s_1 - t_{1,1} & i_1 = 0 \\ (i_1 - \frac{1}{2})s_1 & 1 \le i_1 \le N_1 - 1, \\ (N_1 - \frac{3}{2})s_1 + t_{1,1} & i_1 = N_1 \\ (N_1 - \frac{3}{2})s_1 + t_{1,1} + u_\infty & i_1 = N_1 + 1 \end{cases}$$

and

$$s_k(i_k) = \begin{cases} s_k - t_{k,1} - u_\infty & i_k = 0 \\ s_k - t_{k,1} & i_k = 1 \\ (i_k - 1)s_k & 2 \le i_k \le N_k - 1, \\ (N_k - 2)s_k + t_{k,1} & i_k = N_k \\ (N_k - 2)s_k + t_{k,1} + u_\infty & i_k = N_k + 1 \end{cases}$$

for k = 2,3. If we choose the variables $t_{1,k}$ to be on the order of the correlation scale of u_1 and the number of closest neighbours is chosen so that the assumptions used to derive the approximative solution to the kriging equation can be justified, it is possible to predict the value of the pore velocity u_1 in all the mesh points

$$s_1(i_1)\mathbf{e}_1 + s_2(i_1)\mathbf{e}_2 + s_3(i_3)\mathbf{e}_3$$

for which

$$(i_1 \le 0 \vee i_1 \ge N_1) \vee (i_2 \le 1 \vee i_2 \ge N_2 - 1) \vee (i_3 \le 1 \vee i_3 \ge N_3 - 1).$$

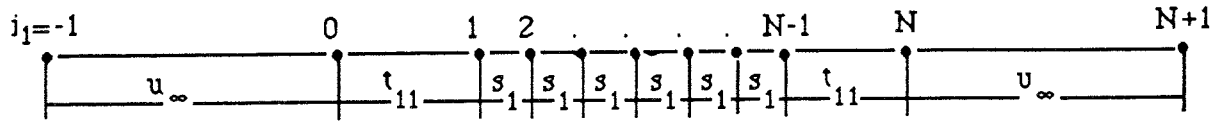

Figure 9.2 *Showing the extended mesh in the 1-direction for the 1-velocity.*

The mesh points distanced u_∞ from the others are inserted in order to continue the tracking "far away". Obviously, in the absence of simulation there is no need for additional node layers beyond the correlation scale. For simplicity the predictions at these infinity nodes are taken to be identical to the corresponding nodes at the correlation scale even though it is not certain that the $|D_1(\mathbf{x})|$ nearest neighbours are the same.[22]

Finally, it should be noted that the algorithm described needs to find the $|D_1(\mathbf{x})|$ closest points of $\mathbf{x}$. As a general problem this is not a trivial one and the obvious algorithms becomes much too laborious. Hence this is made significantly more efficient by the following observation, similar to the one that should be used in a kriging-based interpolaton, mentioned in the end of paragraph 9.1. If $\mathbf{x}$ belongs to the first layer of the extended mesh, to be specific say that $i_1 = 0$, and the set of (indices of) neighbours used $D_1(\mathbf{x})$ is such that a translation, that is $D_1(\mathbf{x}) + (0,j_2,j_3)$, still is a valid set of indices then the kriging equation 9.10 used is unchanged and thus the estimate at $\mathbf{x}_1 = \mathbf{x} + j_2\mathbf{e}_2s_2 + j_3\mathbf{e}_3s_3$ becomes

$$u_1(\mathbf{x} + j_2\mathbf{e}_2s_2 + j\mathbf{e}_3s_3)^* = \sum_{j \in D_1(\mathbf{x})} \lambda_j(\mathbf{x}) u_1(\mathbf{x}_1 + j_2\mathbf{e}_2s_2 + j_3\mathbf{e}_2s_3)$$

---

[22]Note that the predictions can vary beyond the realms of the correlation scale if we allow the kriging neighbourhood to vary. For instance if we choose the kriging neighbourhood to consist of the $|D(\mathbf{x})|$ nearest mesh points it may vary beond the correlation scale. In fact it will vary until it contains nodes on the "surface" only.

10 USING HYDRASTAR IN TRANSPORT MODELLING

To solve the problem of radionuclide transport in SKB 91 a number of methods were originally considered:

- A direct solution of the advection-dispersion equation.
- Random walk methods.
- Stream tube models.

The two first were deemed to be computationally too costly for use in Monte Carlo simulations which left only the stream tube model. The primary approximation in a stream tube model as compared to the other two methods, is neglection of radionuclide transport between different streamtubes i.e neglection of transversal dispersion and transversal diffusion.

When modelling a repository with many canisters as potential sources of radionuclide contamination the ideal strategy, once a stream tube model has been chosen, is to use one stream tube per source. Due to the large number of canisters and to the relative complexity necessary for modelling these processes, such as corrosion, backfill transport, precipitation etc, in the vicinity of the canister this might also be computationally too costly. Therefore the question arises how to cluster stream tubes, or stream lines, into larger stream tubes in the best possible way.

The first idea envisaged is to spatially divide the repository into initial surfaces for the stream tubes and associate a stream tube to each initial surface. The travel time and flow in such a stream tube can then be taken from one release point on the initial surface. However, it is apparent that if one uses a crude spatial division of the repository for reasons of computer costs the resulting approximation will perhaps not be satisfactory due to the fact that the points used may not be representative. A possible improvement, which is not implemented in HYDRASTAR, is to use spatial clustering. This involves the use of more particles for each stream tube and present some integrated measures representing the streamtube. This would do nicely for the streamtube flow but a large spatial cluster will not in general transform its initial surface to a boundary surface. That is some particles on the initial surface of the stream tube may reach the boundary of the computational domain long before the majority of the particles used to represent the stream tube do. If the majority of the particles are much slower than the fast ones they will dominate integrated data such as for instance the travel time of the centroid. The improvement implemented in HYDRASTAR is instead a temporal clustering that is to collect stream lines with approximately the same travel time to the biosphere into stream

tubes. Note that there is no reason to require that a streamtube should have a connected cross section in view of the neglect of transversal dispersion.

For a more detailed discussion of these topics and some suggested improvements see appendix A.

10.1 Clustering algorithms

The division of stream tubes according to the groundwater travel times leads to so called clustering problems. That is, given a set of points, in general in a n-dimensional space, a number C and a measure of the size of a set, how do we find the division of the original point set into subsets, clusters, so that the sizes of the clusters become as small as possible. This kind of problems are the origin of a whole branch of mathematics. In HYDRASTAR a simple variant has been used obtained by minimizing the sum of the diameters[23] of the clusters. In the one dimensional space of traveltimes this problem is simply solved by sorting the travel times and dividing the set by removing the C - 1 longest distances between the travel times.

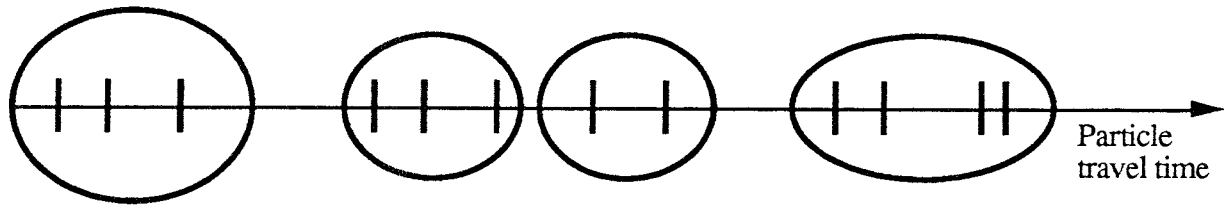

Figure 10.1 *Showing the division of twelve travel times into four clusters that is into four streamtubes using the algorithm in the text.*

[23]The diameter of a set D is in general defined as sup{|x-y|, x,y∈D}.

11 PROPOSALS FOR FUTURE HYDRASTAR DEVELOPMENT

Here follows a list of possible developments of HYDRASTAR. The description of the items in the list are short and no distinction is made between items that will require large amounts of work and those leading to minor changes:

- Include the possibility to simulate the head boundary conditions coupled with the hydraulic conductivity. This is to remedy some of the problems discussed in chapter 8 and would diminish if not unnessecitate the need for an outer hydrological model.
  This would lead to the generalization of the stochastic function generators to coregionalizations, or perhaps a better word vectorvalued stochastic functions. In particular the conditional simulations would need the introduction of cokriging. These developments are also needed in the case one wants to develop HYDRASTAR into more advanced models of the conductivity field such as anisotropic conductivity and linking discrete fracture models with stochastic continuum models in the way proposed in [Norman and Geier, 1991]. For some ideas in the field of coregionalizations and cokriging see [Myers, 1982], [Myers, 1983] and [Myers, 1984].

- For reasons discussed in chapter 9 one could rewrite the streamline equation solver to allow for

  different interpolation schemes

  different equation solvers

  and include random walk as an optional transport modelling.

- Improve the integral approximations for the one dimensional processes in the turning bands approximation, see section 5.2.

- Include the simulation of intrinsic random functions with higher order.

- Include the possibility of a more general mesh. In particular this would be desirable when modelling disturbed zones around the tunnels of a repository. Since the resistance to flow in certain radial flow pattern is centered near the tunnels the mesh resolution in this area should be fine.

12 LIST OF NOTATION

In general vectors and matrices are printed in boldface.The chapter references on the notation do not give all the chapters where the notation occurs but do hopefully contain all chapter references where the same notation has different meaning. This list of notation does not include the appendices.

^{T}	Matrix transpose, chapter 6.
$\sim$	Fourier transform, chapter 5.
$\hat{}$	Signals that this is an estimate or signals this is a unit vector.
$'$	A mean removed form. Chapter 3.
$\grave{}$	Functional operator defined by negating the argument of the argument function, chapter 5.
$\bullet$	Inner tensor product, chapter 6.
$*$	Kriging estimate chapter 6, complex conjugate chapter 5.
$*$	Convolution operator, chapter 5.
$(\cdot, \cdot,)$	The scalar product, chapter 5.
$(\cdot)^+$	The operand if it is positive and zero otherwise. Chapter 2.
$(\cdot)^-$	The negated operand if it is negative and zero otherwise. Chapter 2.
$\lvert\cdot\rvert$	Size of a set or absolute value of a real, chapter 5, 7.
$\lVert\cdot\rVert$	Norm of a vector, chapter 4.
$\{\mathbf{x}:(\cdot)\}$	The set of all $\mathbf{x}$ such that $(\cdot)$.
$f\mid_I$	The function f restricted to the set I, chapter 9.
$\mathbf{1}$	A vector with all components equal to 1.
$\aleph$	A σ-algebra, chapter 6.
a	Range parameter in the spherical covariance model, chapter 4, 5.
b	Grid spacing in the integral approximations in the turning bands method, chapter 5.
$\mathbf{b}$	Arbitrary vector orthogonal to the kriging neighbourhood normal, chapter 4.

χ_I	Characteristic function for the interval (or set) I. That is a function equal to one at points in the set I and to zero at points outside the set I, chapter 2.
$C(\xi)$, $C_Y(\xi)$	Covariance function sometimes subscripted by the stochastic function to which it refers. Chapter 3, 5.
$C_{iso}(\xi)$	Isotropic covariance model, chapter 4.
$C_1(\cdot,\mathbf{l})$	Covariance for a one dimensional process on the line **l**, chapter 5.
$C_p(\mathbf{x})$	Pseudo covariance, chapter 6.
$\mathbf{C_p}$	Pseudo covariance matrix, chapter 6.
C_0	Constant used in defining the pseudo covariance, chapter 6.
$C(\mathbf{0})$	The variance, by definition, chapter 3,6.
$\mathbf{C}$	Generic notation for a covariance matrix with components $C(\mathbf{x}_i-\mathbf{x}_j)$, chapter 6.
$\mathbf{c}$, $\mathbf{c}(\mathbf{x})$	Generic notation for the covariance vector with components $C(\mathbf{x}_i-\mathbf{x})$, chapter 6.
δ	Density of water, chapter 2.
$\mathbf{D}$	Kriging matrix, chapter 6.
$D(i_1, i_2, i_3)$	The (i_1, i_2, i_3):th diagonal element of the numerical hydrology equation, chapter 7.
d	Packer length, chapter 2.
$D(\mathbf{x})$	Kriging neighbourhood, chapter 4, 6.
$D_1(\mathbf{x})$	Kriging neighbourhood for the pore velocity in the 1-direction, chapter 9.
$dS(\mathbf{l})$	Scalar surface measure, chapter 5.
$d\mathbf{S}(\mathbf{l})$	Directed surface measure, chapter 7.
δt	Time step used in the Runge-Kutta solver of the stream line equation, chapter 9.
dF	Spectral measure, chapter 5.
dT	Stochastic measure, chapter 5.
Δh, Δh_i	Difference head, from packer test i, chapter 2.

Δp	Packer test overpressure.
e^{+}_{reg}	Sum of the positive regularization overlap, chapter 2.
e^{-}_{reg}	Sum of the negative regularization overlap, chapter 2.
ε	Tolerance for the step length in the stream line equation solver, chapter 9.
ε_f	Flow porosity, Chapter 9.
ε_p	Positive regularization tolerance.
ε_n	Negative regularization tolerance.
$\mathbf{e}_1, \mathbf{e}_2, \mathbf{e}_3$	The standard basis vectors, chapter 9.
$E(\mathbf{x})$	Kriging set, chapter 4.
$E[\ \cdot\ ]$	Expectation value operator, chapter 3.
$f(\mathbf{x})$	Probability density function on the half unit sphere, chapter 5.
$f(\mathbf{x}),\ g(\mathbf{x})$	Generic functions, chapter 5.
ϕ	Angle coordinate in a spherical system, chapter 5.
g	Constant of gravity, Chapter 2.
G	The matrix of geometrical anisotropy. Chapter 3.
Γ	Semivariogram matrix, chapter 6.
$\gamma,\ \gamma(\mathbf{x})$	Generic notation for the covariance vector with components $C(\mathbf{x}_i\text{-}\mathbf{x})$, chapter 6.
φ	Angle coordinate in a cylindrical coordinate system, chapter 2, and in spherical system chapter 5.
$\gamma_Y(\xi),\ \gamma(\xi)$	The semivariogram. Chapter 3.
η	Coordinate vector in the isotropic (lag)space. Chapter 4.
$h(\mathbf{x})$	The hydraulic potential
$h_0(\mathbf{x})$	The hydraulic potential under natural conditions. Chapter 2.
$\langle h \rangle^s$	Intrinsic average[24] hydraulic head on the averaging scale s, chapter 7.

[24]That is the volume used for the average is the volume of the pores inside the averaging volume.

$h_j(\mathbf{x})$, $\Delta h_j(\mathbf{x})$	The scaled disturbance of the natural head field, head difference due to the induced overpressure between two packers. Chapter 2.
h_{1+2}	The difference field arising from the simultaneous application of unit overpressure in both packer interval 1 and packer interval 2, chapter 2.
i	Generic integer, chapter 5, 6.
i_1, i_2, i_3	Mesh points coordinates, chapter 7.
j	Generic integer, chapter 6.
I_j	Generic interval, chapter 5.
I_{reg}	Interval along a drill hole covered by a regularized measurement, chapter 2.
L_{reg}	Length of a regularized measurement, chapter 2.
$K(\mathbf{x})$, $K_s(\mathbf{x})$	The hydraulic conductivity for a certain averaging scale, s, viewed as a stochastic process, chapter 2,7.
K_{reg}	Regularized measurement value of the conductivity. Chapter 2.
K_i	The conductivity value obtained from packer test i and Moyes formula.
$K_j(i_1, i_2, i_3)$	The conductivity at the (i_1, i_2, i_3):th node of the mesh of the j:th direction, chapter 7.
k	Generic integer, chapter 5.
$\mathbf{k}^1$, $\mathbf{k}^2$, $\mathbf{k}^3$, $\mathbf{k}^4$	Auxillary vector variables in the stream line equation solver, chapter 9.
λ	Wave vector i.e the coordinate in the Fourier space, chapter 5.
λ, $\lambda(\mathbf{x})$	Vector of kriging weigths chapter 6.
λ	One dimensional wave vector i.e the coordinate in the one dimensional Fourier space, chapter 5.
λ	Range parameter in the exponential covariance model, chapter 4, 5.
λ_i	Kriging weights, chapter 6.
$\mathbf{l}$, $\mathbf{l}_i$	A line in the turning bands method, also a point on the half unit sphere, chapter 5.
L_i	Packer interval, chapter 2.
$m_Y(\mathbf{x})$, $m(\mathbf{x})$	Expectation value function, chapter 3, 6.

m_0, $\mathbf{m}_1$, $\mathbf{m}_2$	Trend parameters, chapter 6.
$\mu(\mathbf{x})$	Lagrangian multiplier, chapter 6.
N	The number of lines in the turning bands method, chapter 5. Number of measurements, chapter 6.
N_q	The quotient between bandwitdth and grid spacing in the turning bands method, chapter 5.
N_j	The number of head nodes in the j:th direction, j = 1,2,3, chapter 7.
n	Normal of the kriging neighbourhoods and sets, chapter 4.
n	The number of measurements used in a regularization, chapter 2.
n	Interpolation polynomial for the pore velocity, chapter 9.
$n_{i,j,k}$	Coefficients of the interpolation polynomial, i,j,k $\in$ [0,1], chapter 9.
N_{kn}	Number of measurements in the kn:th kriging neighborhood.
o, w	Overlap and width in the definition of kriging neighbourhoods and sets. Chapter 4.
P	Probability measure, chapter 6.
p, Δp	Pressure, overpressure in a packed off section. Chapter 2
Q,Q_i	Induced packer test flow, from section i. Chapter 2.
q,q_i	Induced packer flow per unit applied difference head, from section i. Chapter 2
R	Parameter that determines the number of values used in the integral approximations in the turning bands method, chapter 5.
$\mathbf{R}^3$, $\Re^3$	Three dimensional real space. Chapter 4.
$\Re^3_{1/2}$	Three dimensional halfspace, chapter 5.
r	Norm of the lag vector, chapter 5.
r_i	Random real from the random number generator, chapter 5.
r_1, r_2, r_3	Coordinates of the radius vector, chapter 9.
r(t)	Radius vector of a water particle at time t given the original position **r**(0), chapter 9.

$\mathbf{r}^n$	The radius vector after completing n time steps in the Runge-Kutta algorithm, chapter 9.
r_i^n	The coordinates of $\mathbf{r}^n$ above, chapter 9.
ρ	Radial coordinate in a cylindrical coordinate system. Chapter 2.
ρ_w	Borehole radius, chapter 2.
s	Characteristic length of an averaging scale, chapter 7.
s	Generic real. Chapter 4,5.
s	Auxillary variable for expressing the solution of the kriging equations, chapter 6.
$\mathbf{s}_1, \mathbf{s}_2, \mathbf{s}_3$	Basis vectors for the prismatic mesh of HYDRASTAR, chapter 7.
s_1, s_2, s_3	Length of the basis vectors for the prismatic mesh of HYDRASTAR, chapter 7.
$s_1(i_1), s_2(i_1), s_3(i_1)$	Variable length of the basis vectors for the prismatic mesh of HYDRASTAR used in the external tracing, chapter 9.
S	Target regularization scale, chapter 2.
Σ	Auxillary variable, chapter 5.
$S_{1/2}$	Half the unit sphere, chapter 5.
S, S_Y	Spectrum, spectrum of the stochastic function Y, chapter 5.
S_l	Spectrum of a stochastic function Y_l on a line $\mathbf{l}$ in the turning bands method, chapter 5.
σ,σ_Y	Standard deviation, chapter 3.
σ_T	Standard deviation of the stochastic measure T, chapter 5.
σ_t	Standard deviation of the integrated stochastic measure t_k, chapter 5.
T	Width of the bands in the turning bands algorithm, chapter 5.
$T_j(i_1, i_2, i_3)$	The transmissivity of the surface represented by the (i_1, i_2, i_3):th node of the mesh of the j:th direction, chapter 7.
t	Time, chapter 9.
$t_{i,j}$	Distance from the mesh boundary in the j:th direction used in predicting the i:th pore velocity component outside the domain.

t_Ω Travel time to the boundary, chapter 9.

t_k Integrated stochastic measure, chapter 5.

$\tau(\mathbf{x},z)$ Travel time function, chapter 9.

$U_j(i_1, i_2, i_3)$ The j:h component of the Darcy velocity at the (i_1, i_2, i_3):th node in the j:th -directional mesh , chapter 7.

U_j Random reals used to generate random rotation vector, chapter 5..

$\mathbf{U}(\mathbf{x})$ The Darcy velocity, or Darcy flux, for a certain averaging scale viewed as a stochastic process.

$\mathbf{u}(\mathbf{x})$ Pore velocity, chapter 9.

$u_1(\mathbf{x})$, $u_1(\mathbf{x})$, $u_1(\mathbf{x})$ Components of the pore velocity, chapter 9.

u Generic real. Chapter 5.

u_∞ Distance between the last and second last node layers used in the external tracking, chapter 9.

V Variance, chapter 5. Arbitrary volume chapter 7.

$V[\ \cdot\ ]$ Centered variance operator, chapter 6.

V_s The averaging volume of characteristic length s, chapter 7.

w Auxillary variable, "Lagrangian correction vector", chapter 6.

Ω Event space, chapter 6 computational domain chapter 9.

Ω_f The void space inside the fractured rock, chapter 7.

ω A point in the event space. It is almost always supressed. Chapter 3.

ω_j Coordinates of a random rotation vector, chapter 5.

$\mathbf{X}$ Trend matrix, chapter 6.

x_i, y_i, z_i Intermediate integers in the random number generator, chapter 5.

x_1, x_2, x_3 Local coordinates in a computational cell, chapter 9.

$\mathbf{x}_i, \mathbf{x}$ General notation for a point in space. The coordinates of this points is given by x1, x2, x3 in Cartesian coordinates. Chapter 2.

$\mathbf{x}_P$ Point defining a kriging neighbourhood.

ξ	Generic notation for a lag vector, chapter 3. Auxillary vector variable chapter 7.
ξ	Generic notation for a lag distance, chaper 5.
$\mathbf{Y}$	The stochastic vector obtained by restricting the function $Y(\cdot)$ to a set of spatial points.
$Y(\mathbf{x},\omega)$, $Y(\mathbf{x})$	The stochastic process defined by $Y(\mathbf{x}) = \log(K(\mathbf{x}))$. Also used as a generic notation for a stochastic process or a representation of an intrinsic random function. The argument ω is the event space vector and is almost always supressed. Chapter 3.
$y(\mathbf{x})$	A realization of the stochastic process $Y(\mathbf{x})$, chapter 6.
$Y_1(\xi)$	One dimensional stochastic function, chapter 5.
$Y_S(\mathbf{x})$	A process that can be used to simulate $Y(\mathbf{x})$.
z	Coordinate in a cylindrical coordinate system with its z-axis along a certain drill hole. Chapter 2. Coordinate corresponding to $\hat{\mathbf{z}}$.
z_i	The lowest point along the drill hole axis of a packed off interval .
$Z(\mathbf{x})$	A stochastic function, chapter 6.

13 ACKNOWLEDGEMENTS

The author wishes to thank:

Mr Anders Ström SKB AB again for his persistence in getting the author going and for proofreading the main part of the manuscript.

Mr Nils Kjellbert for stimulating discussions in general and lately regarding the transport modelling in particular. He also proofread parts of the manuscript.

Mr Lars Lovius Starprog AB for writing the code of the stream line equation solver and a first version of chapter 9. He also proofread the formulas.

Mr Lars Eriksson and Dr Jesper Oppelstrup Starprog AB for numerical hints.

Ms Annica Johansson Starprog AB for getting the author out of his depressions.

Mr Marcus Berglund Starprog AB for discussions about and the writing of the clustering algorithm.

Mr Per Hörnfeldt for proofreading parts of the manuscript, writing the code for the disturbed zone and performing the verification exercise of the FD -solver.

Mr Stefan Jansson for proofreading parts of the manuscript.

Mrs Marita Norman for endurance.

Mr Viktor Norman and Ms Erika Norman for being reasonably well behaved.

14 REFERENCES

[Ahlbom and Tiren, 1991] Ahlbom, K., Tiren, S. Overview of the geological and geohydrological conditions at the Finnsjön site and its surroundings, SKB TR 91-08.

[Bear, 1972] Bear, J. Dynamics of fluids in porous media, American Elsevier Pub. Co, New York 1972

[Braester and Thunvik] Braester, C., Thunvik, R., Numerical simulation of double packer tests. Calculation of rock permeability., SKB TR 82 - 06.

[Brately, Fox and Schrage, 1987] Bratley, P. , Fox, B. L. , Schrage, L. E. , A Guide to Simulation, 2nd Ed. , Springer, New York, 1987.

[Coveyou and MacPherson, 1967] Coveyou, R. L. , MacPherson, R. D. , Fourier Analysis of Uniform Random Number Generators, J. of the Assoc. for Computing Machinery, Vol. 14, No 1, Jan. 1967, pp 100 -116.

[Dahlquist and Björck] Dahlquist, G. , Björck, Å, Numerical Methods, Prentice Hall, 1974

[Darcy, 1856] Darcy, H., Les fontaines publiques de la ville de Dijon, Dalmont, Paris.

[de Marsily, 1986] de Marsily, G., Quantitative Hydrogeology, Academic Press, 1986.

[Delhomme, 1979] Delhomme, J. P., Spatial Variability and Uncertainty in groundwater Flow Parameters: a Geostatistical Approach. Water Resour. Res. 15(2), pp. 269 - 280.

[Eriksson] Eriksson, L. O., MOLCOL an Implementation of One-leg Methods for partitioned Stiff ODE's, TRITA-NA-8319.

[Fisz, 1963] Fisz, M., Probability theory and mathematical statistics, Wiley, 1963.

[Geier et al, 1992] Geier J E, Axelsson C-L, Hässler L, Benabderrahmane A, Discrete fracture modelling of the Finnsjön rock mass: Phase 2, SKB TR 92-07.

[Golub and van Loan] Golub, G. van Loan, Matrix Computations, 2:d edition, Hopkins, July 1989.

[Goode, 1990] Goode, D., J., Particle Velocity Interpolation in Block-Centered Fimite Difference Groundwater models, Water Resour. Res. Vol. 26, No 5, pp 925-940, 1990.

[Gray and O'Neill, 1976] Gray, W. and O'Neill, K., On the General Equations for Flow in Porous Media and their reduction to Darcy´s law, Water Resources Research April 1976, pp. 148 - 154.

[HYDRASTAR] User's Guide to HYDRASTAR 1.2, SKB AR 93-02

[Journel ,1977] Journel, A. G. , Kriging in terms of projections, J. Math. Geol., 9(6), 563-586, 1977.

[Journel and Huijbregts, 1978] Journel, A. G.Huijbregts, Ch. J. , Mining Geostatistics, Academic Press, 1978.

[Journel and Alabert, 1989] Journel A. G. and Alabert, F. 1989, Non-Gaussian data expansion in the earth sciences, Terra Nova, Vol. 1, No. 2, pp 123-134.

[Matheron, 1973] Matheron, G., The Intrinsic Random Functions and their Application, Adv. Appl. Prob. 5, 439-468, 1973.

[McGrath and Irving, 1975] McGrath, E. J. , Irving D. C. , Techniques for Efficient Monte Carlo Simulation ORNL-RSIC-38, Vol. 2, Oak Ridge National Laboratory,.1975

[Moye, 1967] Moye, D. G., Diamond drilling for foundation exploration, Civil engineering transactions, 1967, pp 95 - 100.

[Myers, 1982] Myers D. E., Matrix Formulation of Co-Kriging, Mathematical Geology, Vol. 14, No. 3, 1982

[Myers, 1983] Estimation of Linear Combinations and Co-Kriging, Mathematical Geology, Vol. 15, No 5, 1983.

[Myers, 1984] Myers, D. E., Co-Kriging, New Developments, G. Verly et al. (eds.), Geostatistics for Natural Resources Characterization, Part 1, 295-305., 1984 by D. Reidel Publishing Company.

[Neuman, 1988] Neuman S. P. , A proposed conceptual framework and methods for investigating flow and transport in Swedish crystalline rock, SKB AR 88-37, September 1988.

[Norman, 1991] Norman, S. , Verification of HYDRASTAR - A code for stochastic continuum simulation of groundwater flow, SKB TR 91-27.

[Norman and Geier, 1991] Norman, S., and Geier, J., Interface between discrete fracture network and stochastic continuum models for the SKB 91 safety assesment study. Proposal to SKB 1991.

[Norman and Kjellbert, 1991] Norman, S., Kjellbert N. , A near field radionuclide migration code for use with the PROPER package, SKB TR 91-19.

[Nyberg and Voss, 1991] Problems in modelling ground water systems i limited scale, SKB AR 91-10.

[Pörn, 1986] Pörn, K. , Testing of the Random Number Generator used in PROPER, SKB Memo 1986.

[Tompson, Ababou and Gelhar, 1989] Tompson, A. F. B. , Ababou, R. , Gelhar, L. W. , Implementation of the Three Dimensional Turning Bands Generator, Water Resour. Res. , Vol. 25, No. 10, pp 2227-2234, Oct. 1989.

[Whitaker, 1985] Whitaker, S. Flow in Porous Media 1: A Theoretical Derivation of Darcy´s law, Transport in Porous Media 1 (1986) 3-25, D. Reidel Publishing Company.

[Yaglom, 1962] Yaglom, A. M. , Stationary random functions, Prentice-Hall, 1962 (Dover Publications 1973)

APPENDIX A - TRANSPORT MODELLING WITH HYDRASTAR

The approach used in the SKB 91 study [SKB91, p 114-119] is to take a rather large computational domain and a number of initial positions which signify the starting points of a set of stream tubes covering the repository and perform Monte Carlo simulations that in each iteration use:

- HYDRASTAR to generate a corresponding set of travel times to the boundary of the computational domain for FARF31 and the Darcy velocities at the initial position for use in NEAR21/TULL22,
- NEAR21/TULL22 is used to give the radionuclide inflow rate to the stream tube, for information about NEAR21 see [Norman and Kjellbert, 1991] and for TULL22 see [Kjellbert, 1991],
- FARF31 is used to give the radionuclide outflow rate which is then added up to give the total outflux from the computational domain. For information about FARF31 see [Norman and Kjellbert, 1990].

NEAR21/TULL22 basically handles only one canister and calculates the convective nuclide flow from the redox front. The input to FARF31 is the input flux at the start of the tube. To each streamtube start surface one must then assign a number of canisters in a rather arbitrary fashion and NEAR21/TULL22 is considered to deliver the total flow from all these canisters through the start surface by the following rules:

- If the set of canisters assigned to the streamtube contains one ore more initially damaged canisters the undamaged canisters are neglected, the damaged canisters are treated identically and the resulting influx to the streamtube is calculated as the product of the number of damaged canisters times the inflow from one damaged canister.
- If the set of canisters assigned to the streamtube contains no initially damaged canisters all canisters are treated identically and the resulting influx to the streamtube is calculated as the product of the number of canisters assigned to the streamtube times the inflow from one canister.

Hence, the temporal streamtube clustering method, as described in chapter 10, was not used in SKB 91. If temporal clustering is used, TULL22 is capable of handling canisters exposed to different water fluxes within each streamtube. The canisters seeing the least water flux can also be screened off, cf section A.5.

The travel time for the particle representing the streamtube is taken to be the travel time to the boundary of the computational domain and this is shown to be a reasonable

approximation, [SKB91, p 131] thanks to the well chosen computational domain that returns over 50% of the particles released.

The general method outlined above contain some weak points such as:

- The interface between the nearfield and farfield models are rather crude.
- When using the FARF31 stream tube approximation one work consistently with cross section flow averages. Thus for instance if we use cross sections large in comparison to the velocity correlation scale or large in comparison to the travel time correlation scale it is inconsistent to use single particle tracking. Instead the stream tube should be viewed as the movement of an ensemble of particles.
- One only obtains the outflow from the computational domain. This can be directed through any surface and not at all through the top surface which would be necessary for giving a correct measure of the release to the biosphere.

To remedy the situation some features were added to HYDRASTAR one of which was the external tracking viewed as a shortcut to obtain some of the advantages of a more general idea as described in paragraph 9.3.1. These features were never used in [SKB 91] but are discussed here for completeness.

A.1 Transport modelling with FARF31

Let us start by reviewing the important assumptions employed in the stream tube model. There are three classes:

1. Continum assumptions. That the transport from the outset can be described with a dispersion - advection model.
2. Stream tube cross section averaging. In particular radionuclide transport is only modeled along the stream lines.
3. Stream tube longitudinal averaging of some parameters.

Below we shall only concern ourselves with assumptions of class 2 . In this connection we state formally that with the term stream tube we will mean a collection of stream lines each stream line associated with a initial surface. We especially point out that the inital surfaces of a stream tube taken together need not constitute a connected surface.

It might appear that using stream tubes with disconnected cross sections would enhance the defect resulting from assuming that one can neglect transversal dispersion. This is however not the case since the neglect of transversal dispersion is equally serious when applied inside a stream tube. Hence we conclude that there is no disadvantage involved using stream tubes with disconnected cross sections. Also we note that if we exclude the

computational efficiency point of view the the best approach is to have one stream tube per canister. Thus the only reason for collecting stream lines into stream tubes is to enhance the computational speed. The problem is to do this in a manner that minimizes the incurred errors.

A.2 Interface between NEAR21/TULL22 and FARF31

In a FARF31 stream tube the representative quantity $C_f^{i,tube}(\zeta)$ is defined as

$$C_f^{i,tube}(\zeta) = \int_{A(\zeta)} C_f^i(\xi)\frac{dq(\xi)}{Q_{tube}}.$$

where

ξ is the traveltime coordinate along the streamtube.

$A(\xi)$ is the cross section of the stream tube,

$C_f^i(\xi)$ is the intrinsic average concentration of nuclide i ,

Q_{tube} total water flow in the stream tube,

$dq(\xi)$ infinitesimal flow through the surface elements $dA(\xi)$.

The output from NEAR21/TULL22 is written

$$Q_{near,out}C_{near,out,i} \qquad \text{A.1}$$

where

$C_{near,out,i}$ is the concentration of substance i at the interface between the nearfield and the farfield models and

$Q_{near,out}$ is the flow through the interfacial surface calculated as

$$Q^j_{near,out} = \left|U(\mathbf{x}_j)\right| P(R_j).$$

Here

$\mathbf{x}_j$ is the location of canister j

R_j is the surface of the interface between canister j and the stream tube. This is calculated differently in NEAR21 and TULL22, see [Kjellbert 1991].

$|U(\mathbf{x}_j)|$ is the magnitude of the Darcy velocity at $\mathbf{x}_j$

$P(R_j)$ is the area of the surface of the interface between canister j and the stream tube projected along $U(\mathbf{x}_j)$.

Thus it is natural to assume that the initial surface A(0) of the stream tube is built up of a number of R_j:s and thus

$$C_f^{i,tube}(0,t) = \int_{A(0)} C_f^i(\xi,t)\frac{dq(\xi)}{Q_{tube}} \approx \frac{\sum_j C^j_{near,out,i}(t)Q^j_{near,out}}{\sum_j Q^j_{near,out}}$$

i e replacing the nuclide flux boundary condition, used in SKB 91 and implemented in FARF31, with a nuclide concentration boundary condition.

For this approach we need to assume that each point on A(0) is intersected at most once by every stream line. Or differently put, there is no stream line connecting interfacial surfaces from different canisters. This is already assumed implicitly in NEAR21/TULL22 since the inflowing water is assumed to be uncontaminated and is, luckily, a conservative assumption. Note again that we do not need to assume that the R_j:s taken together makes up a connected surface.

A disadvantage with this proposal is that it does not guarantee the conservation of mass in the system constituted by the near and farfield models. This is the output from the nearfield, i.e what is removed from the nearfield model, is calculated using the nearfield model only from A.1. There is no guarantee that this equals the input to the farfield model

$$Q_{tube}\left(C_f(\zeta,t) - \frac{t_w}{Pe}\frac{\partial C_f(\zeta,t)}{\partial\zeta}\right)\Bigg|_{\zeta=0},$$

see [Norman and Kjellbert, 1990] formula (3.9), and this is the reason for for choosing the flux boundary condition and thus accepting the concentration mismatch. The only way to satisfy both the flux and concentration requrements is to remove the division of the transport model into two parts. Then the amount removed from the nearfield could be calculated from

$$F^i_{out}(t) = \sum_{j=i}^{N}\int_0^t C_{in}(t)C_f^{i,j}(0,t-\tau)d\tau$$

and the output from the stream tube as before

$$F^i_{far,out}(t) = \sum_{j=i}^{N}\int_0^t C_{in}(t)C_f^{i,j}(t_w,t-\tau)d\tau$$

where $C_f^{i,j}$ are the response function for nuclide i from a Dirac concentration pulse in nuclide j placed above i in the decay chain. These response function is calculated in principle by FARF31; only the minor changes below have to be made.

Now returning to the discussion of concentration type boundary conditions it may be proposed that the reasonable model for the surficial interfaces is that the R_j:s are disjoint patches. Then one could fill out the gaps with patches having zero concentration thus obtaining a new initail value for the stream tube

$$C_f^{i,tube}(0,t) = \frac{\sum_j C^j_{near,out,i}(t) Q^j_{near,out}}{\sum_j Q^j_{near,out} + \sum_j Q^j_{gap}}$$

where Q^j_{gap} are the flow through patches covering the gap between the interfaces. This looks like a uniqeness problem but is not since by linearity the solution to this modified problem is identical to the old one save only the multiplicative factor

$$\frac{\sum_j Q^j_{near,out}}{\sum_j Q^j_{near,out} + \sum_j Q^j_{gap}}.$$

Thus it results in the same outflow from the stream tube since the outflow of the stream tube is proportional to the water flow Q_{tube} in the stream tube. See [Norman and Kjellbert,1990], equation 3.12. We conclude that if all other parameters are fixed the addition of patches with zero concentration to the initial surface do not alter anything. This is most illustrative if we should like to study one canister only. Thus the conclusion of this discussion is that the witdth of the tube does not matter if all other parameters are fixed. The question however is which parameters are changed as the width of the stream tube increases. This is the topic of the next section that treats the parameters Pe and t_w.

A.3 Changes in FARF31

Changing the boundary conditions to concentration boundary conditions results in one simple change in the solution of the transport equations used in FARF31 as described in [Norman and Kjellbert, 1990] Appendix C.

The solution to the homogeneous $\tilde{C}_f^i$ -equation is written as

$$H^i_f(\zeta, s) = A_i e^{f_i(s)\zeta}$$

but A_i is now determined as

$$A_i(s) = \tilde{C}^i_{in}(s)$$

where $\tilde{C}^{i}_{in}(s)$ is the Laplace transform of the concetration of nuclide i at the initial surface of the stream tube. This may be compared with the previously used formula

$$A_i = \frac{\tilde{F}^{i}_{in}(s)}{Q_{tube}\left(1 - \frac{t_w}{Pe} f_i(s)\right)}$$

where $\tilde{F}^{i}_{in}(s)$ is the Laplace transform of the input flux into the stream tube of nuclide i. The results regarding holomorphy domains of the solution proven in [Norman and Kjellbert, 1990] Appendix C remains unchanged.

A.4 Stream tube division

First, how do we define travel time for a stream tube that widens. Clearly the concept of travel time prevails however "the initial surfaces do not transform into boundary surfaces" thus we do not get the whole stream tube i.e all particles comprising it, to exit simultaneously instead the calculation of it should stop when one part of the surface reaches the boundary. Thus the stream tube end surface can be located to a large extent in the interior of the computational domain. Hence the difficulty becomes rather do define when the stream tube hits the biosphere since it may hit with a edge only and the interesting thing is the flux through that edge and not through the stream tube cross section. This outflow may in certain cases be uniteresting. Thus it is natural to collect the stream lines into stream tubes with respect to travel times to the biosphere.

Another question that arises is if the Peclet number varies with the width of the stream tube. This is influenced by the replacement of the pore velocity by its stream tube cross section average, see [Norman and Kjellbert,1990] Appendix A. Hence if one is to join stream lines into stream tubes and minimize the effect of the averaging procedures, one should take stream lines with approximately equal velocity together. Which leads to the same conclusion as above i e that it is natural to collect the stream lines into stream tubes with respect to travel times to the biosphere.

A.5 Reduction of the number of canisters treated

A practical problem with the approach outlined above is that we in principle need to calculate $C_{near,out,i}$ for all canisters. Thus the computational time and storage requirements may be prohibitive even considering the documented effectiveness of the nearfield model NEAR21/TULL22. However we see that due to the weighting with $Q^{j}_{near,out}$ in the calculation of the boundary conditions of the stream tube we could content ourselves with taking only the canisters which together takes a large fraction, f

,of the flow. Stated formally for each stream tube we order the $Q^{j}_{near,out}$´s in descending order $Q^{j(k)}_{near,out}$ and define the set H(f) recursively as

$$\begin{cases} Q^{j(1)}_{near,out} \in H(f) \\ Q^{j(k+1)}_{near,out} \in H(f) \text{ if } Q^{j(k)}_{near,out} \in H(f) \text{ and } \sum_{l=1}^{k+1} Q^{j(l)}_{near,out} < f \sum_{j} Q^{j}_{near,out} \end{cases}.$$

The resulting boundary condition for the stream tube would then become

$$C_f^{i,tube}(0,t) = \frac{\sum_{j \in H(f)} C^{j}_{near,out,i}(t) Q^{j}_{near,out}}{\sum_{j} Q^{j}_{near,out}}.$$

In order for this to be efficient, the target parameters under study must be fairly strongly dependent on Darcy velocity, which was not the case in SKB 91.

A.6 References

[Kjellbert, 1991] Kjellbert, N., Tullgarn - A nearfield radionuclide migration code, SKB AR 91-25.

[Norman and Kjellbert, 1990] Norman, S., Kjellbert, N., FARF31 - A far field radionuclide migration code for use with the PROPER package, SKB TR 90-01.

[Norman and Kjellbert, 1991] Norman, S., Kjellbert N. , A near field radionuclide migration code for use with the PROPER package, SKB TR 91-19.

[SKB 91] SKB 91, Final disposal of spent nuclear fuel. Importance of the bedrock for safety, SKB TR 92-20.

APPENDIX B - MOYE'S FORMULA

This appendix derives Moye's formula [Moye, 1967] and is inserted solely for the conveniance of the reader.

B.1 Derivation of Moye's formula

We study the packer test by using the mathematical model expressed by the formulas 2.4 and 2.5. In particular we repeat the approximation that the flow per difference head q_1 is written using the notation of section 2.1 as

$$q_1 := \frac{Q_1}{2\pi\Delta h_1} = \int_{z_1}^{z_1+L_1} K(\mathbf{x})\left(\frac{1}{\Delta h_1}\frac{\partial h_0(\mathbf{x})}{\partial \rho} + \frac{\partial h_1(\mathbf{x})}{\partial \rho}\right)\rho_w dz \approx$$

$$\int_{z_1}^{z_1+L_1} K(\mathbf{x})\frac{\partial h_1(\mathbf{x})}{\partial \rho}\rho_w\, dz \qquad \text{B.1}$$

Now the flow resulting from the overpressure is assumed to be purely cylindrical up to a radial distance of L/2, see fig B.1. Assuming the conductivity to be a constant K_1 in a neighbourhood of the packer test we solve the steady state hydrology equation in a cylindrical system of coordinates shown in 2.1 to obtain for the head

$$h_1(\rho) = A\ln(\rho) + B,$$

where A and B are constants to be determined, and for the radial component U_ρ of the Darcy velocity

$$U_\rho(\rho) = -K_1\frac{A}{\rho}.$$

Since the total flux Q_1 is known we have

$$A = -\frac{Q_1}{2\pi L K_1}$$

and the head on the boundary of the pressurized section is by the boundary conditions 2.5 given as

$$h_1(\rho_w) = \Delta h_1.$$

This gives

$$B = \Delta h_1 + \frac{Q_1}{2\pi L_1 K_1}\ln(\rho_w)$$

and thus

$$h_1(\rho) = \Delta h_1 + \frac{Q_1}{2\pi L_1 K_1} \ln\left(\frac{\rho_w}{\rho}\right).$$

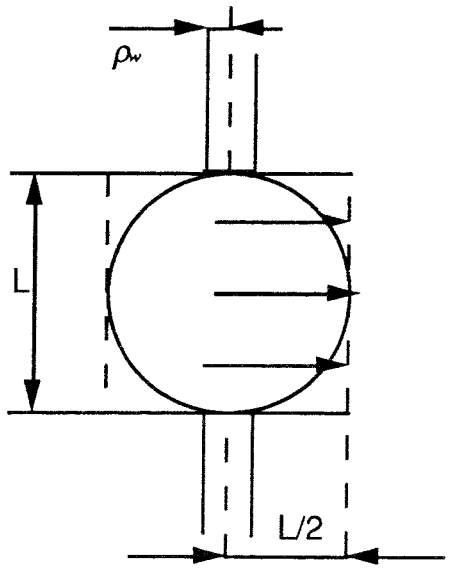

Figure B.1 *Illustrating a packer test and the corresponding derivation of Moye's formula.*

Assume that the flux changes abruptly from radial to spherical at ρ = r = L/2 . For spherical flux in a homogeneous medium we have for the head

$$h_1(r) = \frac{A}{r} + B$$

and for the Darcy velocity

$$U_r(r) = K\frac{A}{r^2}.$$

It follows from the boundary conditions 2.5 and the underlying assumption that the position of the measurement is far from the the boundary that

$$\lim_{r\to\infty} h_1(r) = 0$$

giving B = 0 above. Next transferring the head from the radial case at ρ = r = L/2 gives

$$A = \frac{L_1}{2}\Delta h_1 + \frac{Q_1}{4\pi K_1} \ln\left(\frac{2\rho_w}{L_1}\right)$$

and thus if we equate the total flow in the radial and spherical regions we get

$$Q_1 = 4\pi K_1 \frac{L_1}{2} \Delta h_1 + Q_1 \ln\left(\frac{2\rho_w}{L_1}\right)$$

from which we derive Moye´s formula

$$K_1 = \frac{Q_1\left(1 - \ln\left(\frac{2\rho_w}{L_1}\right)\right)}{2\pi L_1 \Delta h_1} = q_1 \frac{\left(1 - \ln\left(\frac{2\rho_w}{L_1}\right)\right)}{L_1} \qquad \text{B.1}$$

B.2 References

[Moye, 1967] Moye, D. G., Diamond drilling for foundation exploration, Civil engineering transactions, 1967, pp 95 - 100.

APPENDIX C - INTRINSIC RANDOM FUNCTIONS

The objective of this appendix is to explore the theory of intrinsic random functions in more detail. For that purpose we have to start with some more exact definitions of a stochastic function.

C.1 Mathematical definition of a stochastic function

First we define what we will mean with a **stochastic function**. In order to do that we first introduce the event space Ω which is a so-called measure space. The meaning of that notion is that there is defined an σ–algebra $\aleph$[25] of subsets to Ω. The sets in this algebra are known in the language of probability theory as **events**. Finally there also exists a positive probability measure P defined on the members of $\aleph$ such that $P(\Omega) = 1$ and that

$$P\left(\bigcup_i O_i\right) = \sum_i P(O_i)$$

if the sets O_i are disjoint, that is the events O_i are independent.

We define the space $L(\Omega, \aleph, P)$ as the real (or complex) valued functions X that are measurable with respect to $\aleph$[26]. In the language of probability theory X is a **stochastic variable**. We also define $L^2(\Omega, \aleph, P)$ as the subset of $\{X \in L(\Omega, \aleph, P)\}$ whose members satisfy

$$\int_\Omega X(\omega)^2 dP(\omega) < \infty \qquad \text{C.1}$$

Then X is a stochastic variable with the extra quality of having a finite variance.

Now define a **stochastic function** on $\mathbf{R}^3$ as a mapping

$$Y : \mathbf{R}^3 \rightarrow L^2(\Omega, \aleph, P) \qquad \text{C.2}$$

---

[25] A collection $\aleph$ of subsets of a set Ω is said to be a σ-algebra in Ω if $\aleph$ has the following properties

(i) $\Omega \in \aleph$

(ii) If $O \in \aleph$ then $O^C \in \aleph$ where O^C denotes the complement of O relative to Ω.

(iii) If $O = \bigcup_{i=1}^{\infty} O_i$ and if each $O_i \in \aleph$ then $O \in \aleph$.

[26] A realvalued function F is measurable with respect to $\aleph$ if for every open set O in R the inverse image $F^{-1}(O)$ belongs to $\aleph$.

this is to say that a stochastic function is a mapping that assigns a stochastic variable to each point $\mathbf{x} \in \mathbf{R}^3$. This can of course also be written in the same manner as in chapter 3 i.e. as $Y(\mathbf{x},\omega)$.

In order to avoid misunderstanding it is appropriate to insert a short discussion of the event space Ω. The element or "points" ω of Ω can be taken to consist of mappings $\omega:\mathbf{R}^3 \rightarrow \mathbf{R}^1$ [27]. The mapping C.2 is then the map $Y:\mathbf{x} \rightarrow Y(\mathbf{x})(\omega) = \omega(\mathbf{x})$. Thus in particular the distribution function of the stochastic variable $Y(\mathbf{x})$ is $P(Y(\mathbf{x}) \leq \alpha) = P(\{\omega : \omega(\mathbf{x}) \leq \alpha\})$ and the requirement C.1 is reformulated as

$$\int_{\Omega} \omega(\mathbf{x})^2 dP(\omega) < \infty \qquad \text{C.3}$$

for all $\mathbf{x} \in \mathbf{R}^3$. The formulas C.3 and C.1 are usually expressed by the phrase that the stochastic function is of second order. Note that this has nothing to do with stationarity.

After these preliminaries we define the expectation value function or trend of a second order stochastic function as

$$m_Y(\mathbf{x}) = E[Y(\mathbf{x})] = \int_{\Omega} Y(\mathbf{x}, \omega) dP(\omega) < \infty$$

and the covariance

$$C_Y(\mathbf{x}_1, \mathbf{x}_2) = E\left[(Y(\mathbf{x}_1) - m_Y(\mathbf{x}_1))(Y(\mathbf{x}_2) - m_Y(\mathbf{x}_2))\right] =$$

$$\int_{\Omega}\int_{\Omega} (Y(\mathbf{x}_1, \omega_1) - m_Y(\mathbf{x}_1))(Y(\mathbf{x}_2, \omega_2) - m_Y(\mathbf{x}_2)) dP(\omega_1) dP(\omega_2) < \infty$$

That these integrals exist as finite values is a consequence of the second-order assumption and the Cauchy Schwarz inequality. Finally $Y(\mathbf{x})$ is a **weakly (second order) stationary** stochastic function if $m_Y(\mathbf{x})$ is a constant and $C_Y(\mathbf{x}_1, \mathbf{x}_2)$ depends only on the difference $\mathbf{x}_1 - \mathbf{x}_2$.

C.2 Mathematical definition of intrinsic random functions

To make the definition of an intrinsic random function precise we follow [Matheron, 1973] and start by introducing the class Λ of measures on $\mathbf{R}^3$ with **finite support** i.e. measures λ such that

---

[27] That is we take Ω to consist of all possible realizations. This is equivalent to take the sample space equal $N_6 = \{1,2,3,4,5,6\}$ in the standard example case of tossing of a die and $N_6 \otimes N_6 \otimes \ldots$ in the case of an infinite, or undetermined, number of tosses.See [Doob, 1990].

$$\int f(\mathbf{x})d\lambda(\mathbf{x}) = \sum_i f(\mathbf{x}_i)\lambda_i$$

holds for any continuous function f:$\mathbf{R}^3 \rightarrow \mathbf{R}$. The above sum contains only finitely many terms. Next we define a translation operator τ_ξ on this class of measures by the requirement that

$$\int f(\mathbf{x})d(\tau_\xi\lambda)(\mathbf{x}) = \sum_i f(\mathbf{x}_i + \xi)\lambda_i$$

should hold for all continuous functions f.[28]

Now define Λ' as the class of all finitely supported measures λ which annihilate the constant functions, i.e. measures λ such that

$$\int_{\mathbf{R}^3} d\lambda = \sum_{i=1}^{n} \lambda_i = 0 \qquad \text{C.4}$$

We will say that Z is a **generalized second order random function** on Λ' if it is a linear map $Z : \Lambda' \rightarrow L^2(\Omega, \aleph, P)$.

A generalized random function on Λ' is an **intrinsic random function of order zero** if the stochastic function (of **x**) $Y(\tau_{\mathbf{x}}\lambda)$ is second-order stationary for any choice of λ in Λ'. That this stochastic function is second-order stationary is equivalent to the requirement that

$$E[Z(\lambda)Z(\lambda')] = E[Z(\tau_\xi\lambda)Z(\tau_\xi\lambda')]$$

for any choices of measures λ and λ' in Λ'. Expanding this gives

$$E\left[\sum_{i=1}^{n}\lambda_i Z(\mathbf{x}_i)\sum_{j=1}^{n'}\lambda'_j Z(\mathbf{x}'_j)\right] = E\left[\sum_{i=1}^{n}\lambda_i Z(\mathbf{x}_i + \xi)\sum_{j=1}^{n}\lambda'_j Z(\mathbf{x}'_j + \xi)\right]$$

and thus in particular

$$E\left[(Z(\mathbf{x}_1) - Z(\mathbf{x}_2))^2\right] = E\left[(Z(0) - Z(\mathbf{x}_2 - \mathbf{x}_1))^2\right] = 2\gamma(\mathbf{x}_2 - \mathbf{x}_1)$$

where $\gamma(\mathbf{h})$ is the semivariogram of Z. This shows that the above definition of an intrinsic random order function implies the definition in section 3.2.

---

[28]The choice of the continuous functions is natural since the measures of compact support is the dual space of the continuous functions.

Conversely let us show that this definition of an intrinsic random function follows from the definition of an intrinsic random function as contained in 3.1 and 3.2 in the case of zero order. In fact

$$E[Z(\lambda)Z(\lambda')] =$$

$$E\left[\sum_{i=1}^{n}\sum_{j=1}^{n}\lambda_i\lambda'_j Z(\mathbf{x}_i)Z(\mathbf{x}'_j)\right] = -\frac{1}{2}E\left[\sum_{i=1}^{n}\sum_{j=1}^{n}\lambda_i\lambda'_j\left(Z(\mathbf{x}_i) - Z(\mathbf{x}'_j)\right)^2\right] =$$

$$-\sum_{i=1}^{n}\sum_{j=1}^{n}\lambda_i\lambda'_j\gamma(\mathbf{x}_i - \mathbf{x}_j) \qquad \text{C.5}$$

where we used C.4 in the second equality. Clearly this and 3.1 proves our case and it also shows in particular by choosing $\lambda = \lambda'$ that the semivariogram is conditionally negative semi-definite, i.e. that

$$-\sum_{i=1}^{n}\sum_{j=1}^{n}\lambda_i\lambda_j\gamma(\mathbf{x}_i - \mathbf{x}_j) \geq 0 \qquad \text{C.6}$$

for any λ in Λ' and that the semivariogram is the generalized covariance of order zero as defined in [Matheron, 1973, p 450] and [de Marsily, 1986, p 314].

C.3 Representations of an intrinsic stochastic function

As seen there is a major difference between stochastic functions as defined in section C.1 and intrinsic stochastic functions in that the latter are defined on a space of finite measures. Now we say that a stochastic function $Y(\mathbf{x})$ is a **representation** of the intrinsic random function $Z(\lambda)$ if

$$Z(\lambda) = \int Y(\mathbf{x})d\lambda(\mathbf{x}) \qquad \forall\ \lambda \in \Lambda'$$

First we consider the question of the existence of a representation. It would be tempting to put $\lambda = \delta(\mathbf{x} - \mathbf{x}')$ in the above formula, where $\delta(\cdot)$ is the Dirac measure, but this measure does not belong to Λ' . However this is easily rectified by taking

$$\lambda(\mathbf{x}) = \delta(\mathbf{x} - \mathbf{x}') - \delta(\mathbf{x})$$

where $\mathbf{x}'$ is an arbitrary point and thus deriving as a necessary condition

$$Z(\delta(\mathbf{x} - \mathbf{x}') - \delta(\mathbf{x})) = Y(\mathbf{x}') - Y(\mathbf{0}) .$$

We easily see that this condition is also sufficient since taking any measure λ in Λ' then integrating the above formula with respect to $\mathbf{x}'$ we have

$$\int Y(\mathbf{x}')d\lambda(\mathbf{x}') = \int Z(\delta(\mathbf{x}-\mathbf{x}') - \delta(\mathbf{x}))d\lambda(\mathbf{x}') \qquad \text{C.7}$$

since obviously

$$\int Y(\mathbf{0})d\lambda(\mathbf{x}') = Y(\mathbf{0})\int d\lambda(\mathbf{x}') = 0$$

Now since λ is a finite measure the right hand side of C.7 is written

$$\sum_j Z\left(\delta\left(\mathbf{x}-\mathbf{x}'_j\right) - \delta(\mathbf{x})\right)\lambda_j$$

for some set of points $\{\mathbf{x}'_j\}$ and moreover since, by definition, Z is a linear mapping this is equal to

$$Z\left(\sum_j\left(\delta\left(\mathbf{x}-\mathbf{x}'_j\right) - \delta(\mathbf{x})\right)\lambda_j\right).$$

Finally it is clear that

$$\sum\left(\delta\left(\mathbf{x}-\mathbf{x}'_j\right) - \delta(\mathbf{x})\right)\lambda_j = \sum\lambda_j\delta\left(\mathbf{x}-\mathbf{x}'_j\right) = \lambda(\mathbf{x})$$

and thus

$$\int Y(\mathbf{x}')d\lambda(\mathbf{x}') = Z(\lambda)$$

which was what we wanted to show.

Now the above reasoning can also be used to obtain all representations of an intrinsic function Z. To that end let us assume that Y_1 and Y_2 are two representations of the intrinsic random function Z. Thus by definition

$$\int Y_1(\mathbf{x})d\lambda(\mathbf{x}) = \int Y_2(\mathbf{x})d\lambda(\mathbf{x}) \qquad \forall\ \lambda \in \Lambda'$$

and in particular choosing $\lambda \in \Lambda$' as

$$\lambda(\mathbf{x}) = \delta(\mathbf{x}-\mathbf{x}') - \delta(\mathbf{x})$$

we have

$$Y_1(\mathbf{x}') = Y_2(\mathbf{x}') + X$$

for all points $\mathbf{x}'$ and where X is a stochastic variable given by i.e

$$X = \left(Y_2(\mathbf{0}) - Y_1(\mathbf{0})\right) \in L^2(\Omega, \aleph, P)$$

Note that the integrals written here all refer to functions with values in the Hilbert space $L^2(\Omega, \aleph, P)$. A very nice discussion of such (abstract) integrals is found in [Ladas and Lakshmikantham, p 1- 20].

C.4 Relations to kriging

As pointed out in [Delfiner, 1976, p. 57] and as shown in section C.3 an intrinsic function (of order zero) is an equivalence class of stochastic functions that differ only by an arbitrary trivial random function $X(\omega)\cdot 1$. Furthermore the key equation is the special case of C.5 with $\lambda' = \lambda$

$$E\left[Y(\lambda)^2\right] = -\sum_{i=1}^{n}\sum_{j=1}^{n}\lambda_i\lambda_j\gamma(\mathbf{x}_i - \mathbf{x}_j)$$

since this may be interpreted as expressing estimation error solely in terms of the variogram. In fact choosing λ such that

$$\int f(\mathbf{x}')d\lambda(\mathbf{x}') = f(\mathbf{x}) - \sum_{i\in D(x)}\lambda_i(\mathbf{x})f(\mathbf{x}_i)$$

for any continuous function $f(\mathbf{x})$ where the weights λ_i satisfy the nonbias condition, we see that the kriging error is expressible as

$$E\left[\left(Y(\mathbf{x}) - \sum_{i\in D(x)}\lambda_i(\mathbf{x})Y(\mathbf{x}_i)\right)^2\right] =$$

$$2\sum_{i=1}^{n}\sum_{j=1}^{n}\lambda_i(\mathbf{x})\gamma(\mathbf{x} - \mathbf{x}_j) - \sum_{i=1}^{n}\sum_{j=1}^{n}\lambda_i(\mathbf{x})\lambda_j(\mathbf{x})\gamma(\mathbf{x}_i - \mathbf{x}_j)$$

Thus the point, [Delfiner, 1976], if the interest is to predict the values of the intrinsic random function, we do not need the covariance of a representation but only the variogram (generalized covariance) which is the covariance for the intrinsic random function.

C.5 References

[Ladas and Lakshmikantham, 1972] Ladas, G. E., Lakshmikantham, V., Differential equations in abstract spaces, Academic Press 1972

[Matheron, 1973] Matheron, G., The Intrinsic Random Functions and their Application, Adv. Appl. Prob. 5, 439-468, 1973.

[de Marsily, 1986] de Marsily, G., Quantitative Hydrogeology, Academic Press, 1986.

[Doob, 1990] Doob, J. L., Stochastic Processes, Wiley 1990.

[Delfiner, 1976] Delfiner, P., Linear Estimation of Non Stationary Spatial Phenomena, in M. Guarascio et al. (eds.), Advanced Geostatistics in the Mining industry, 49-68, D. 1976, Reidel puplishing Company, Dordrecht-Holland.

List of SKB reports

Annual Reports

1977-78
TR 121
KBS Technical Reports 1 – 120
Summaries
Stockholm, May 1979

1979
TR 79-28
The KBS Annual Report 1979
KBS Technical Reports 79-01 – 79-27
Summaries
Stockholm, March 1980

1980
TR 80-26
The KBS Annual Report 1980
KBS Technical Reports 80-01 – 80-25
Summaries
Stockholm, March 1981

1981
TR 81-17
The KBS Annual Report 1981
KBS Technical Reports 81-01 – 81-16
Summaries
Stockholm, April 1982

1982
TR 82-28
The KBS Annual Report 1982
KBS Technical Reports 82-01 – 82-27
Summaries
Stockholm, July 1983

1983
TR 83-77
The KBS Annual Report 1983
KBS Technical Reports 83-01 – 83-76
Summaries
Stockholm, June 1984

1984
TR 85-01
Annual Research and Development Report 1984
Including Summaries of Technical Reports Issued during 1984. (Technical Reports 84-01 – 84-19)
Stockholm, June 1985

1985
TR 85-20
Annual Research and Development Report 1985
Including Summaries of Technical Reports Issued during 1985. (Technical Reports 85-01 – 85-19)
Stockholm, May 1986

1986
TR 86-31
SKB Annual Report 1986
Including Summaries of Technical Reports Issued during 1986
Stockholm, May 1987

1987
TR 87-33
SKB Annual Report 1987
Including Summaries of Technical Reports Issued during 1987
Stockholm, May 1988

1988
TR 88-32
SKB Annual Report 1988
Including Summaries of Technical Reports Issued during 1988
Stockholm, May 1989

1989
TR 89-40
SKB Annual Report 1989
Including Summaries of Technical Reports Issued during 1989
Stockholm, May 1990

1990
TR 90-46
SKB Annual Report 1990
Including Summaries of Technical Reports Issued during 1990
Stockholm, May 1991

1991
TR 91-64
SKB Annual Report 1991
Including Summaries of Technical Reports Issued during 1991
Stockholm, April 1992

Technical Reports
List of SKB Technical Reports 1992

TR 92-01
GEOTAB. Overview
Ebbe Eriksson[1], Bertil Johansson[2], Margareta Gerlach[3], Stefan Magnusson[2], Ann-Chatrin Nilsson[4], Stefan Sehlstedt[3], Tomas Stark[1]
[1]SGAB, [2]ERGODATA AB, [3]MRM Konsult AB [4]KTH
January 1992

TR 92-02
Sternö study site. Scope of activities and main results
Kaj Ahlbom[1], Jan-Erik Andersson[2], Rune Nordqvist[2], Christer Ljunggren[3], Sven Tirén[2], Clifford Voss[4]
[1]Conterra AB, [2]Geosigma AB, [3]Renco AB,
[4]U.S. Geological Survey
January 1992

TR 92-03
Numerical groundwater flow calculations at the Finnsjön study site – extended regional area
Björn Lindbom, Anders Boghammar
Kemakta Consultants Co, Stockholm
March 1992

TR 92-04
Low temperature creep of copper intended for nuclear waste containers
P J Henderson, J-O Österberg, B Ivarsson
Swedish Institute for Metals Research, Stockholm
March 1992

TR 92-05
Boyancy flow in fractured rock with a salt gradient in the groundwater – An initital study
Johan Claesson
Department of Building Physics, Lund University, Sweden
February 1992

TR 92-06
Characterization of nearfield rock – A basis for comparison of repository concepts
Roland Pusch, Harald Hökmark
Clay Technology AB and Lund University of Technology
December 1991

TR 92-07
Discrete fracture modelling of the Finnsjön rock mass: Phase 2
J E Geier, C-L Axelsson, L Hässler,
A Benabderrahmane
Golden Geosystem AB, Uppsala, Sweden
April 1992

TR 92-08
Statistical inference and comparison of stochastic models for the hydraulic conductivity at the Finnsjön site
Sven Norman
Starprog AB
April 1992

TR 92-09
Description of the transport mechanisms and pathways in the far field of a KBS-3 type repository
Mark Elert[1], Ivars Neretnieks[2], Nils Kjellbert[3], Anders Ström[3]
[1]Kemakta Konsult AB
[2]Royal Institute of Technology
[3]Swedish Nuclear Fuel and Waste Management Co
April 1992

TR 92-10
Description of groundwater chemical data in the SKB database GEOTAB prior to 1990
Sif Laurent[1], Stefan Magnusson[2], Ann-Chatrin Nilsson[3]
[1]IVL, Stockholm
[2]Ergodata AB, Göteborg
[3]Dept. of Inorg. Chemistry, KTH, Stockholm
April 1992

TR 92-11
Numerical groundwater flow calculations at the Finnsjön study site – the influence of the regional gradient
Björn Lindbom, Anders Boghammar
Kemakta Consultants Co., Stockholm, Sweden
April 1992